Energy extraction from black holes and the jet formation

Nektarios Vlahakis

University of Athens

Outline

- **Lecture 1**
  - Introduction
  - Classes of relativistic jets
  - Observations relevant to jet physics (apparent motion, polarization, Faraday rotation)
  - Accretion disks and their magnetic field
  - Unipolar inductors and energy extraction
- **Lecture 2**
  - Magnetohydrodynamic modeling of jets
  - Bulk acceleration
  - Collimation
  - The role of the outflow environment
  - Jet kinematics

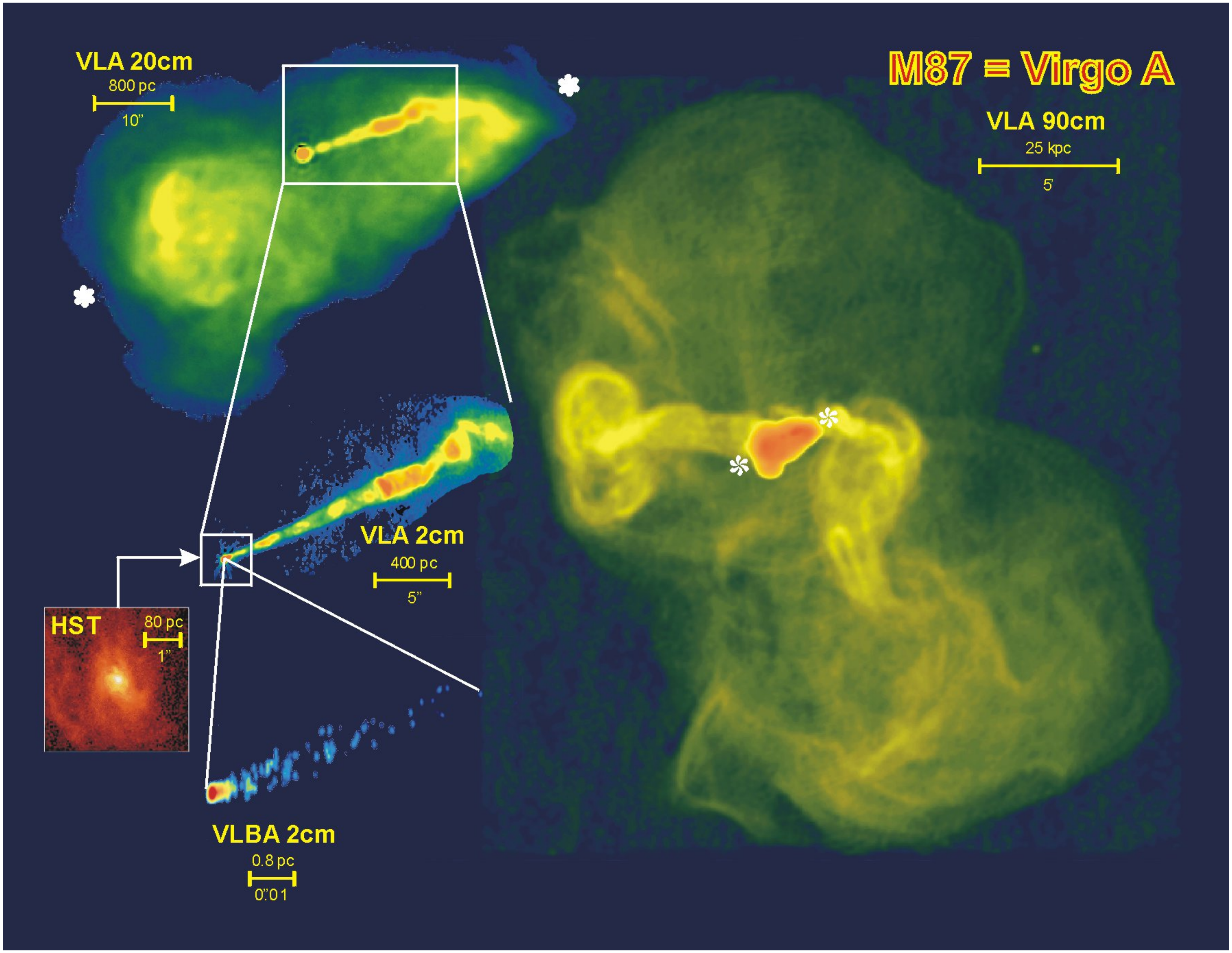
M87 = Virgo A
VLA 20cm
800 pc
10"
VLA 90cm
25 kpc
5'
VLA 2cm
400 pc
5"
HST
80 pc
1"
VLBA 2cm
0.8 pc
0."01

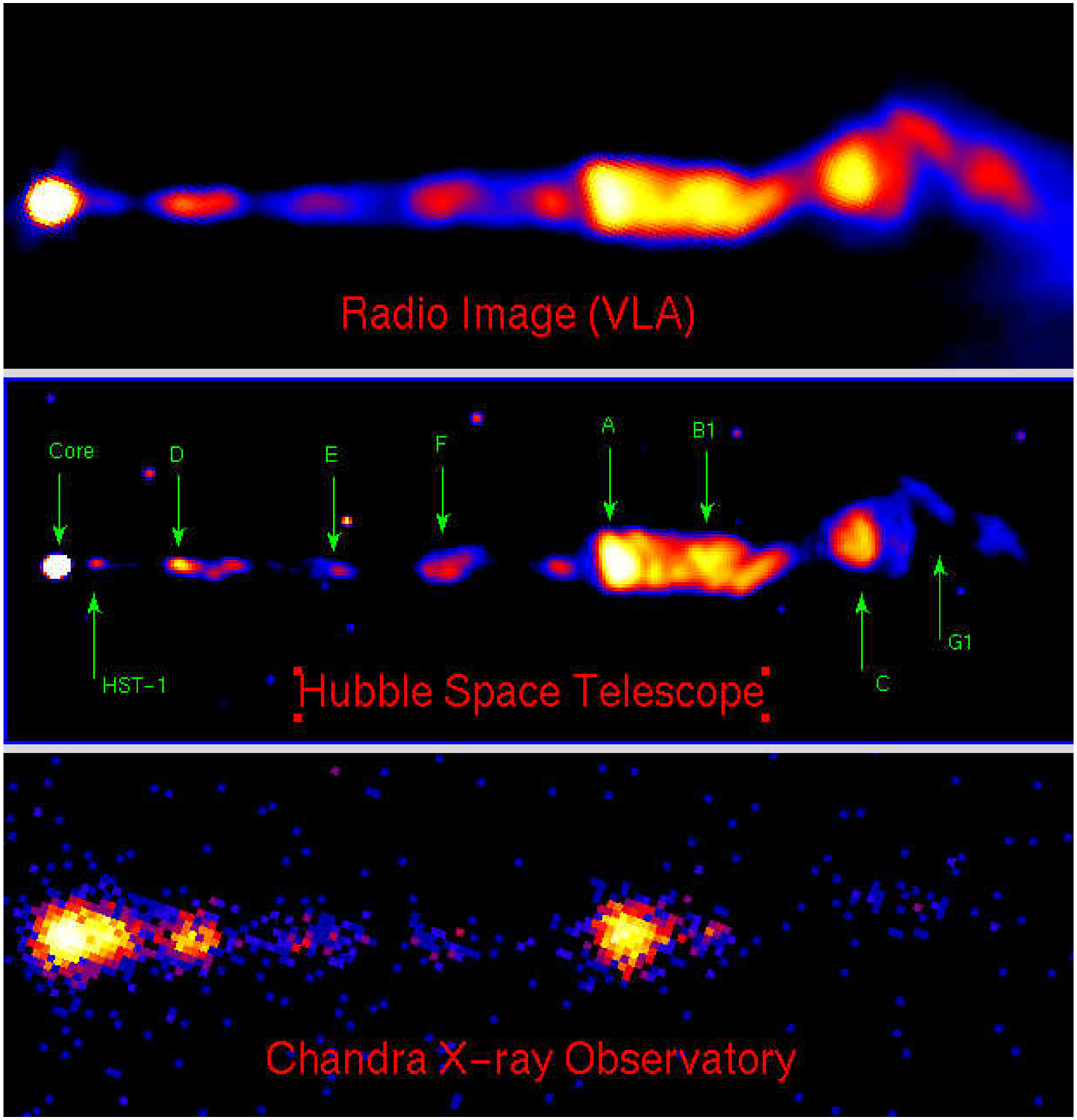
Radio Image (VLA)
Core
D
E
F
A
B1
HST-1
G1
C
Hubble Space Telescope
Chandra X-ray Observatory

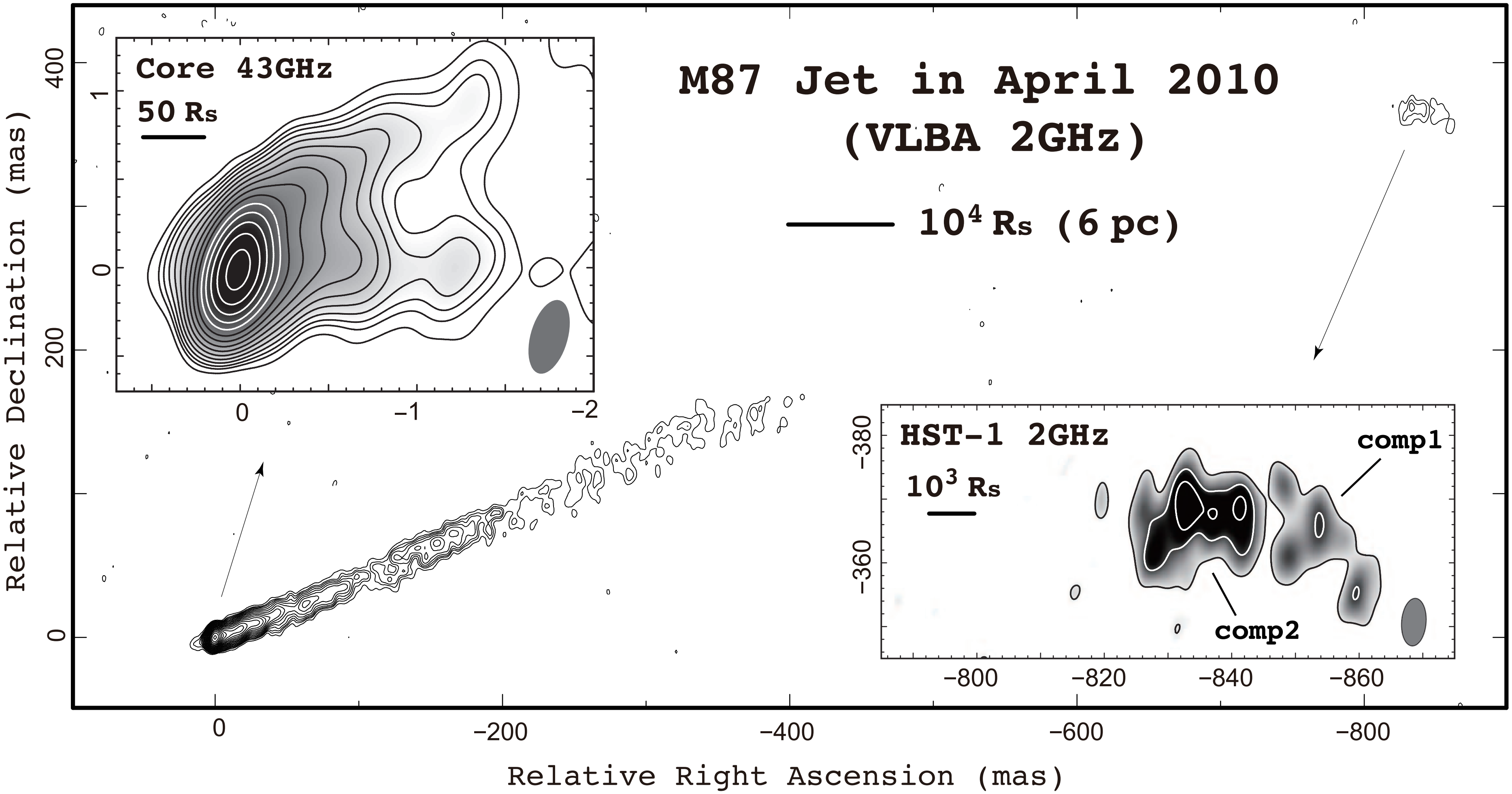

(Hada+)
collimation at ∼100 Schwarzschild radii

(Asada & Nakamura 2011)

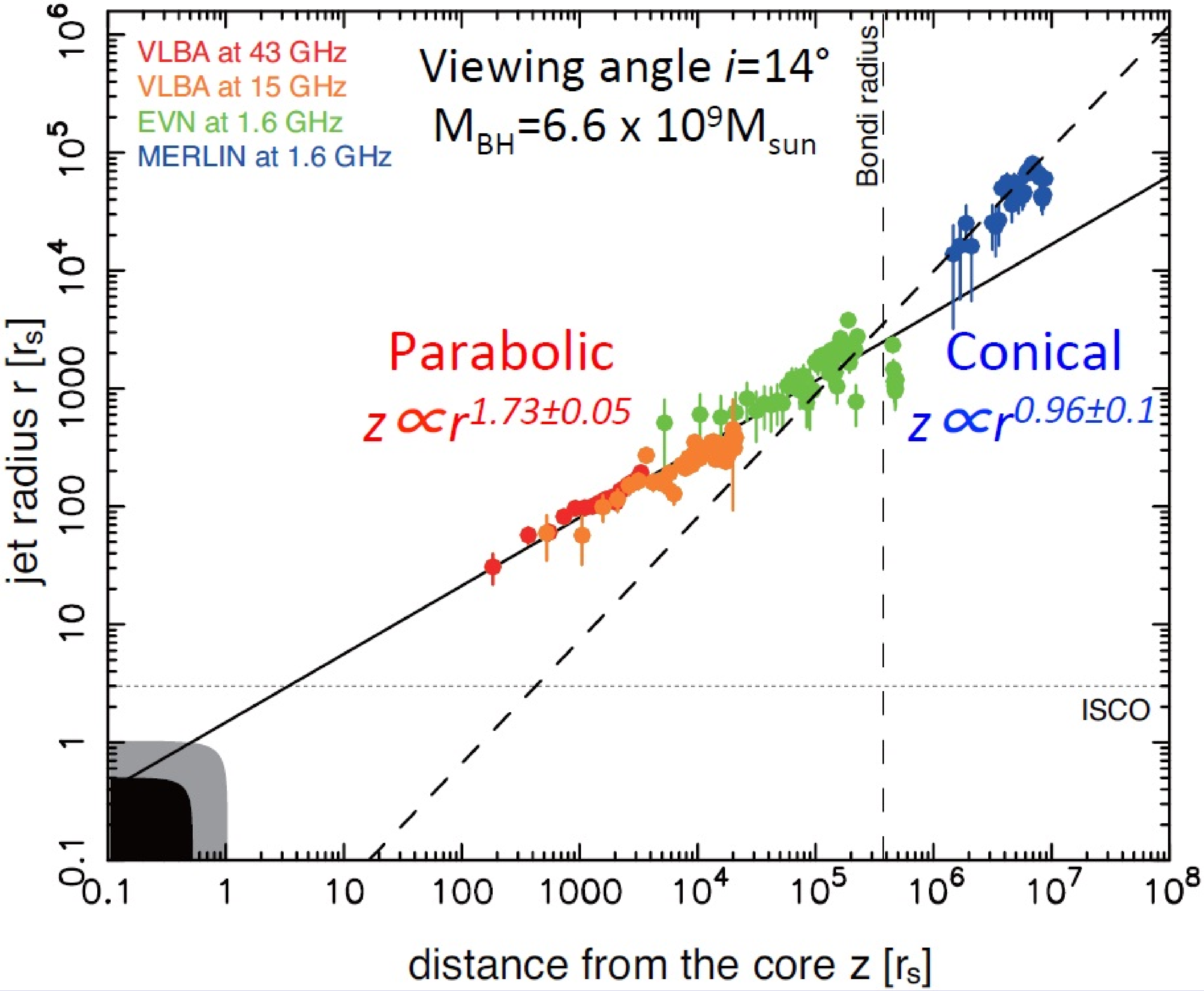

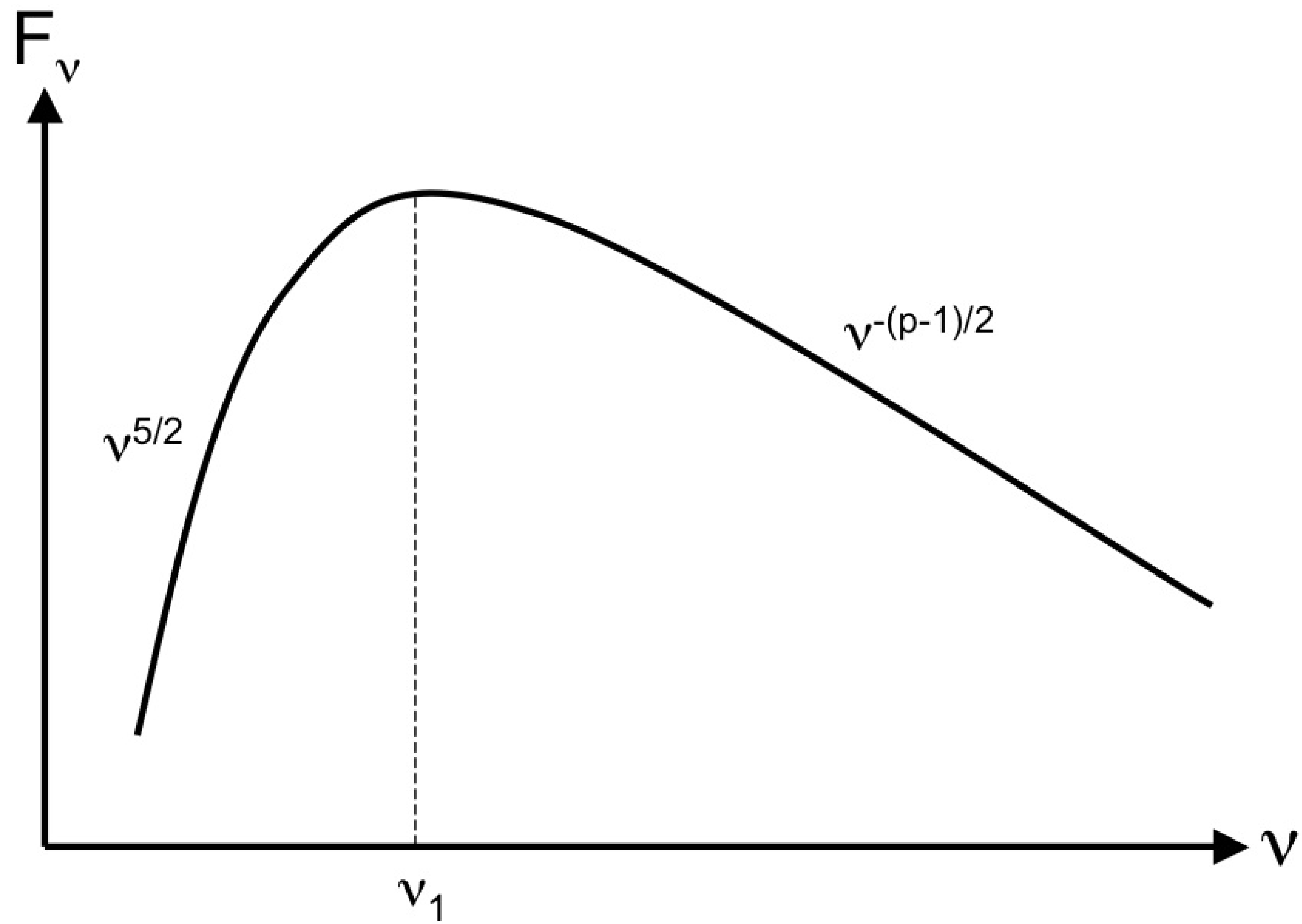
F_ν
$\nu^{5/2}$
$\nu^{-(p-1)/2}$
ν_1
ν

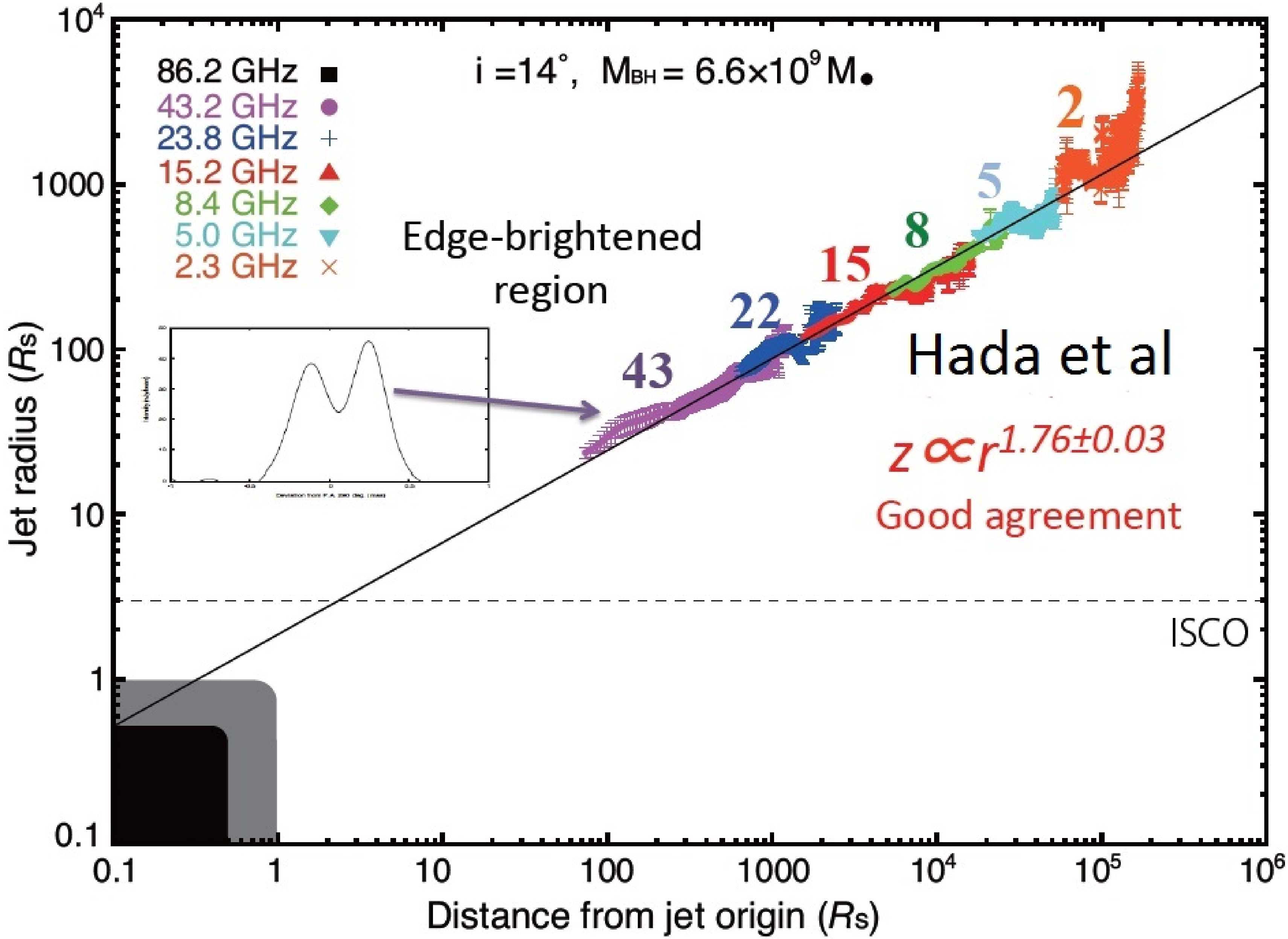

i =14°, M_{BH} = 6.6×10^9 $M_\odot$
86.2 GHz
43.2 GHz
23.8 GHz
15.2 GHz
8.4 GHz
5.0 GHz
2.3 GHz
Edge-brightened region
Hada et al
$z \propto r^{1.76\pm0.03}$
Good agreement
43
22
15
8
5
2
ISCO
Jet radius (Rs)
Distance from jet origin (Rs)

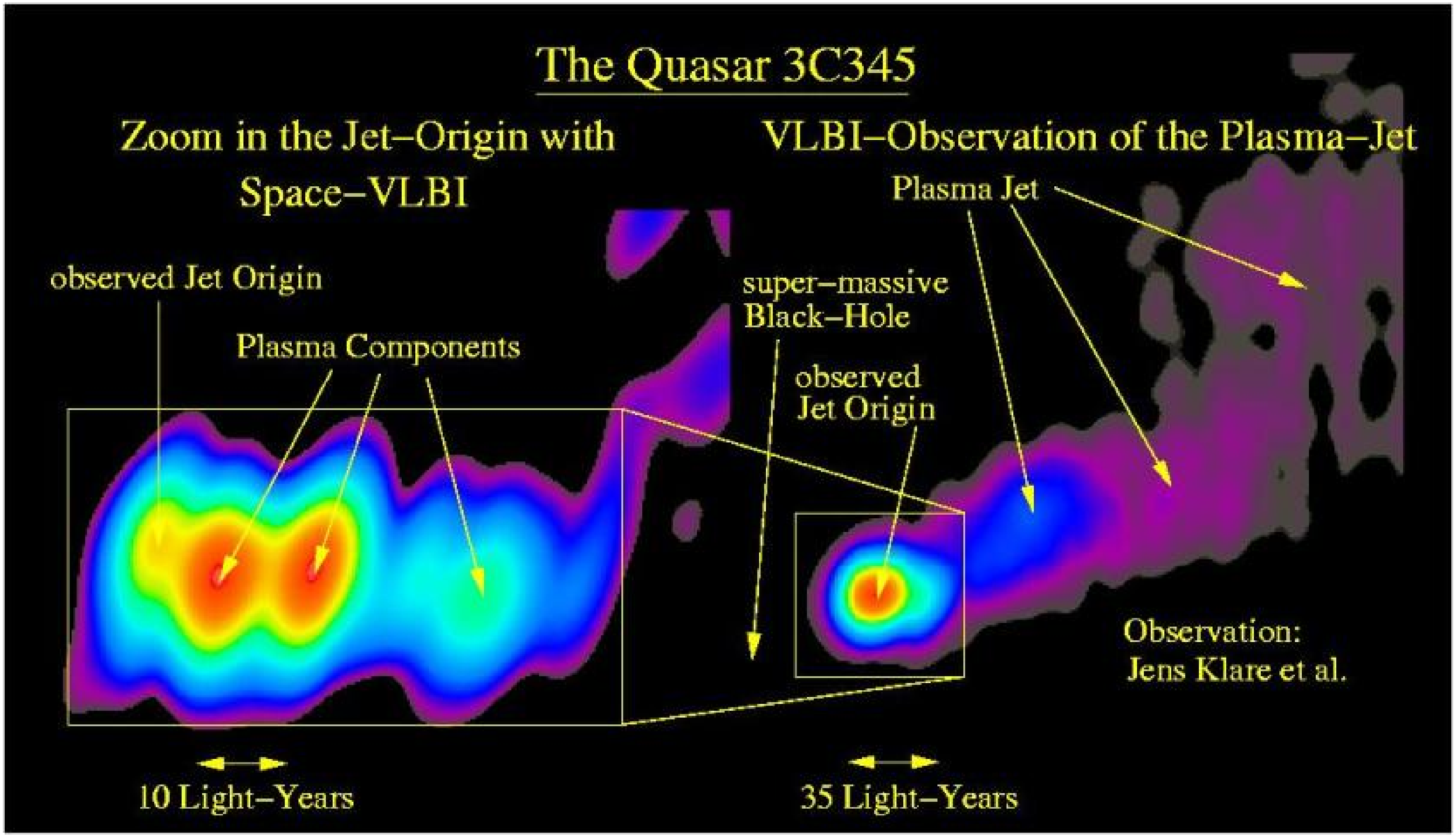

(credit: Klare+)

The plasma components move with superluminal apparent speeds

They travel on curved trajectories

The trajectories differ from one component to the other

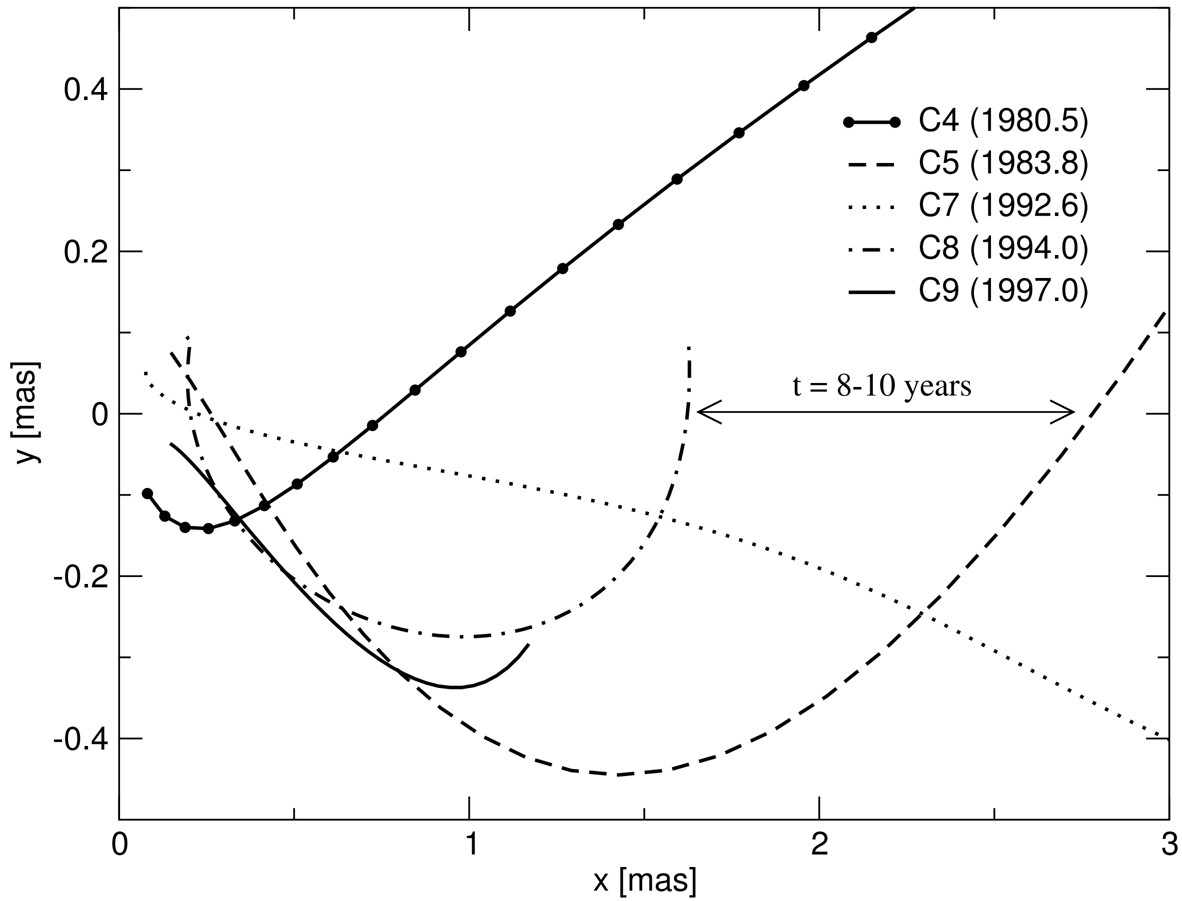

(credit Klare+)

microquasars

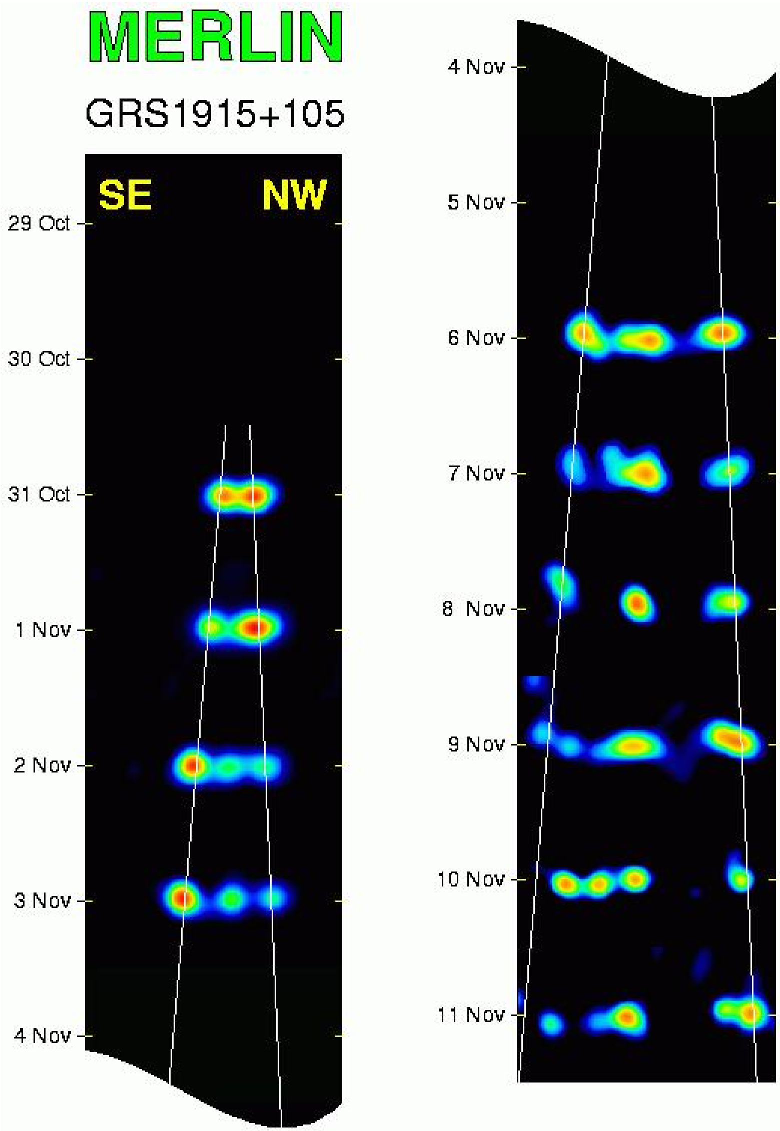

scale-down of quasars

speed $\sim 0.9 - 0.99c$

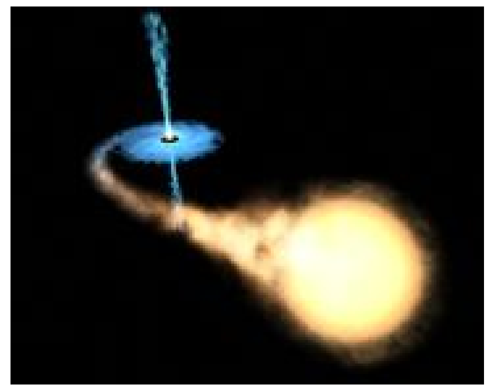

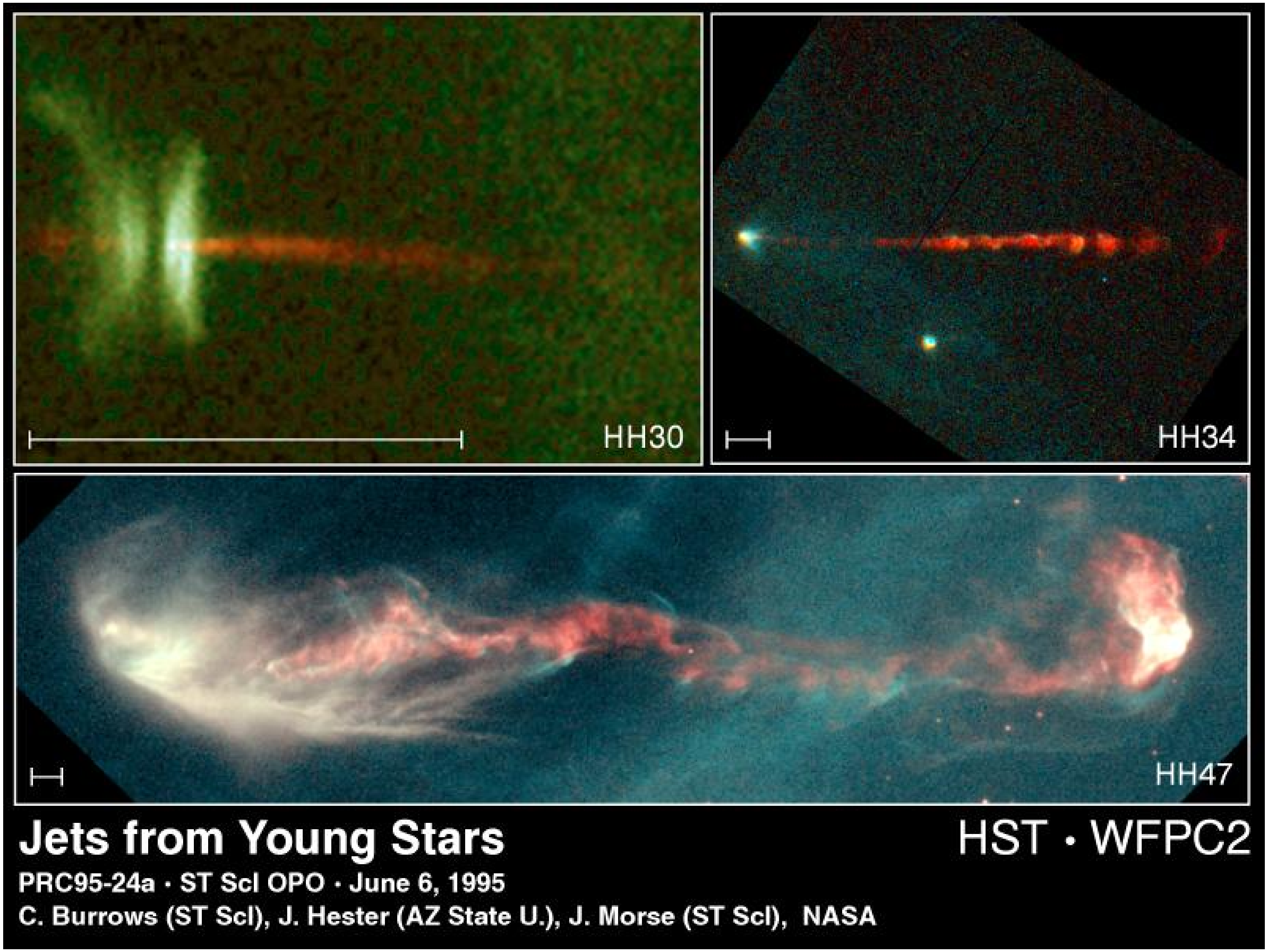

(scale =1000 AU, $V_{\infty} = a few 100$km/s)


Herbig-Haro 49/50
NASA / JPL-Caltech / J. Bally (Univ. of Colo.)
Spitzer Space Telescope • IRAC
sig06-002

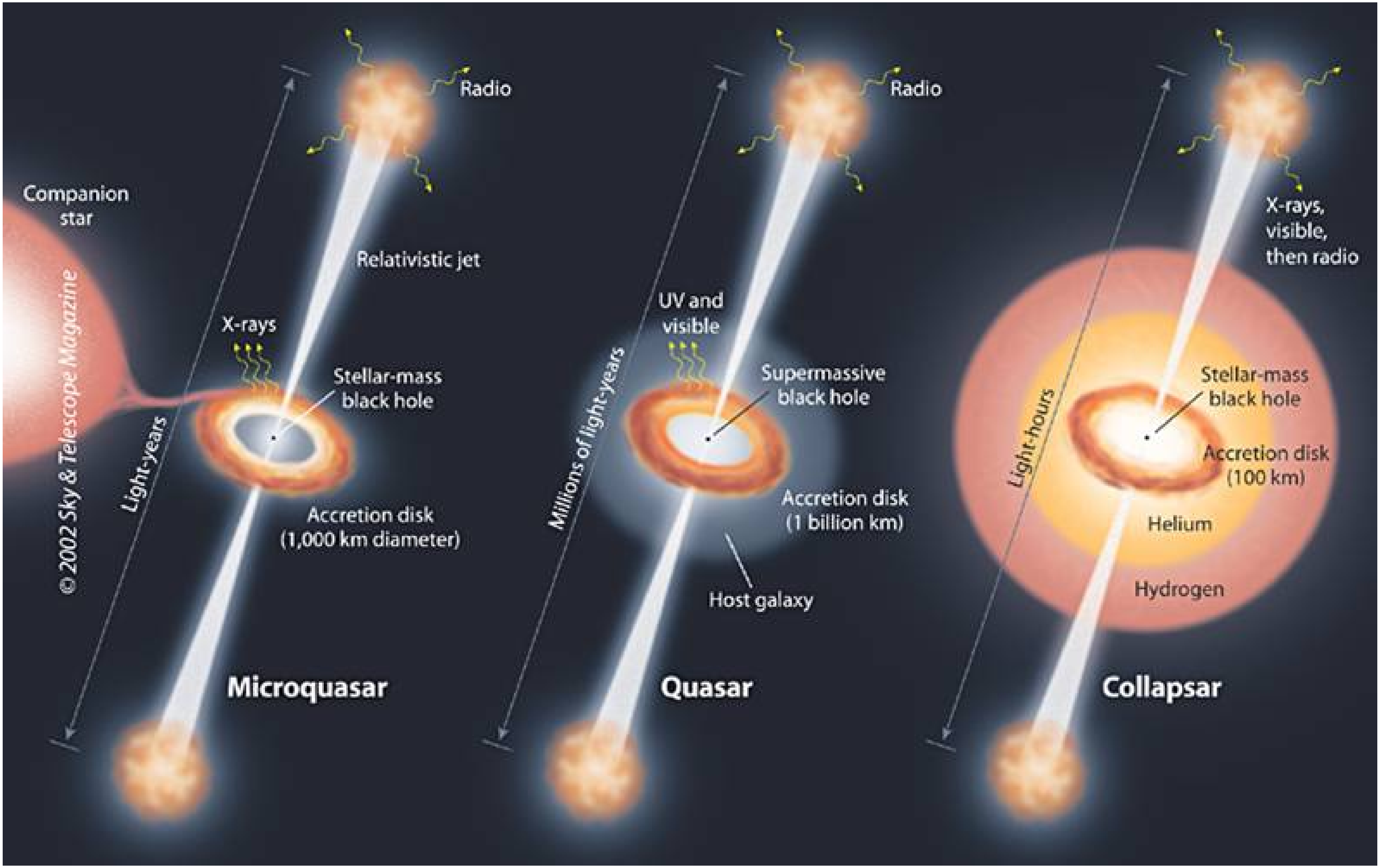

Companion star
Radio
Relativistic jet
X-rays
Stellar-mass black hole
Accretion disk (1,000 km diameter)
Light-years
© 2002 Sky & Telescope Magazine
Microquasar
Radio
UV and visible
Supermassive black hole
Accretion disk (1 billion km)
Host galaxy
Millions of light-years
Quasar
X-rays, visible, then radio
Stellar-mass black hole
Accretion disk (100 km)
Helium
Hydrogen
Light-hours
Collapsar

GRB prompt emission

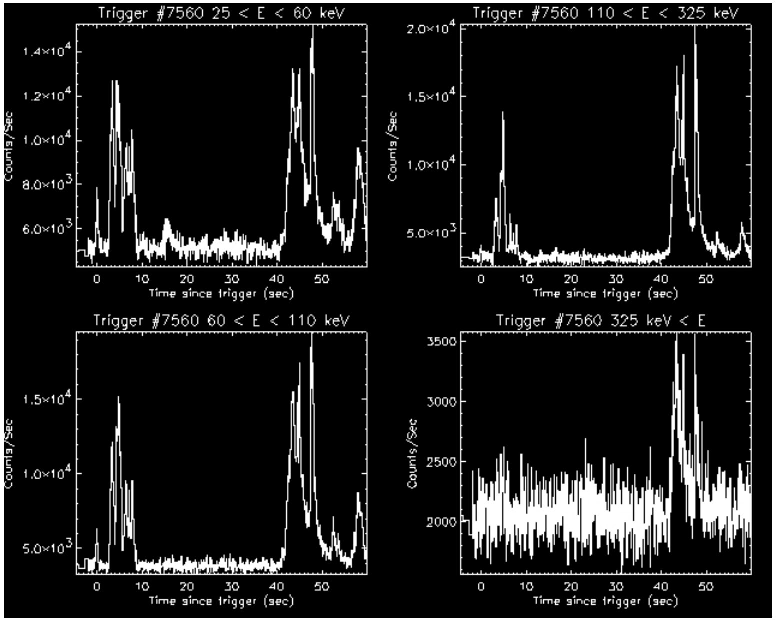

Variability timescale δt

compact source $R < c\,\delta t \sim 1000$ km

huge optical depth for $\gamma\gamma \to e^+e^-$

compactness problem: how the photons escape?

relativistic motion $\gamma \gtrsim 100$
- $R < \gamma^2 c\,\delta t$
- blueshifted photon energy
- beaming
- optically thin

Jet speed

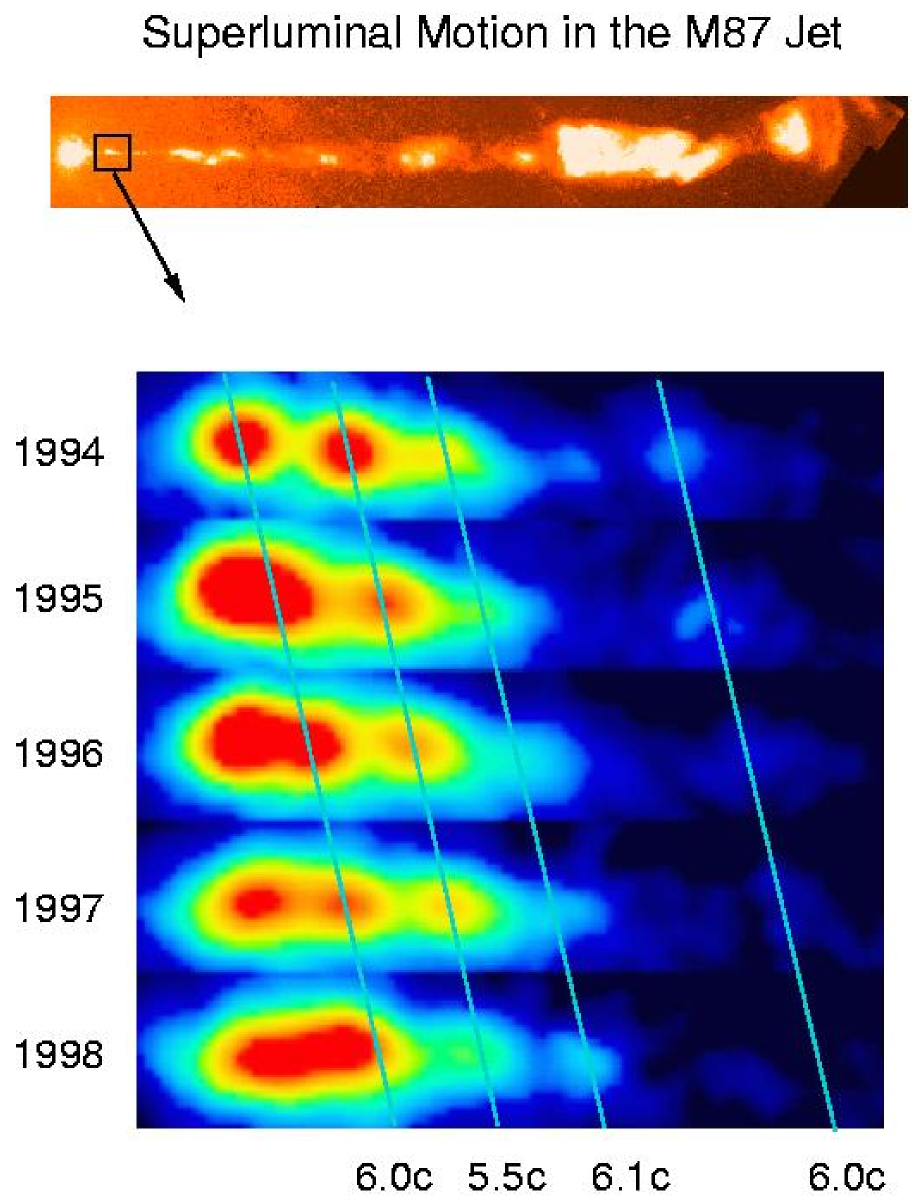

Superluminal Motion in the M87 Jet
1994
1995
1996
1997
1998
6.0c
5.5c
6.1c
6.0c

- Superluminal apparent motion: $\beta_{\rm app}$ is a lower limit of real γ
- **If** we know both $\beta_{\rm app} = \dfrac{\beta \sin\theta_n}{1-\beta\cos\theta_n}$ and $\delta \equiv \dfrac{1}{\gamma\,(1-\beta\cos\theta_n)}$
  we find $\theta_n(t_{\rm obs})$, $\beta(t_{\rm obs})$ and $v = c\beta$, $\gamma = 1/\sqrt{1-v^2/c^2}$
  Rough estimates of δ from:
  - comparison of radio and high energy emission (SSC)
    e.g., for the C7 component of 3C 345 Unwin+ argue that δ changes from ≈ 12 to ≈ 4 ($t_{\rm obs} =$ 1992 – 1993) $\Longrightarrow$ acceleration from $\gamma \sim 5$ to $\gamma \sim 10$ over $\sim 3-20$ pc from the core (θ_n changes from ≈ 2 to $\approx 10^o$)
    Similarly Piner+2003 inferred an acceleration from $\gamma = 8$ at $R < 5.8$pc to $\gamma = 13$ at $R \approx 17.4$pc in 3C 279
  - variability timescale (compared to the light crossing time), Jorstad, Marscher+

On the bulk acceleration

- More distant components have higher apparent speeds
- Brightness temperature increases with distance

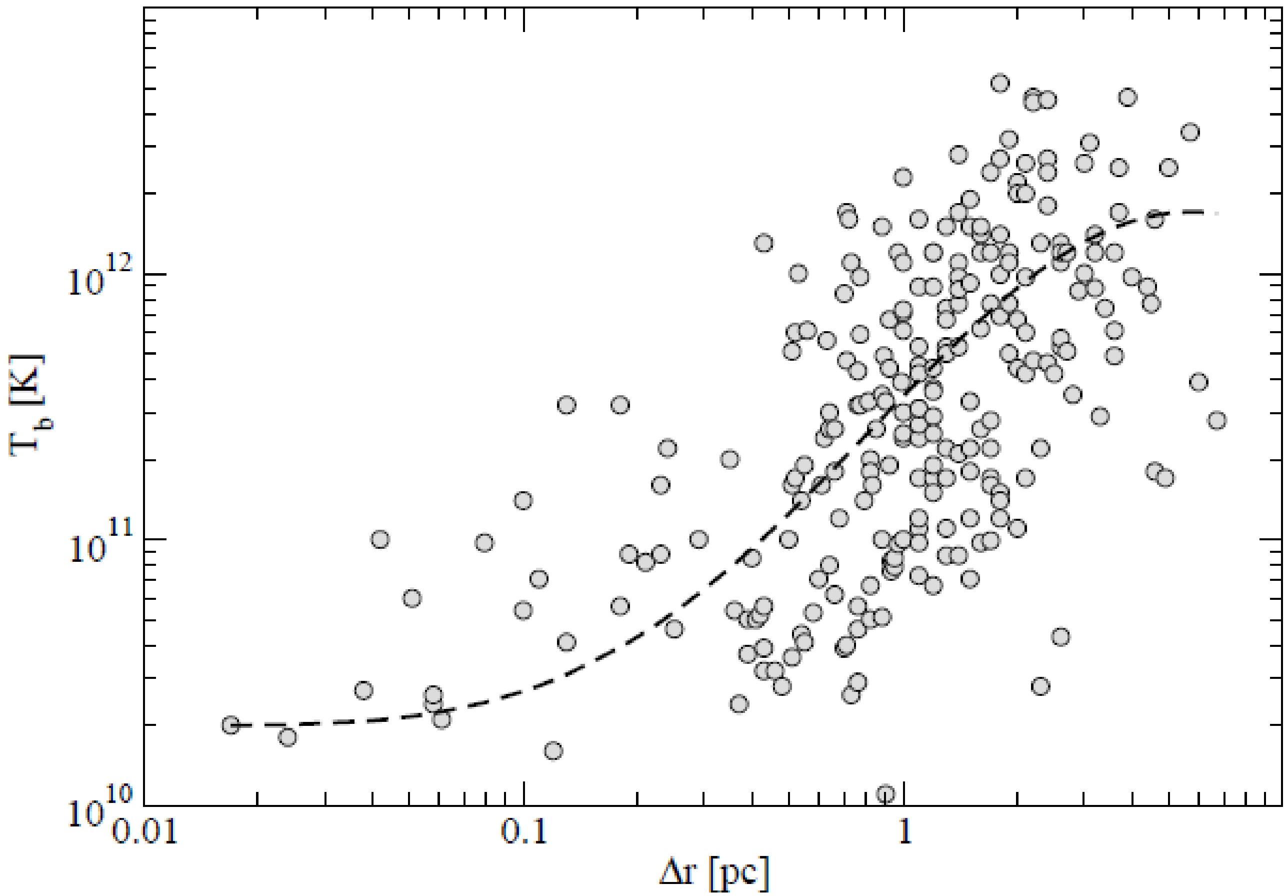

(Lee and Lobanov)

- recent measurements of apparent velocity in M87, along and across the jet (Mertens and Lobanov)

- A more general argument on the acceleration (Sikora+):
  - $\star$ lack of bulk-Compton features $\rightarrow$ small ($\gamma < 5$) bulk Lorentz factor at $\lesssim 10^3 r_g$
  - $\star$ the γ saturates at values $\sim$ a few 10 around the blazar zone $(10^3 - 10^4 r_g)$

  So, relativistic AGN jets undergo the bulk of their acceleration on parsec scales ($\gg$ size of the central black hole)

- Sikora+ also argue that the protons are the dynamically important component in the outflow.

Polarization

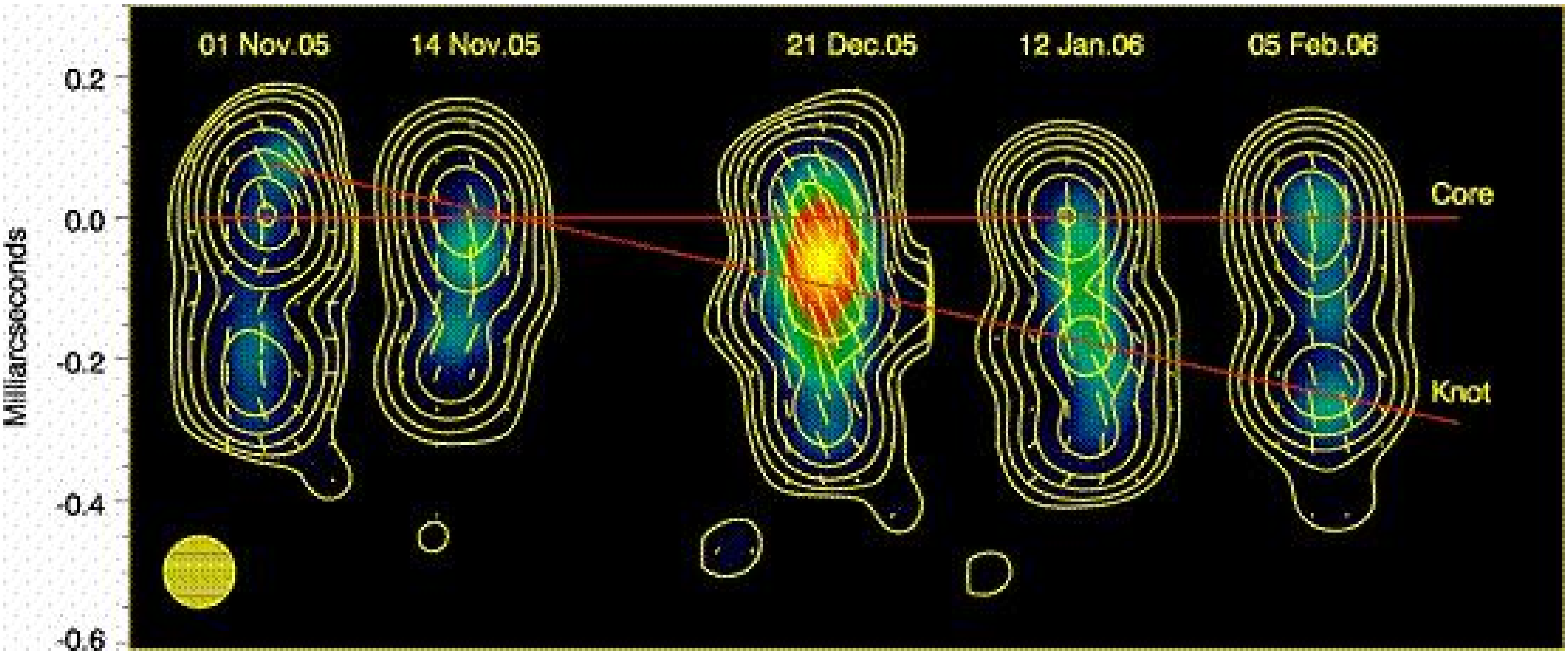

(Marscher+2008 Nature)

helical motion and field rotate the EVPA as the blob moves

observed $\boldsymbol{E}_{rad} \perp \boldsymbol{B}_{rad}$ and $\boldsymbol{B}_{rad}$ is $\parallel$ $\boldsymbol{B}_{\perp los}$
(modified if the jet is relativistic)

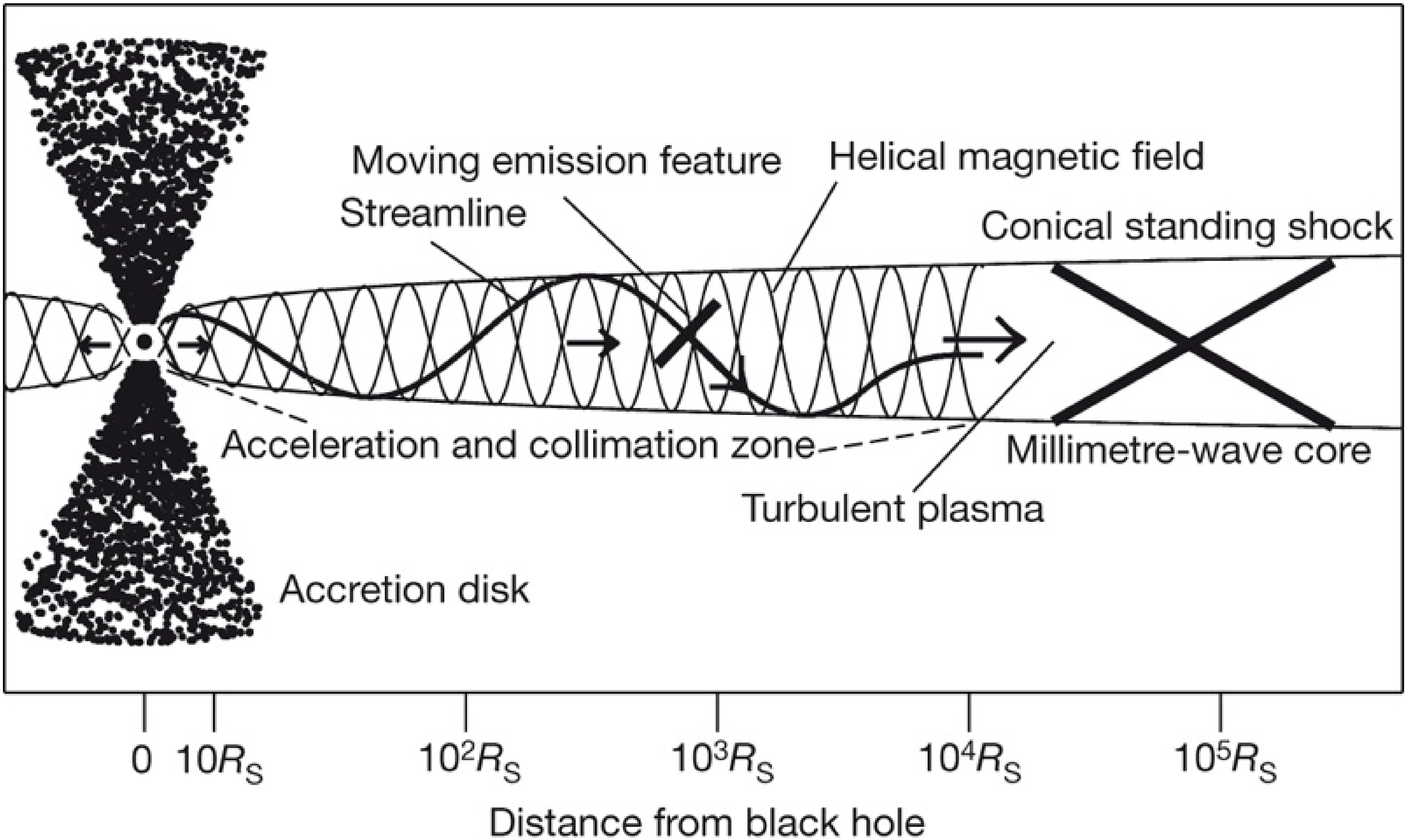

(from Marscher+)

Faraday rotation

Faraday rotation – the plane of LP rotates when polarized EM wave passes through a magnetized plasma, due to different propagation velocities of the RCP and LCP components of the EM wave in the plasma.

If internal, there is also depolarization (fractional polarization depends on λ).

If external, the amount of rotation is proportional to the square of the observing wavelength, and the sign of the rotation is determined by the direction of the line of sight B field:

$$\chi = \chi_0 + (RM)\lambda^2$$

$$(RM) \propto \int n_e B_{\| los} d\ell$$

Faraday RM gradients across the jet

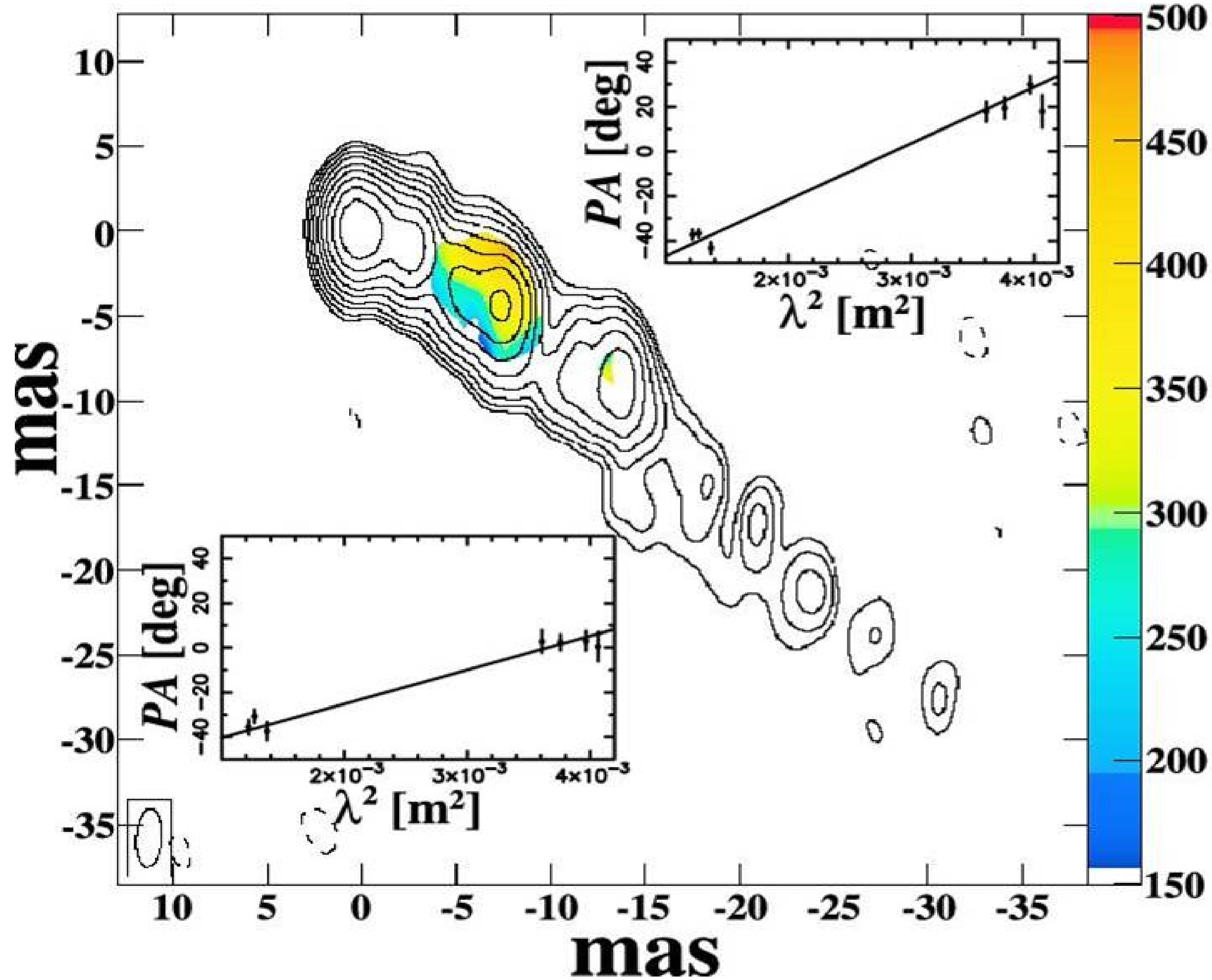

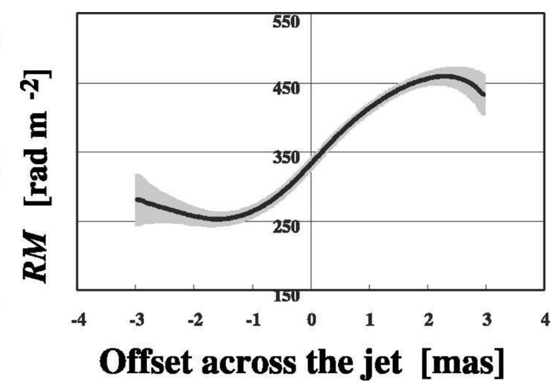

(from Asada+)

helical field surrounding the emitting region

Theory: Hydro-Dynamics

Hard to explain bulk acceleration.

- In case $n_e \sim n_p$, $\gamma_{\max} \sim kT_i/m_p c^2 \sim 1$ even with $T_i \sim 10^{12} K$
- If $n_e \neq n_p$, $\gamma_{\max} \sim (n_e/n_p) \times (kT_i/m_p c^2)$ could be $\gg 1$
- With some heating source, $\gamma_{\max} \gg 1$ is in principle possible

However, even in the last two cases, HD is unlikely to work because the HD acceleration saturates at distances comparable to the sonic surface where gravity is still important, i.e., very close to the disk surface (certainly at $\ll 10^3 r_g$)

We need magnetic fields

- ⋆ They extract energy (Poynting flux)
- ⋆ extract angular momentum
- ⋆ transfer energy and angular momentum to matter
- ⋆ explain relatively large-scale acceleration
- ⋆ collimate outflows and produce jets
- ⋆ needed for synchrotron emission
- ⋆ explain polarization and RM maps

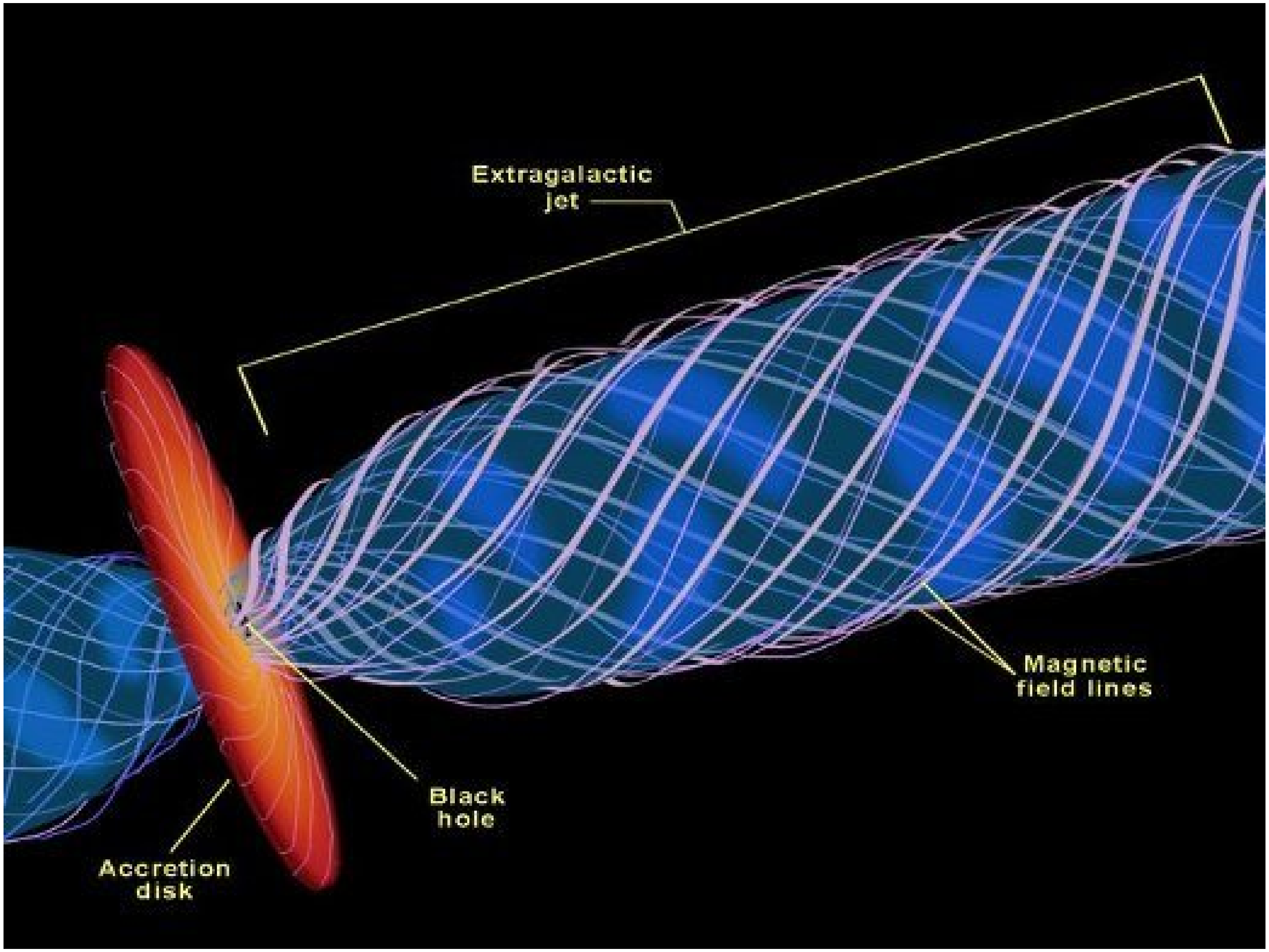

B field from advection, or dynamo, or cosmic battery (Poynting-Robertson drag).

Origin of magnetic fields ?

$$\frac{\partial \boldsymbol{B}}{\partial t} = -c\nabla \times \boldsymbol{E}$$ and

$$m_e n_e \frac{d\boldsymbol{v}_e}{dt} = -\nabla P_e - e n_e \left(\boldsymbol{E} + \frac{\boldsymbol{v}_e}{c} \times \boldsymbol{B}\right) + (\ldots)(\boldsymbol{v} - \boldsymbol{v}_e)\,,$$ with

$\boldsymbol{v}_e = \boldsymbol{v} - \frac{\boldsymbol{J}}{en}$, give (neglecting the electron's inertia)

$$\frac{\partial \boldsymbol{B}}{\partial t} \approx -c\nabla \times \left(-\frac{\boldsymbol{v}}{c} \times \boldsymbol{B} + \frac{\boldsymbol{J}}{en} \times \boldsymbol{B} - \frac{1}{en}\nabla P_e + \frac{\boldsymbol{J}}{\sigma}\right)$$

- Biermann battery (for non-barotropic plasmas)
- $\alpha\omega$ dynamo
- Contopoulos and Kazanas battery

Advection by accretion ?   MRI?

A unipolar inductor

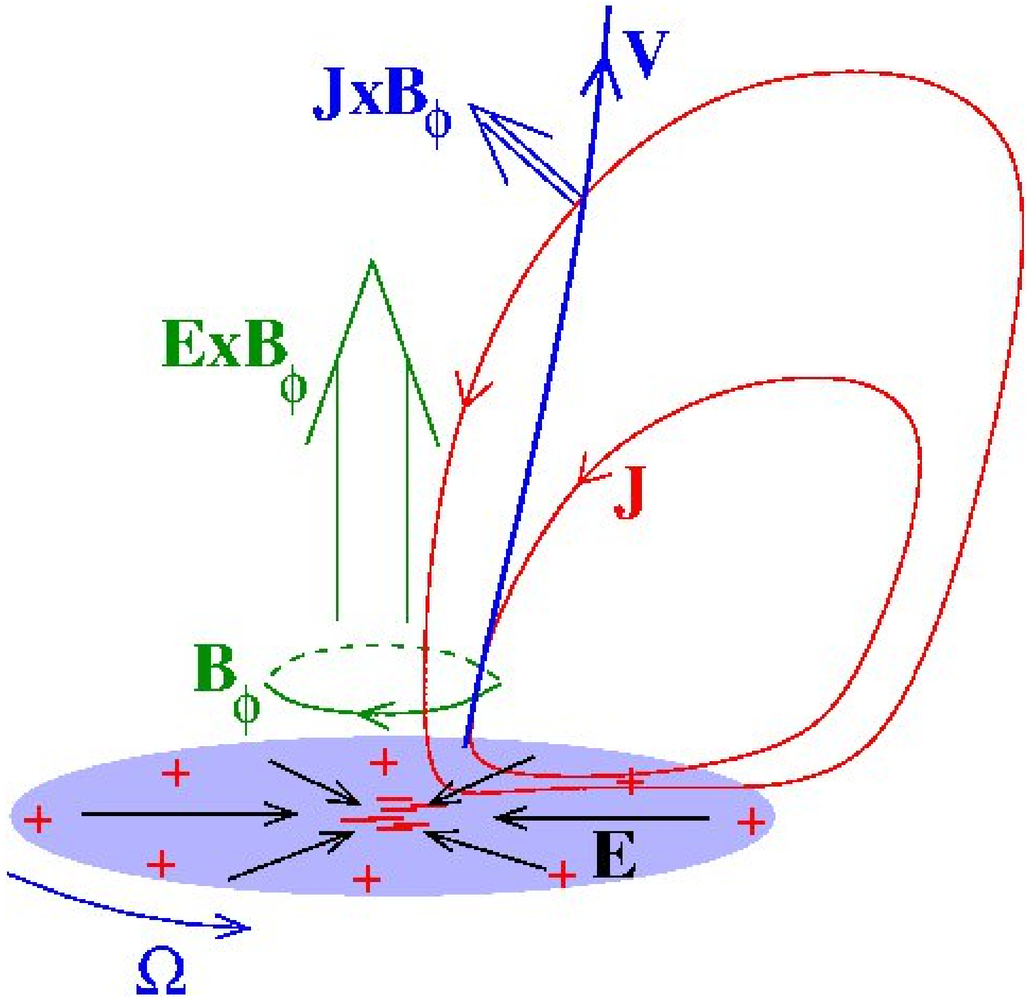

current $\leftrightarrow B_\phi$
Poynting flux $\frac{c}{4\pi} E B_\phi$ is extracted (angular momentum as well)

The Faraday disk could be the rotating accretion disk, or the frame dragging if energy is extracted from the ergosphere of a rotating black hole (Blandford & Znajek mechanism)

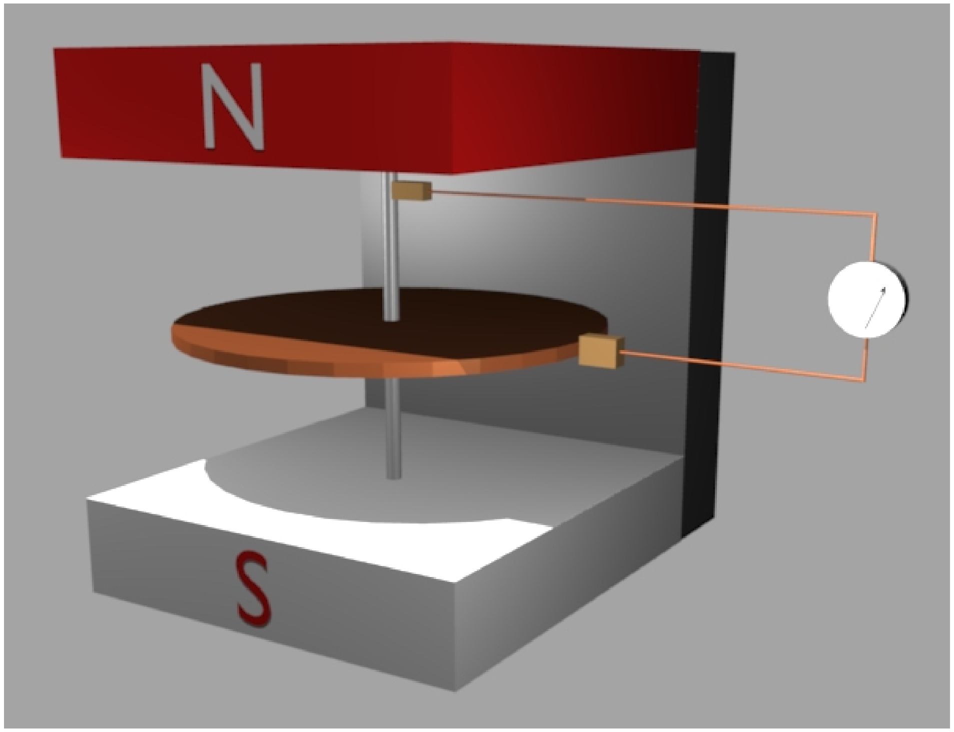
N
S

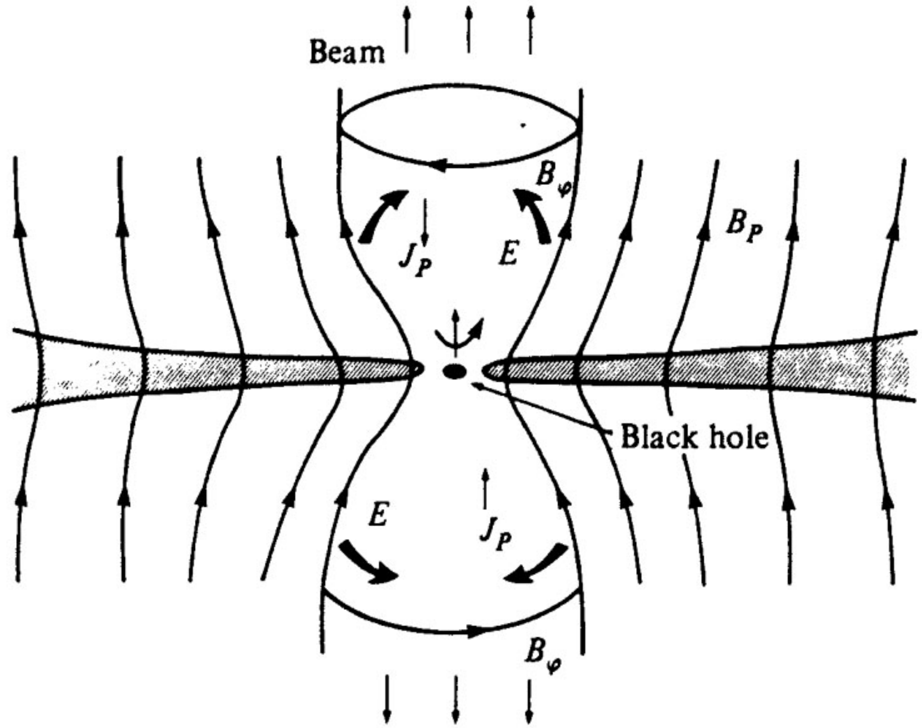
Beam
B_φ
B_P
J_P
E
Black hole
E
J_P
B_φ

How to model magnetized outflows?

- ⋆ as pure electromagnetic energy (force-free, magnetodynamics, electromagnetic outflows):
  – ignore matter inertia (reasonable near the origin)
  – this by assumption does not allow to study the transfer of energy form Poynting to kinetic
  – wave speed $= c \rightarrow$ no shocks
  – there may be some dissipation (e.g. reconnection) $\rightarrow$ radiation

- ⋆ as magneto-hydro-dynamic flow
  – the force-free case is included as the low inertia limit
  – MHD can also describe the back reaction from the matter to the field (this is important even in the superfast part of the regime where $\sigma \gg 1$)

Magnetized outflows

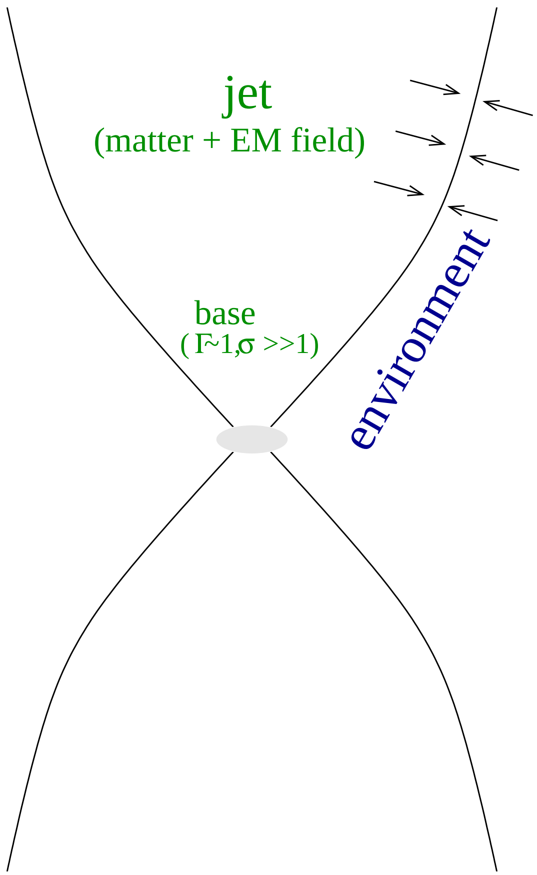

- Extracted energy per time $\dot{\mathcal{E}}$
mainly in the form of Poynting flux
(magnetic fields tap the rotational energy
of the compact object or disk)

$$\dot{\mathcal{E}} = \frac{c}{4\pi} \underbrace{\frac{r\Omega}{c} B_p}_{E} B_\phi \times (\text{ area }) \approx \frac{c}{2} B^2 r^2$$

- Ejected mass per time $\dot{M}$

- The $\mu \equiv \dot{\mathcal{E}}/\dot{M}c^2$ gives the maximum
possible bulk Lorentz factor of the flow

- Magnetohydrodynamics:
matter (velocity, density, pressure)
+ large scale electromagnetic field

Source of energy

If BZ, rotation of black hole, $\dot{\mathcal{E}} = 10^{42} a^2 (B/10^4\mathrm{G})^2 M_8^2$ erg/s

If extraction from disk, $\dot{\mathcal{E}} = b\dfrac{GM\dot{M}_a}{2r_i}$

Thin disk physics $\dot{M}_a = 2\pi r \times 2H \times \rho|V_r|$, $H = \dfrac{c_s}{\Omega}$, $c_s = \sqrt{\dfrac{P}{\rho}}$

slow Mach number $M_s = \dfrac{|V_r|}{c_s}$, plasma beta $\beta = \dfrac{8\pi P}{B^2}$

So, $\dfrac{\dot{\mathcal{E}}_{BZ}}{\dot{\mathcal{E}}_{disk}} = 3 \times 10^{-3} \dfrac{a^2}{b\beta M_s} \left(\dfrac{r_i}{r_g}\right)^{-3/2}$

E.g., for $a = 1$, $r_i = r_g$ and JED with $b \sim 0.5$, $\beta \sim M_s \sim 1$, $\dot{\mathcal{E}}_{BZ}$ is only a few percent on $\dot{\mathcal{E}}_{disk}$ (Ferreira)

Other disk models ?

MHD (Magneto-Hydro-Dynamics)

- matter: velocity $\boldsymbol{V}$, density ρ, pressure P
- large scale electromagnetic field: $\boldsymbol{E}\,, \boldsymbol{B}\,, \boldsymbol{J}\,, \delta$

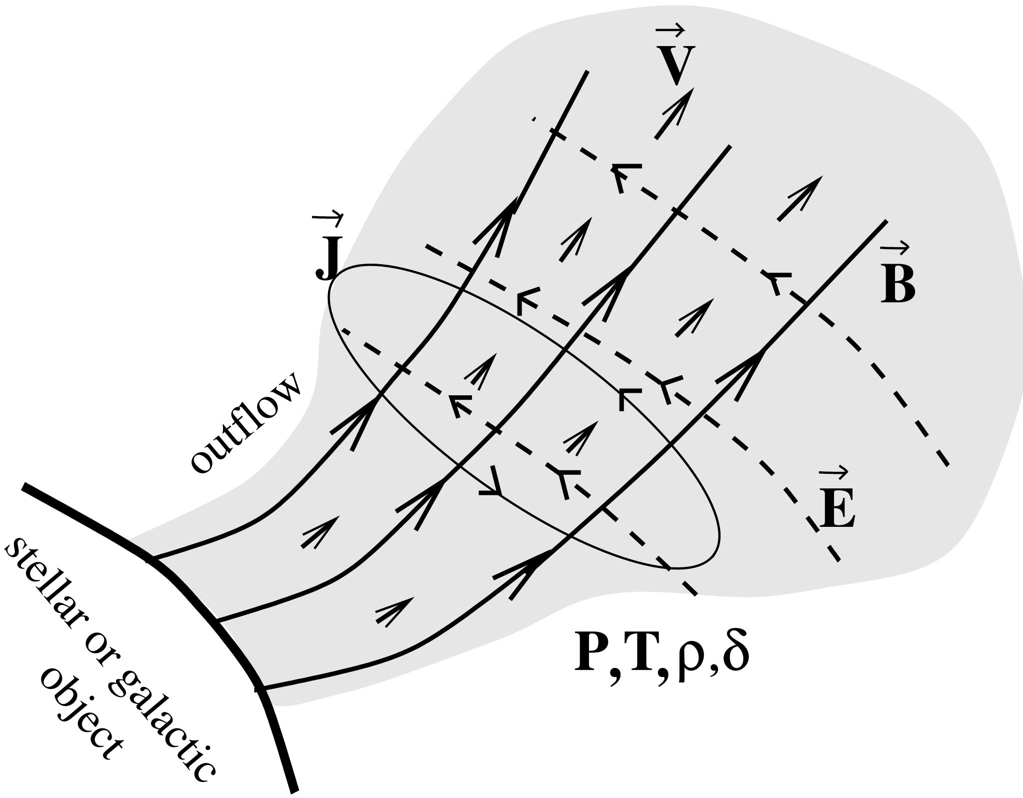

The flow can be relativistic wrt

- bulk velocity $\boldsymbol{V} \approx c$, $\gamma \gg 1$

- random motion in comoving frame $k_{\mathrm{B}}T/m/c^2 \gg 1$, or,
  $P \gg \rho_0 c^2$, where $\rho_0 = \rho/\gamma$ the density in comoving frame
  Define specific enthalpy
  $\xi c^2 = \frac{\mathrm{mass} \times c^2 + \mathrm{internal\ energy} + P \times \mathrm{volume}}{\mathrm{mass}} = c^2 + \frac{1}{\Gamma - 1}\frac{P}{\rho_0} + \frac{P}{\rho_0}$, or,
  $\xi = 1 + \frac{\Gamma}{\Gamma - 1}\frac{P}{\rho_0 c^2} \gg 1$

- gravity $r \sim \mathcal{GM}/c^2$
  Define lapse function $h = \sqrt{1 - \frac{2\mathcal{GM}}{c^2 r}}$

In nonrelativistic flows, γ, ξ, h, all are ≈ 1

- Ohm: $\boldsymbol{E} + \dfrac{\boldsymbol{V}}{c} \times \boldsymbol{B} = 0$

- Maxwell:

$$\nabla \cdot \boldsymbol{B} = 0 = \nabla \times \boldsymbol{E} + \frac{\partial \boldsymbol{B}}{c\partial t}\,,\ \boldsymbol{J} = \frac{c}{4\pi}\nabla \times \boldsymbol{B} - \frac{1}{4\pi}\frac{\partial \boldsymbol{E}}{\partial t}\,,\ \delta = \frac{1}{4\pi}\nabla \cdot \boldsymbol{E}$$

- mass conservation: $\dfrac{\partial(\gamma\rho_0)}{\partial t} + \nabla \cdot (\gamma\rho_0\boldsymbol{V}) = 0$

- momentum:

$$\gamma\rho_0\left(\frac{\partial}{\partial t} + \boldsymbol{V}\cdot\nabla\right)(\xi\gamma\boldsymbol{V}) = -\nabla P + \delta\boldsymbol{E} + \frac{\boldsymbol{J}\times\boldsymbol{B}}{c} - \gamma^2\rho_0\xi\frac{\mathcal{GM}}{r^2}\hat{r}$$

- energy: $\left(\dfrac{\partial}{\partial t} + \boldsymbol{V}\cdot\nabla\right)\left(\dfrac{1}{\Gamma - 1}\dfrac{P}{\rho_0}\right) + P\left(\dfrac{\partial}{\partial t} + \boldsymbol{V}\cdot\nabla\right)\dfrac{1}{\rho_0} = \dfrac{q}{\rho_0}$

On the energy equation

- no heating/cooling (adiabatic):
$$\left(\frac{\partial}{\partial t}+\boldsymbol{V}\cdot\nabla\right)\left(\frac{1}{\Gamma-1}\frac{P}{\rho_0}\right)+P\left(\frac{\partial}{\partial t}+\boldsymbol{V}\cdot\nabla\right)\frac{1}{\rho_0}=0$$
$\Leftrightarrow (\partial/\partial t+\boldsymbol{V}\cdot\nabla)\left(P/\rho_0^{\Gamma}\right)=0$ (entropy conservation)

- with $q\neq 0$ two approaches:
  - polytropic: Give appropriate q such that the energy eq has a similar to the adiabatic form $(\partial/\partial t+\boldsymbol{V}\cdot\nabla)\left(P/\rho_0^{\Gamma_{\rm eff}}\right)=0$ (in steady-state $\frac{q}{\rho_0}=\frac{\Gamma-\Gamma_{\rm eff}}{\Gamma-1}P\boldsymbol{V}\cdot\nabla\frac{1}{\rho_0}$)
  like adiabatic with $\frac{2}{\Gamma_{\rm eff}-1}$ degrees of freedom
  - non-polytropic: ignore the energy equation, use it only a posteriori to find q (after solving for the dynamics)

  In essence, the pressure is also eliminated in this method, by replacing the poloidal momentum eq with $\nabla\times\nabla P=0$ (e.g., in nonrelativistic steady-state, with $\nabla\times\left[-\rho(\boldsymbol{V}\cdot\nabla)\boldsymbol{V}+\boldsymbol{J}\times\boldsymbol{B}/c-\rho\mathcal{G}\mathcal{M}/r^2\right]=0$)

Assumptions

- ideal MHD
  zero resistivity: $0 = \boldsymbol{E}_{\rm co} = \gamma \left(\boldsymbol{E} + \frac{\boldsymbol{V}}{c} \times \boldsymbol{B} \right) - (\gamma - 1) \left(\boldsymbol{E} \cdot \frac{\boldsymbol{V}}{V} \right) \frac{\boldsymbol{V}}{V}$
  $\Leftrightarrow \boldsymbol{E} = -\frac{\boldsymbol{V}}{c} \times \boldsymbol{B}$

- one fluid approximation
  $\boldsymbol{V}_+ \approx \boldsymbol{V}_-$, or, $J \ll \frac{\rho}{m}|e|V$ with $\boldsymbol{J} = n_+ q_+ \boldsymbol{V}_+ + n_- q_- \boldsymbol{V}_-$
  quasi-neutrality $\delta = n_+ q_+ + n_- q_- \ll \frac{\rho}{m}|e|$
  $n_+ \approx n_- \approx \rho / m_p$ for $e^- p$ plasma

- further assume steady-state $\partial / \partial t = 0$

- axisymmetry $\partial / \partial \phi = 0$ in cylindrical $(z\,, \varpi\,, \phi)$ or spherical $(r\,, \theta\,, \phi)$ coordinates

Integrals of motion

From $\nabla \cdot \boldsymbol{B} = 0 \Rightarrow \nabla \cdot \boldsymbol{B}_p = 0$

$$\boldsymbol{B}_p = \frac{\nabla A \times \hat{\phi}}{\varpi}, \text{ or, } \boldsymbol{B}_p = \nabla \times \left(\frac{A\, \hat{\phi}}{\varpi} \right)$$

$$A = \frac{1}{2\pi} \iint \boldsymbol{B}_p \cdot d\boldsymbol{S}$$

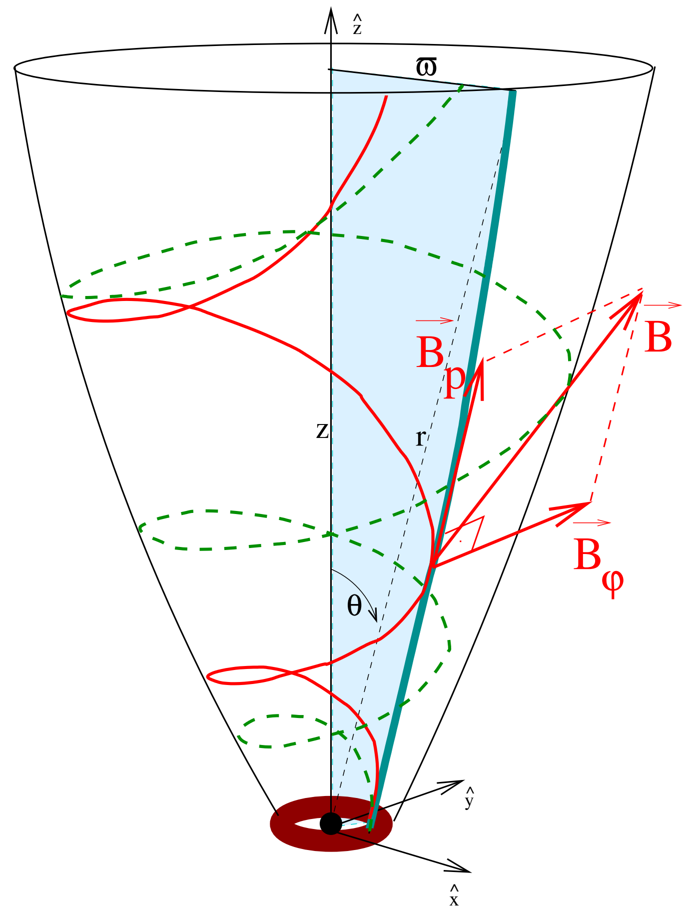

From $\nabla \times \boldsymbol{E} = 0$, $\boldsymbol{E} = -\nabla\Phi$
Because of axisymmetry $E_\phi = 0$.
Combining with Ohm's law
$(\boldsymbol{E} = -\boldsymbol{V} \times \boldsymbol{B}/c)$ we find $\boldsymbol{V}_p \parallel \boldsymbol{B}_p$.

Because $\boldsymbol{V}_p \parallel \boldsymbol{B}_p$ we can write

$$\boldsymbol{V} = \frac{\Psi_A}{4\pi\gamma\rho_0}\boldsymbol{B} + \varpi\Omega\hat{\boldsymbol{\phi}}\,, \quad \frac{\Psi_A}{4\pi\gamma\rho_0} = \frac{V_p}{B_p}\,.$$

$$\left(V_\phi = \frac{B_\phi}{B_p}V_p + \varpi\Omega\right)$$

The Ω and Ψ_A are constants of motion, $\Omega = \Omega(A)$, $\Psi_A = \Psi_A(A)$.

- $\Omega =$ angular velocity at the base
- $\Psi_A =$ mass-to-magnetic flux ratio

The electric field $\boldsymbol{E} = -\boldsymbol{V} \times \boldsymbol{B}/c = -(\varpi\Omega/c)\hat{\boldsymbol{\phi}} \times \boldsymbol{B}_p$ is a poloidal vector, normal to $\boldsymbol{B}_p$. Its magnitude is $E = \frac{\varpi\Omega}{c}B_p$.

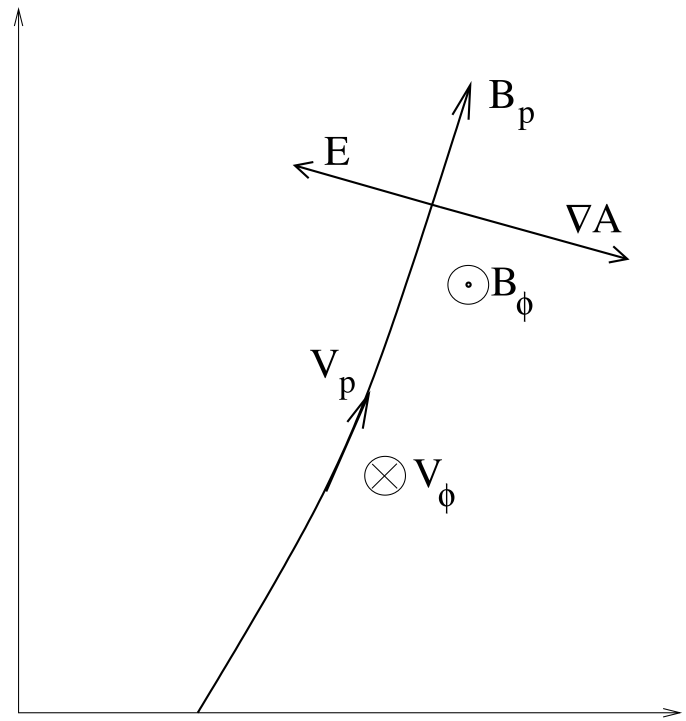

So far, we've used Maxwell's eqs, Ohm's law and the continuity.

The energy and momentum equations remain. The latter:

$$\gamma\rho_0\left(\boldsymbol{V}\cdot\nabla\right)\left(\xi\gamma\boldsymbol{V}\right) = -\nabla P + \delta\boldsymbol{E} + \frac{\boldsymbol{J}\times\boldsymbol{B}}{c} - \gamma^2\rho_0\xi\frac{\mathcal{GM}}{r^2}\hat{r}$$

or,

$$\gamma\rho_0\left(\boldsymbol{V}\cdot\nabla\right)\left(\xi\gamma\boldsymbol{V}\right) = -\nabla P + \frac{(\nabla\cdot\boldsymbol{E})\boldsymbol{E} + (\nabla\times\boldsymbol{B})\times\boldsymbol{B}}{4\pi} - \gamma^2\rho_0\xi\frac{\mathcal{GM}}{r^2}\hat{r}$$

Due to axisymmetry, the toroidal component can be integrated to give the total angular momentum-to-mass flux ratio:

$$\xi\gamma\varpi V_\phi \quad \underbrace{-\frac{\varpi B_\phi}{\Psi_A}}_{\dfrac{-\varpi B_p B_\phi/4\pi}{\rho V_p}} \quad = L(A)$$

For polytropic flows:

- the energy eq gives $P/\rho_0^{\Gamma_{\rm eff}} = Q(A)$
(the effective entropy is a constant of motion).

- the momentum along $\boldsymbol{V}_p$ gives $(h\xi\gamma - 1)c^2 - h\varpi\Omega B_\phi/\Psi_A = \mathcal{E}(A)$
  - In relativistic MHD,

$$h\xi\gamma - h\varpi\Omega B_\phi/\Psi_A c^2 = 1 + \mathcal{E}/c^2 \equiv \mu(A) \text{ = maximum } \gamma$$

  - In nonrelativistic, expansion wrt $(\ldots)/c^2$ gives

$$\frac{V^2}{2} + \frac{\Gamma_{\rm eff}}{\Gamma_{\rm eff}-1}\frac{P}{\rho} - \frac{\mathcal{GM}}{r} \underbrace{-\frac{\varpi\Omega B_\phi}{\Psi_A}}_{\frac{(c/4\pi)E|B_\phi|}{\rho V_p}} = \mathcal{E}(A)$$

Info from integrals (nonrelativistic case)

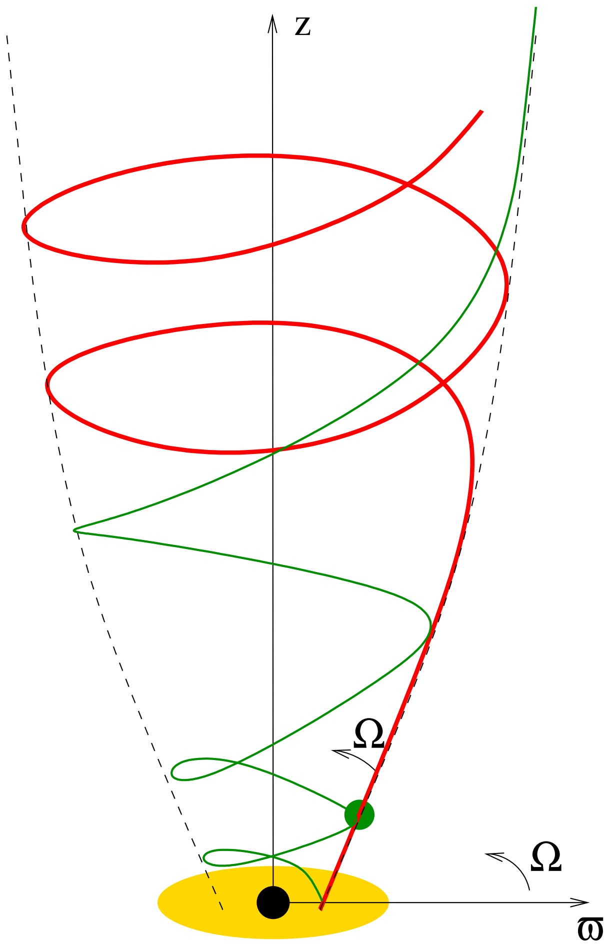

- – near the source,
  $V_\phi = V_p B_\phi / B_p + \varpi \Omega \to V_\phi \approx \varpi \Omega$
  for disk-driven flows $\Omega \approx \Omega_{\rm K}$
  solid-body rotation (rotating wires up to Alfvén surface – $|B_\phi|/B_p$ increases)
  – at large distances
  $\varpi V_\phi - \frac{\varpi B_\phi}{\Psi_A} = L(A) \to V_\phi \sim L/\varpi$
- $A =$const $\to B_p \propto 1/\varpi^2$
  $\rho V_p \propto B_p \to \rho V_p \propto 1/\varpi^2$
- near the source, for Poynting-dominated flows $\mathcal{E} \approx -\varpi \Omega B_{\phi i}/\Psi_A \to B_{\phi i} \approx \frac{-\Psi_A \mathcal{E}}{\varpi_i \Omega}$.
- Alfvén surface: combination of integrals $\to$
  $B_\phi = -\frac{L \Psi_A}{\varpi} \frac{1 - \varpi^2 \Omega / L}{1 - M^2} \to \varpi_A = \sqrt{L/\Omega}$
  ($M = V_p \sqrt{4\pi\rho}/B_p =$ Alfvén Mach)
  $L = \Omega \varpi_A^2$, ϖ_A= lever arm for L-extraction
- maximum asymptotic velocity $V_\infty = \sqrt{2\mathcal{E}} \approx \sqrt{2L\Omega} = \varpi_A \Omega \sqrt{2} = \frac{\varpi_A}{\varpi_i} \sqrt{2} V_{\phi i}$
- $L \approx \varpi_\infty V_{\phi\infty}$, so $V_\infty \approx \sqrt{2 \varpi_\infty V_{\phi\infty} \Omega}$
  (connection between V_∞ , $V_{\phi\infty}$, $\varpi_\infty - \varpi_i$)

The partial integration of the system, the relations between the integrals, and the definition of $M = V_p/(B_p/\sqrt{4\pi\rho})$, yield

$$\boldsymbol{B} = \frac{\nabla A \times \hat{\phi}}{\varpi} - \frac{L\Psi_A}{\varpi}\frac{1-\varpi^2\Omega/L}{1-M^2}\hat{\phi}\,,$$

$$\boldsymbol{V} = \frac{M^2}{\Psi_A}\frac{\nabla A \times \hat{\phi}}{\varpi} + \frac{L}{\varpi}\frac{\varpi^2\Omega/L - M^2}{1-M^2}\hat{\phi}\,,$$

$$\rho = \frac{\Psi_A^2}{4\pi M^2}$$

Thus, we have only two unknowns, the A and M, given by the two poloidal components of the momentum equation

~~M comes from momentum along the flow and A from the transfield~~

these two eqs are coupled!

Poloidal components of the momentum eq

$$\gamma\rho_0 \left(\boldsymbol{V}\cdot\nabla\right)\left(\xi\gamma\boldsymbol{V}\right) = -\nabla P + \frac{(\nabla\cdot\boldsymbol{E})\boldsymbol{E} + (\nabla\times\boldsymbol{B})\times\boldsymbol{B}}{4\pi} \Leftrightarrow$$
$$0 = \boldsymbol{f}_G + \boldsymbol{f}_T + \boldsymbol{f}_C + \boldsymbol{f}_I + \boldsymbol{f}_P + \boldsymbol{f}_E + \boldsymbol{f}_B$$

$$\left.\begin{array}{lll}
\boldsymbol{f}_G = -\gamma\rho_0\xi\left(\boldsymbol{V}\cdot\nabla\gamma\right)\boldsymbol{V} & & \\
\boldsymbol{f}_T = -\gamma^2\rho_0\left(\boldsymbol{V}\cdot\nabla\xi\right)\boldsymbol{V} & : & \text{“temperature” force} \\
\boldsymbol{f}_C = \hat{\boldsymbol{\varpi}}\gamma^2\rho_0\xi V_\phi^2/\varpi & : & \text{centrifugal force} \\
\boldsymbol{f}_I = -\gamma^2\rho_0\xi\left(\boldsymbol{V}\cdot\nabla\right)\boldsymbol{V} - \boldsymbol{f}_C & &
\end{array}\right\} \text{inertial force}$$

$$\begin{array}{lll}
\boldsymbol{f}_P = -\nabla P & : & \text{pressure force} \\
\boldsymbol{f}_E = \left(\nabla\cdot\boldsymbol{E}\right)\boldsymbol{E}/4\pi & : & \text{electric force} \\
\boldsymbol{f}_B = \left(\nabla\times\boldsymbol{B}\right)\times\boldsymbol{B}/4\pi & : & \text{magnetic force}
\end{array}$$

Acceleration mechanisms

- thermal (due to ∇P) $\rightarrow$ velocities up to C_s
- magnetocentrifugal (beads on wire)
  - initial half-opening angle $\vartheta > 30^o$ (only for cold flows)
  - velocities up to $\lesssim \varpi_i \Omega$
  - in reality due to magnetic pressure: the constancy of the integral L gives $f_{C\|} = -\rho V_\phi \partial V_\phi / \partial \ell + (V_\phi / V_p)(B_p / |B_\phi|) f_{B\|}$
- relativistic thermal (thermal fireball) gives $\gamma \sim \xi_i$, where $\xi = \dfrac{\text{enthalpy}}{\text{mass} \times c^2}$.
- magnetic due to $f_{B\|} \propto$ gradient of $\varpi B_\phi \rightarrow$ velocities up to complete matter domination (not always the case)

All acceleration mechanisms can be seen in

$$\frac{V^2}{2} + \frac{\Gamma_{\rm eff}}{\Gamma_{\rm eff} - 1} \frac{P}{\rho} - \frac{\mathcal{GM}}{r} - \frac{\Omega}{\Psi_A} \varpi B_\phi = \mathcal{E} \text{ , or, } \xi\gamma - \frac{\Omega}{\Psi_A c^2} \varpi B_\phi = \mu$$

So $V, \gamma \uparrow$ when $P/\rho_0 \, , \xi \downarrow$ (thermal, relativistic thermal), or, $\varpi |B_\phi| \downarrow$ (magnetocentrifugal, magnetic).

On the magnetic acceleration

$$(\nabla \times \boldsymbol{B}) \times \boldsymbol{B} = \underbrace{(\nabla \times \boldsymbol{B}_p) \times \boldsymbol{B}_p}_{\perp \boldsymbol{B}_p} + \underbrace{(\nabla \times \boldsymbol{B}_p) \times \boldsymbol{B}_\phi}_{0} + \underbrace{(\nabla \times \boldsymbol{B}_\phi) \times \boldsymbol{B}_p}_{\parallel \hat{\phi}} + \underbrace{(\nabla \times \boldsymbol{B}_\phi) \times \boldsymbol{B}_\phi}_{-\frac{B_\phi^2}{\varpi}\hat{\varpi} - \nabla \frac{B_\phi^2}{2} = -\frac{B_\phi}{\varpi}\nabla(\varpi B_\phi)}$$

$$f_{B\parallel} = -\frac{B_\phi}{4\pi\varpi}\frac{\partial}{\partial \ell}(\varpi B_\phi)$$

ϖB_ϕ is related to the poloidal current
$\boldsymbol{J}_p = \frac{c}{4\pi}\nabla \times \boldsymbol{B}_\phi = \frac{1}{2\pi\varpi}\nabla I \times \hat{\phi}$, with
$I = \iint \boldsymbol{J}_p \cdot d\boldsymbol{S} = \frac{c}{2}\varpi B_\phi$

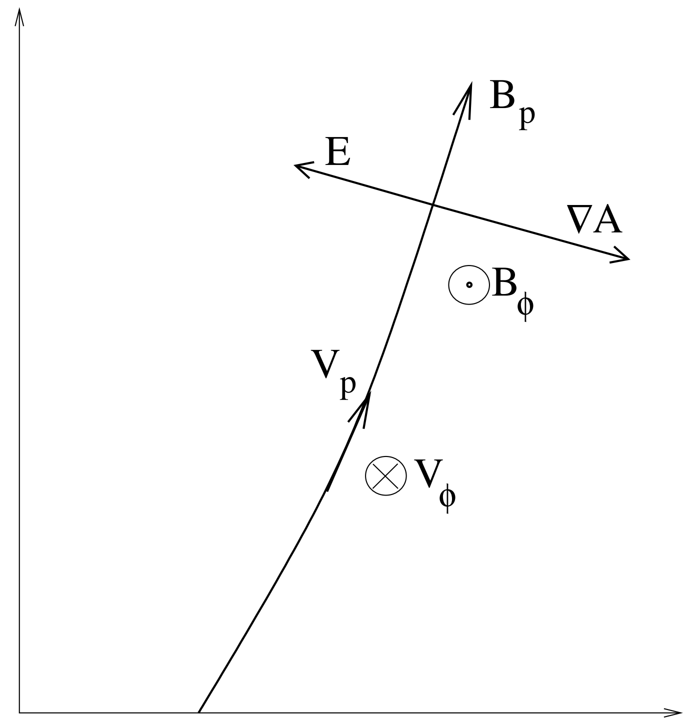

Currents or magnetic fields?

Although in MHD $\boldsymbol{B}$ drive the currents and not the opposite (since $\boldsymbol{J} = ne(\boldsymbol{V}_+ - \boldsymbol{V}_-)$ with $|\boldsymbol{V}_+ - \boldsymbol{V}_-| \ll V$), currents are usefull in understanding acceleration/collimation

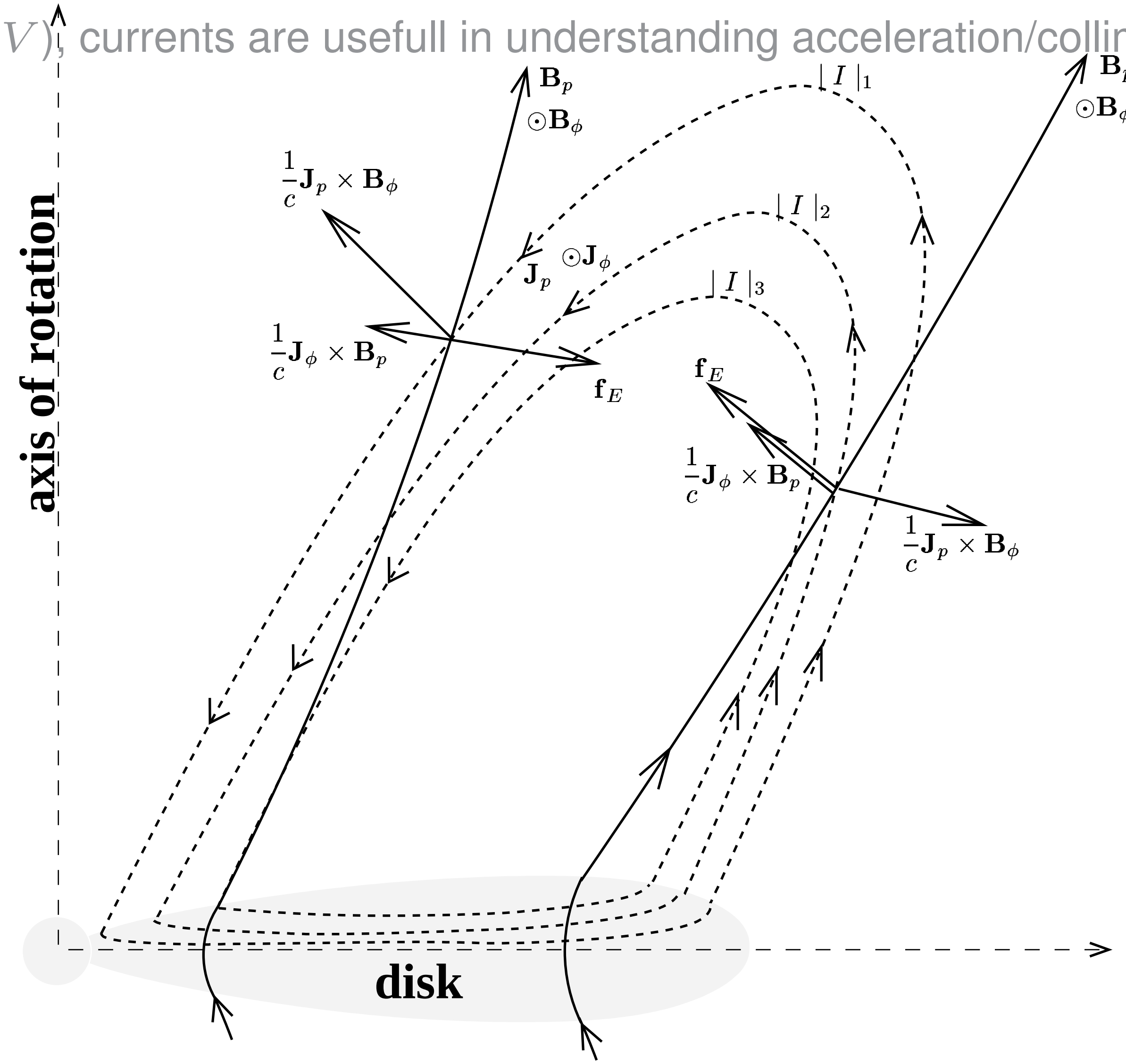

The efficiency of the magnetic acceleration

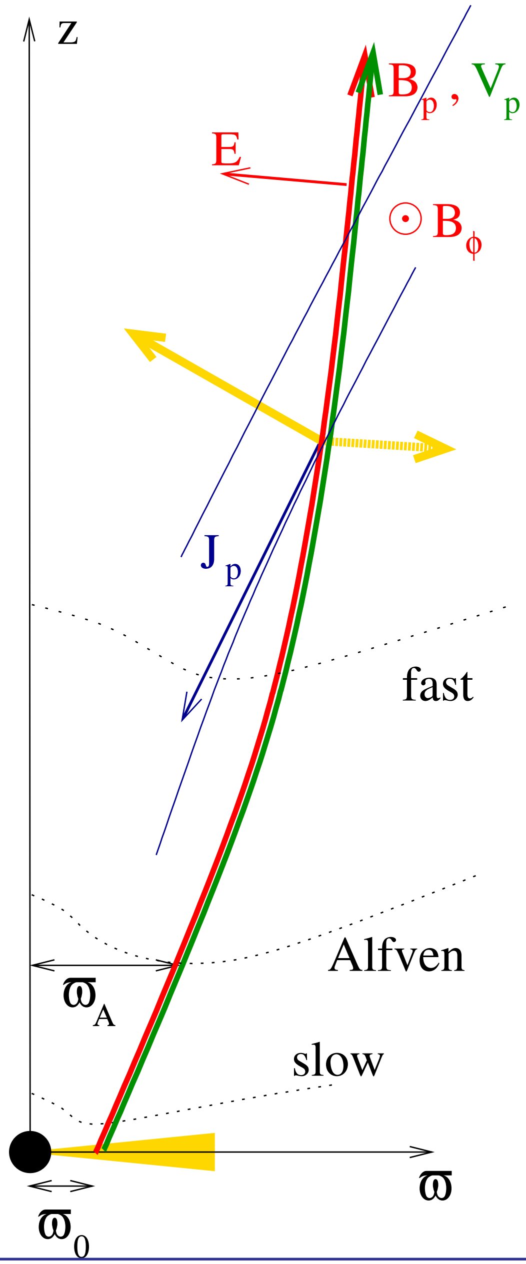

The $\boldsymbol{J}_p \times \boldsymbol{B}_\phi$ force strongly depends on the angle between field-lines and current-lines (for zero angle no acceleration at all)

Are we free to choose these two lines? NO! All MHD quantities are related to each other and should be found by solving the full system of equations.

At classical fast surface $V_p \approx B/\sqrt{4\pi\rho}$,

$$\frac{\text{kinetic}}{\text{Poynting}} = \frac{V_p^2/2}{-\varpi\Omega B_\phi/\Psi_A} \approx \frac{1}{2}\left(1 - \frac{V_\phi}{\varpi\Omega}\right)\frac{B^2}{B_\phi^2} \sim \frac{1}{2}$$

(using $\Psi_A = 4\pi\rho V_p/B_p$ and $V_\phi = \varpi\Omega + V_p B_\phi/B_p$)

For relativistic flows $\gamma_f \approx \mu^{1/3}(\ll \mu)$ and this ratio is $\mu^{-2/3} \ll 1$!

$V_p = (M^2/\Psi_A)B_p$ (from $M^2 = 4\pi\rho V_p^2/B_p^2$ and $\Psi_A = 4\pi\rho V_p/B_p$)

At $M \gg 1$, $\varpi \gg \varpi_{\rm A}$, $-\dfrac{\varpi\Omega B_\phi}{\Psi_A} \approx \dfrac{\Omega^2 B_p \varpi^2}{\Psi_A V_p}$

(from $B_\phi = -\dfrac{L\Psi_A}{\varpi}\dfrac{1-\varpi^2\Omega/L}{1-M^2} \approx -\dfrac{L\Psi_A}{\varpi}\dfrac{\varpi^2\Omega/L}{M^2}$ at large distances)

The $\dfrac{\text{kinetic}}{\text{Poynting}} = 1/2$ at fast gives

$$V_f = \left(\frac{\Omega^2 B_p \varpi^2}{\Psi_A}\right)^{1/3}$$

(The relativistic version is $\gamma_f = \mu^{1/3}$.)

Acceleration continues after the fast (crucial especially for relativistic flows)

Defining the constant of motion

$$\sigma_m = \frac{A\Omega^2}{\Psi_A \mathcal{E} V_\infty} = \frac{A\Omega^2(1+\mathcal{E}/c^2)}{\Psi_A \mathcal{E}^{3/2}\sqrt{2+\mathcal{E}/c^2}}$$

we find (by combining the integral relations)

$$\frac{\text{Poynting}}{\text{total energy flux}} = \sigma_m \left(1 - \frac{V_\phi}{\varpi\Omega}\right) \frac{V_\infty}{V_p} \frac{B_p \varpi^2}{A} \propto \frac{B_p \varpi^2}{A}$$

So, the transfield force-balance determines the acceleration through the "bunching function" $B_p \varpi^2 / A$.

Another ways to see it: Poynting $\propto \varpi B_\phi$ and $B_\phi / B_p \approx E/B_p \approx \varpi\Omega/c$, so Poynting $\propto \varpi^2 B_p$

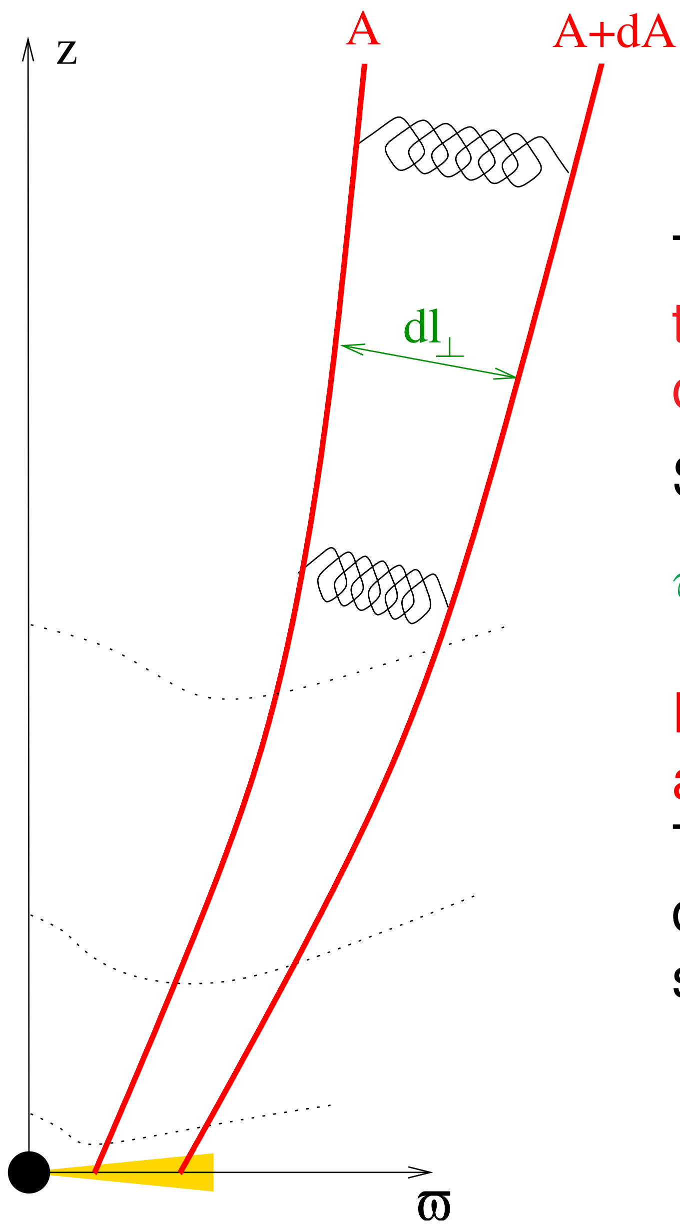

The magnetic field minimizes its energy under the condition of keeping the magentic flux constant.

So, $\varpi B_\phi \downarrow$ for decreasing

$$\varpi^2 B_p = \frac{\varpi^2}{2\pi\varpi dl_\perp}(\underbrace{B_p dS}_{dA}) \propto \frac{\varpi}{dl_\perp}.$$

Expansion with increasing $dl_\perp/\varpi$ leads to acceleration

The expansion ends in a more-or-less uniform distribution $\varpi^2 B_p \approx A$ (in a quasi-monopolar shape).

Conclusions on the magnetic acceleration

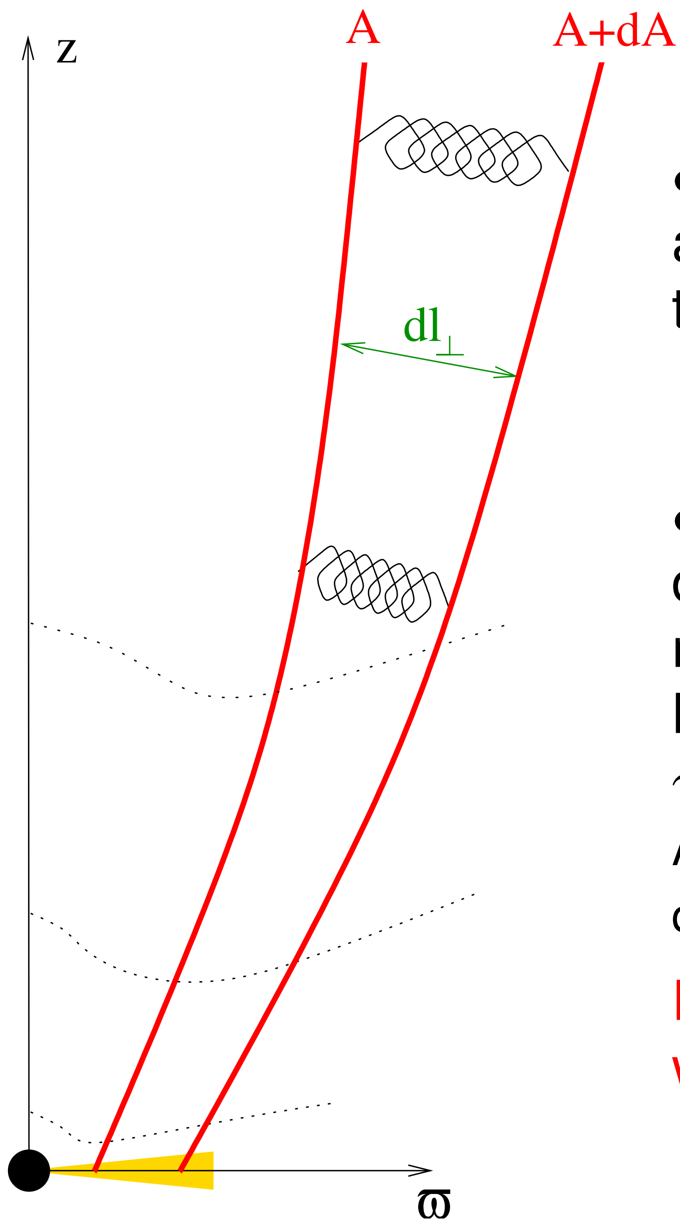

• In nonrelativistic flows efficiency $\sim 1/3$ already at classical fast (increases further – the final value depends on the fieldline shape).

• in relativistic flows: If we start with a uniform distribution the magnetic energy is already minimum $\rightarrow$ no acceleration. Example: Michel's (1969) solution which gives $\gamma_\infty \approx \mu^{1/3} \ll \mu$.

Also Beskin+1998; Bogovalov 2001 who found quasi-monopolar solutions.

For any other (more realistic) field distribution we have efficient acceleration!

The acceleration efficiency in relativistic flows

Applying $$\frac{\text{Poynting}}{\text{total energy flux}} = \sigma_m \left(1 - \frac{V_\phi}{\varpi\Omega}\right) \frac{V_\infty}{V_p} \frac{B_p \varpi^2}{A}$$

at fast, we get $\sigma_m \approx (A/B_p\varpi^2)_{\rm fast}$

Applying the same relation at infinity – where $B_p\varpi^2 \approx A$ – yields (Poynting/total energy flux)$_\infty = \sigma_m$, or, $\dfrac{\mathcal{E} - \gamma_\infty c^2}{\mathcal{E}} = \sigma_m \rightarrow$

$$\boxed{\gamma_\infty \approx \frac{\mathcal{E}}{c^2}(1 - \sigma_m) \approx \frac{\mathcal{E}}{c^2}\left(1 - \frac{A}{(\varpi^2 B_p)_f}\right)}$$

The more bunched the fieldlines near the fast surface the higher the acceleration efficiency.

$I = c\varpi B_\phi/2 \approx -c\varpi E/2 \approx -c\varpi(\varpi\Omega B_p/c)/2 = (A\Omega/2)(\varpi^2 B_p/A)$.
So, $\gamma_\infty \approx (\mathcal{E}/c^2)(1 - A\Omega/2I_f)$

Since the flow is force-free up to the fast, $I_i \approx I_f$ and we connect the acceleration efficiency with conditions at the base of the flow
$\gamma_\infty \approx (\mathcal{E}/c^2)(1 - A\Omega/2I_i)$

On the collimation

hoop-stress:

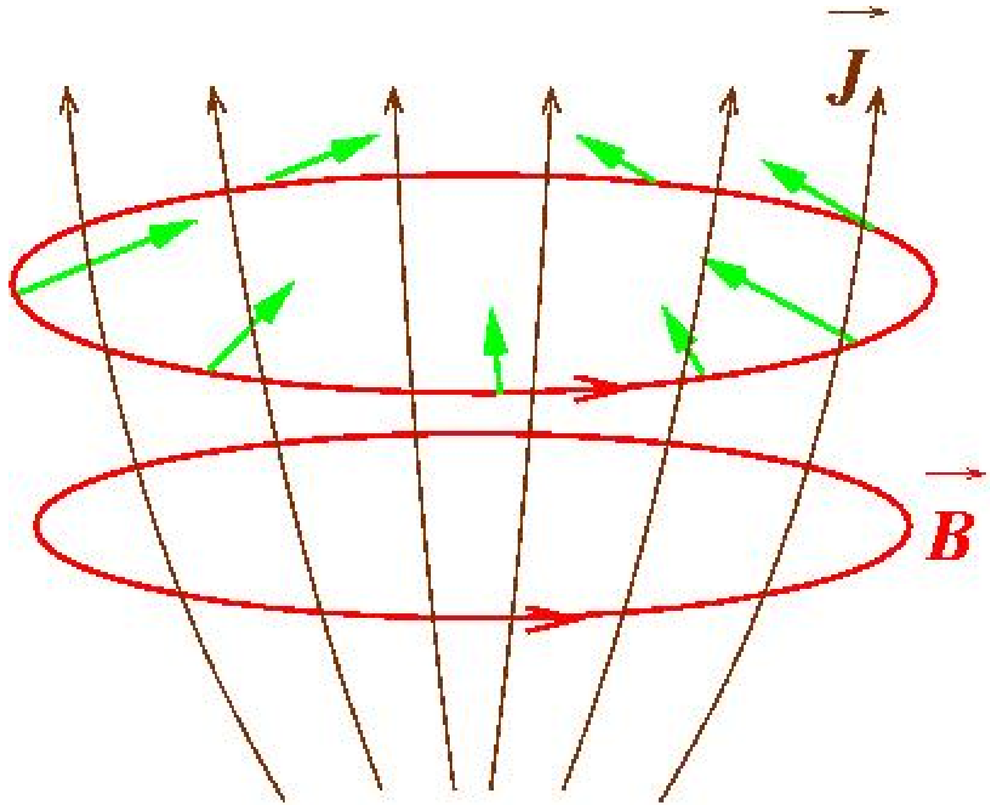

+ electric force

degree of collimation ?   Role of environment?

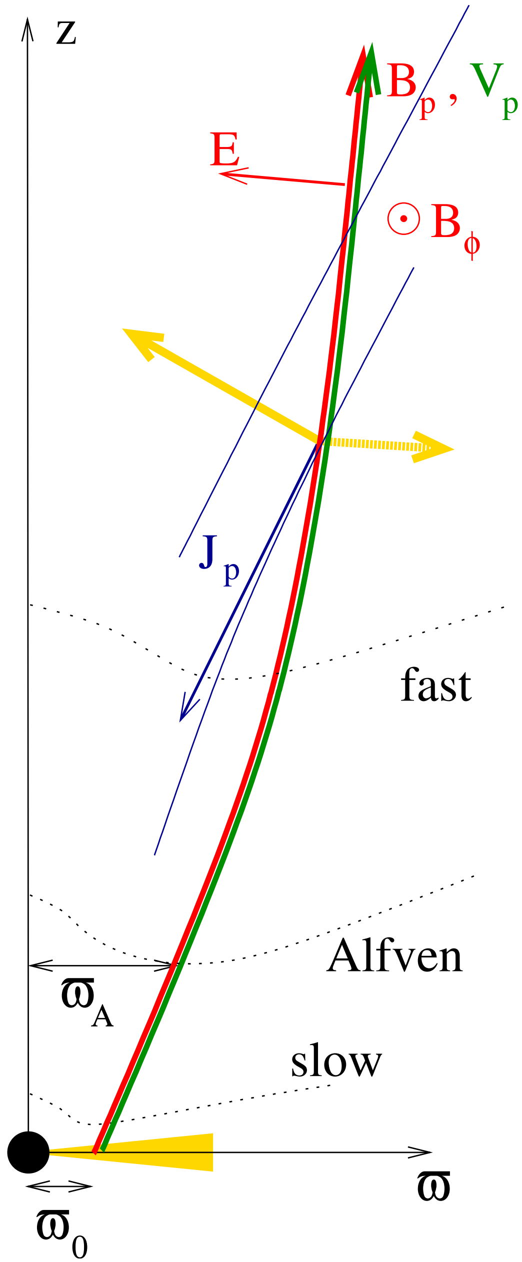

The $\boldsymbol{J}_p \times \boldsymbol{B}_\phi$ force contributes to the collimation (hoop-stress paradigm).
In nonrelativistic flows works fine.
In relativistic flows the electric force plays an opposite role (a manifestation of the high inertia of the flow).

- collimation by an external wind

- self-collimation mainly works at small distances where the velocities are mildly relativistic

- surrounding medium plays a role

some key steps on MHD modeling

- Michel 1969: assuming monopole flow (crucial) $\rightarrow$ inefficient acceleration with $\gamma_\infty \approx \mu^{1/3} \ll \mu$
- Li, Chiueh & Begelman 1992; Contopoulos 1994: cold self-similar model $\rightarrow \gamma_\infty \approx \mu/2$ (50% efficiency)
- Vlahakis & Königl 2003, 2004: generalization of the self-similar model (including thermal and radiation effects) $\rightarrow \gamma_\infty \approx \mu/2$ (50% efficiency)
- Vlahakis 2004: complete asymptotic transfield force-balance connect the flow-shape (collimation) with acceleration explain why Michel's model is inefficient
- Beskin & Nokhrina 2006: parabolic jet with $\gamma_\infty \approx \mu/2$

some key steps (cont'd)

- Komissarov, Barkov, Vlahakis & Königl 2007 and Komissarov, Vlahakis, Königl & Barkov 2009: possible for the first time to simulate high γ MHD flows and follow the acceleration up to the end
  + analytical scalings
  + role of causality, role of external pressure

- Tchekhovskoy, McKinney & Narayan, 2009: simulations of nearly monopolar flow (more detailed than in Komissarov+2009)
  Even for nearly monopolar flow the acceleration is efficient near the rotation axis

some key steps (cont'd)

- Lyubarsky 2009:
  generalization of the analytical results of Vlahakis 2004 and Komissarov+2009
- recent simulations by McKinney, Tchekhovskoy, Blandford, and Tchekhovskoy, McKinney, Narayan
- Contopoulos, The Force-free Magnetosphere of a Rotating Black Hole

"Standard" model for magnetic acceleration

☞ component of the momentum equation

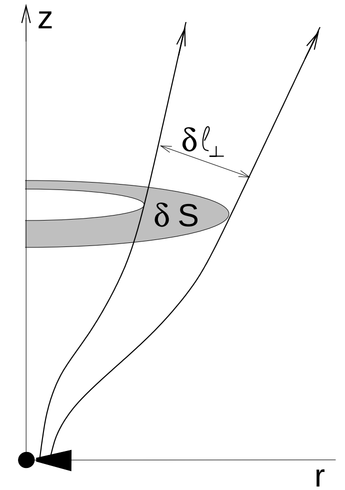

$$\gamma\rho_0(\boldsymbol{V}\cdot\nabla)\,(\gamma\xi\boldsymbol{V}) = -\nabla p + J^0\boldsymbol{E} + \boldsymbol{J}\times\boldsymbol{B}$$

along the flow (wind equation): $\gamma \approx \mu - \mathcal{F}$

where $\mathcal{F} \propto \varpi^2 B_p$

since $B_p \delta S =$ const,

$\mathcal{F} \propto \varpi^2/\delta S \propto \varpi/\delta\ell_\perp$

acceleration requires the separation between streamlines to increase faster than the cylindrical radius

the collimation-acceleration paradigm:
$\mathcal{F}\downarrow$ through stronger collimation of the inner streamlines relative to the outer ones (differential collimation)

☞ transfield component of the momentum equation

$$\frac{\gamma^2 \varpi}{\mathcal{R}} \approx \frac{\left(\frac{2I}{\Omega B_p \varpi^2}\right)^2 \varpi \nabla_\perp \ln \left|\frac{I}{\gamma}\right|}{1 + \frac{4\pi\xi\rho_0 u_p^2}{B_p^2}\frac{\varpi_{\rm lc}^2}{\varpi^2}} - \gamma^2 \frac{\varpi_{\rm lc}^2}{\varpi^2}\nabla_\perp \varpi,$$ with $\nabla_\perp \sim \frac{1}{\varpi}$,

$\varpi_{\rm lc} = \frac{c}{\Omega}$,

simplifies to $$\underbrace{\frac{\gamma^2 \varpi}{\mathcal{R}}}_{inertia} \approx \underbrace{1}_{EM} - \underbrace{\gamma^2 \frac{\varpi_{\rm lc}^2}{\varpi^2}}_{centrifugal}$$

- if centrifugal negligible then $\gamma \approx z/\varpi$ (since $\mathcal{R}^{-1} \approx -\frac{d^2\varpi}{dz^2} \approx \frac{\varpi}{z^2}$) power-law acceleration regime (for parabolic shapes $z \propto \varpi^a$, γ is a power of ϖ)
- if inetria negligible then $\gamma \approx \varpi/\varpi_{\rm lc}$ linear acceleration regime
- if electromagnetic negligible then ballistic regime

☞ role of external pressure

$p_{\rm ext} = B_{\rm co}^2/8\pi \simeq (B^{\hat\phi})^2/8\pi\gamma^2 \propto 1/\varpi^2\gamma^2$

Assuming $p_{\rm ext} \propto z^{-\alpha_p}$ we find $\gamma^2 \propto z^{\alpha_p}/\varpi^2$.

Combining with the transfield $\frac{\gamma^2\varpi}{\mathcal{R}} \approx 1 - \gamma^2\frac{\varpi_{\rm lc}^2}{\varpi^2}$ we find the funnel shape (we find the exponent a in $z \propto \varpi^a$).

- if the pressure drops slower than z^{-2} then
  - ⋆ shape more collimated than $z \propto \varpi^2$
  - ⋆ linear acceleration $\gamma \propto \varpi$
- if the pressure drops as z^{-2} then
  - ⋆ parabolic shape $z \propto \varpi^a$ with $1 < a \leq 2$
  - ⋆ first $\gamma \propto \varpi$ and then power-law acceleration $\gamma \sim z/\varpi \propto \varpi^{a-1}$
- if pressure drops faster than z^{-2} then
  - ⋆ conical shape
  - ⋆ linear acceleration $\gamma \propto \varpi$ (small efficiency)

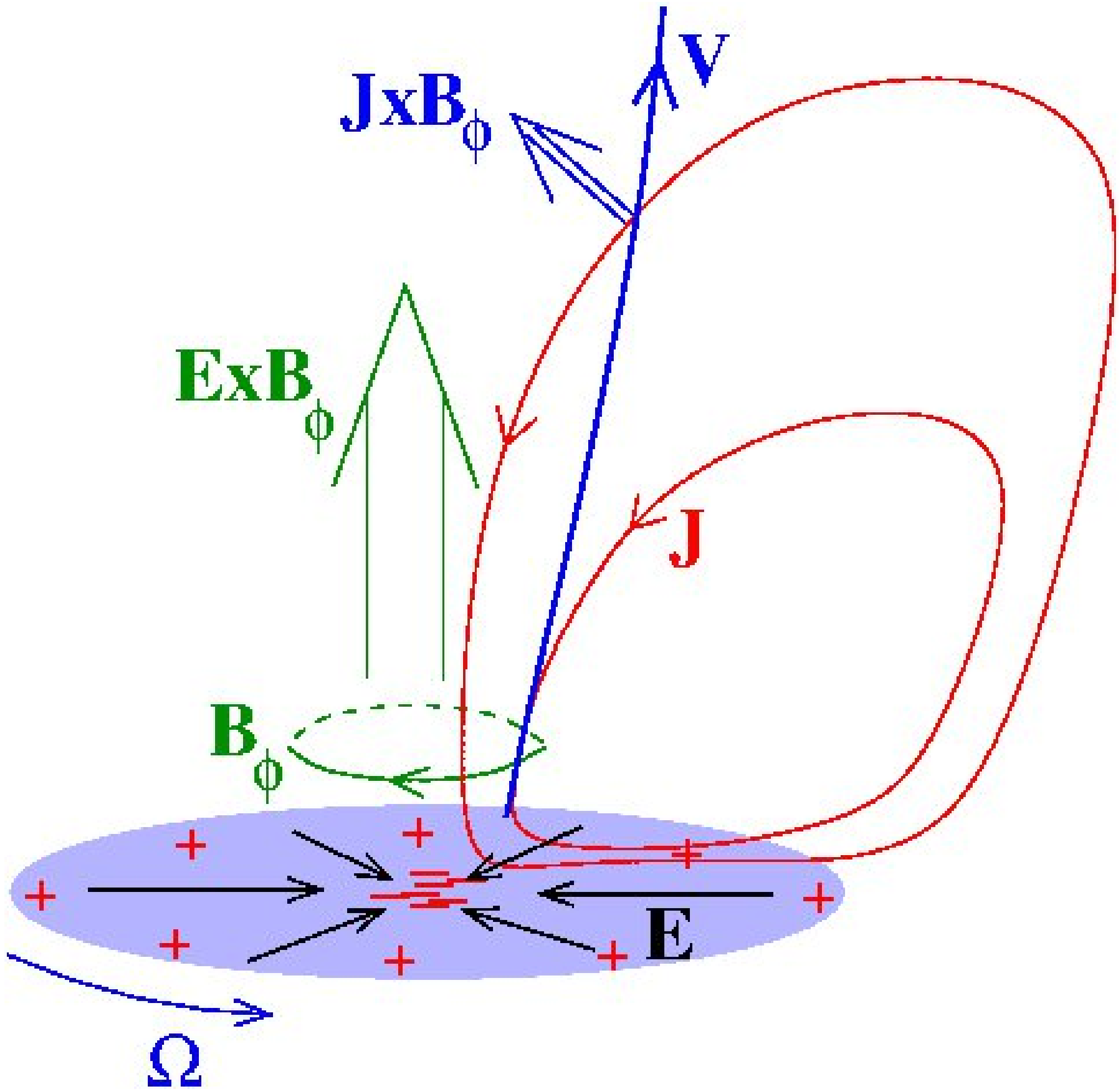

V
JxB$_\phi$
ExB$_\phi$
J
B$_\phi$
E
Ω

Asymptotic flow-shape

From
$$\frac{\text{Poynting}}{\text{total energy flux}} = \sigma_m \left(1 - \frac{V_\phi}{\varpi\Omega}\right) \frac{V_\infty}{V_p} \frac{B_p \varpi^2}{A}$$
we find
$$\sigma_m \left(1 - \frac{V_\phi}{\varpi\Omega}\right) \frac{B_p \varpi^2}{A} = \frac{V_p}{V_\infty} \frac{\text{Poynting}}{\text{total energy flux}} < 1\,.$$
For $V_\phi \ll \varpi\Omega$, this gives $B_p \varpi^2 / A < 1/\sigma_m$ (same as in Heyvaerts & Norman asymptotic analysis).

Assume two lines that cross a given cylinder $\varpi =$const, one reference line A_i and another A that crosses the cylinder at higher z (so $A < A_i$).

The $\hat{\varpi}$ component of $\boldsymbol{B}_p = \nabla A \times \hat{\phi}/\varpi$ is $B_\varpi = -(1/\varpi)\partial A/\partial z$, or, $\partial z/\partial A = -1/(\varpi B_\varpi)$ and can be integrated along the cylinder to give $z(A,\varpi) = z(A_i,\varpi) + \int_A^{A_i} dA/(\varpi B_\varpi)$.

But, $B_\varpi < B_p < A/(\varpi^2 \sigma_m)$, and thus,

$$z(A,\varpi) > z(A_i,\varpi) + \varpi \int_A^{A_i} \frac{\sigma_m}{A} dA$$

lines cannot bend towards equator, they are situtated above some minimal cone

From
$$\frac{\text{Poynting}}{\text{total energy flux}} = \sigma_m \left(1 - \frac{V_\phi}{\varpi \Omega}\right) \frac{V_\infty}{V_p} \frac{B_p \varpi^2}{A}$$
with Poynting $= -\varpi \Omega B_\phi / \Psi_A = -2I\Omega/(c\Psi_A)$ and $B_p/V_p = 4\pi\rho/\Psi_A$ we find

$$\frac{I}{\gamma} = -2\pi c \frac{\Omega}{\Psi_A} \rho_0 \varpi^2$$

- if $\rho_0 \varpi^2 \stackrel{\varpi \to \infty}{\longrightarrow} f(A)$ (conical lines $z/\varpi \stackrel{\varpi \to \infty}{\longrightarrow}$const) then
  $I_\infty(A)/\gamma_\infty(A) =$const
  this constant is independent of A, from

$$\frac{\gamma^2 \varpi}{\mathcal{R}} \approx \left[\frac{\left(\frac{2I}{\Omega B_p \varpi^2}\right)^2 \varpi \nabla \ln \left|\frac{I}{\gamma}\right|}{1 + \frac{4\pi\rho\gamma^2 V_p^2}{B_p^2} \frac{\varpi_{lc}^2}{\varpi^2}} - \gamma^2 \frac{\varpi_{lc}^2}{\varpi^2} \hat{\varpi} \right] \cdot \frac{\nabla A}{|\nabla A|} \text{ with } \mathcal{R}/\varpi \stackrel{\varpi \to \infty}{\longrightarrow} \infty$$

- if $\rho_0 \varpi^2 \stackrel{\varpi \to \infty}{\longrightarrow} 0$ (parabolic lines $z/\varpi \stackrel{\varpi \to \infty}{\longrightarrow} \infty$) then $I_\infty/\gamma_\infty = 0$
  (100% acceleration efficiency)

$I_\infty(A)/\gamma_\infty(A) =$const: solvability condition at infinity

(Heyvaerts & Norman 1989; Chiueh, Li, & Begelman 19991; see also Vlahakis 2004 for generalized analysis)

- nonrelativistic case: $I_\infty(A) =$const
  - no current $\boldsymbol{J}_p$ flows between lines
  - If the flow carries some finite Poynitng flux at infinity, the corresponding $\boldsymbol{J}_p$ flows inside a cylindrical core (this is the only way to have I smoothly varying from zero on the axis to I_∞ at the edge of the core).
  - Note that for cylindrical lines the previous analysis (based on $\varpi \to \infty$) doesn't hold.

- relativistic case:
  again the cylindrical core is the only way to have $I_\infty(A=0)=0$ and $I_\infty(A)/\gamma_\infty(A) =$const $\neq 0$ at larger A

Self-similarity

- simple 1-D models (e.g., Weber & Davis, or sperically summetric, monopole-like) cannot describe jets
- giving the flow-shape and solve for velocity is incomplete (solving the transfield is crucial for the acceleration)
- self-similarity: 1-D from mathematical point of view (ODEs), 2-D from physical
  we need an algorithm to produce all lines from a reference one
  Example: $A = r^x f(\theta)$:
  If a line A starts from r_0 at $\theta = \pi/2$, then $A = r_0^x f(\pi/2)$ and so,
  $r = r_0 \left[f(\pi/2)/f(\theta) \right]^{1/x}$.
  If we know one line – we know $f(\theta)$ – from the eq above we find all other lines.
  choose a coordinate system on the poloidal plane
  give the dependence on the one coordinate
  solve for the dependence on the other

r self-similarity

This model corresponds to boundary conditions at a cone $\theta = \theta_i$:
$V_r = D_1 r^{-1/2}$, $V_\theta = D_2 r^{-1/2}$, $V_\phi = D_3 r^{-1/2}$, $\rho = D_4 r^{2x-3}$, $P = D_5 r^{2x-4}$, $B_\phi = D_6 r^{x-2}$, $B_r = D_7 r^{x-2}$.

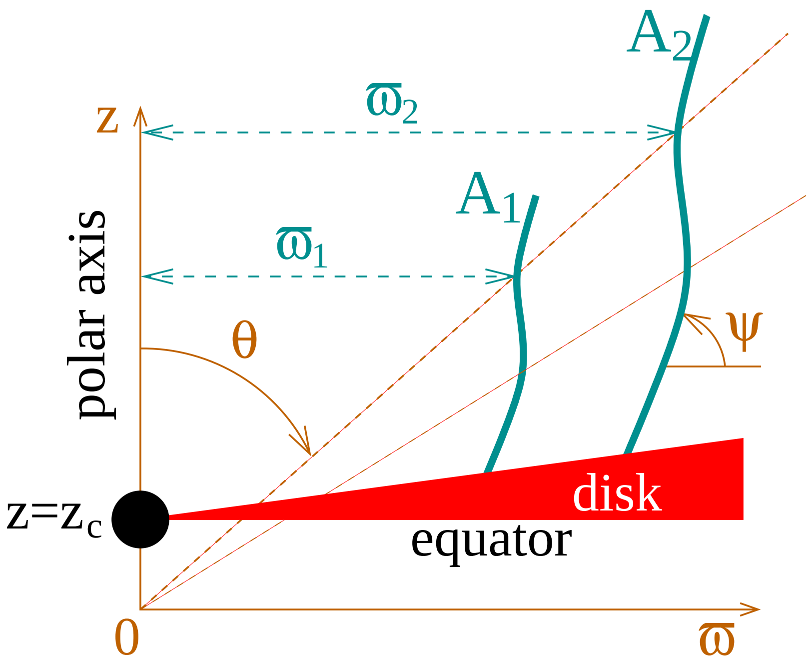

self-similar ansatz $r = \mathcal{F}_1(A)\,\mathcal{F}_2(\theta)$

For points on the same cone $\theta = const$,
$$\frac{\varpi_1}{\varpi_2} = \frac{r_1}{r_2} = \frac{\mathcal{F}_1(A_1)}{\mathcal{F}_1(A_2)}.$$

ODEs
$$\left\{ \begin{array}{l} \psi = \psi(G\,,M\,,\theta)\,, \text{(Bernoulli)} \\ \dfrac{dG}{d\theta} = \mathcal{N}_0(G\,,M\,,\psi\,,\theta)\,, \text{(definition of } \psi) \\ \dfrac{dM}{d\theta} = \dfrac{\mathcal{N}(G\,,M\,,\psi\,,\theta)}{\mathcal{D}(G\,,M\,,\psi\,,\theta)}\,, \text{(transfield)} \end{array} \right\}$$

$\mathcal{D} = 0$: singular points
(Alfvén, modified slow - fast)

conical Alfvén surface

caveats: singular at $A = 0$, absence of scale (need to give $A_{\rm in}$, $A_{\rm out}$)

Vlahakis+2000

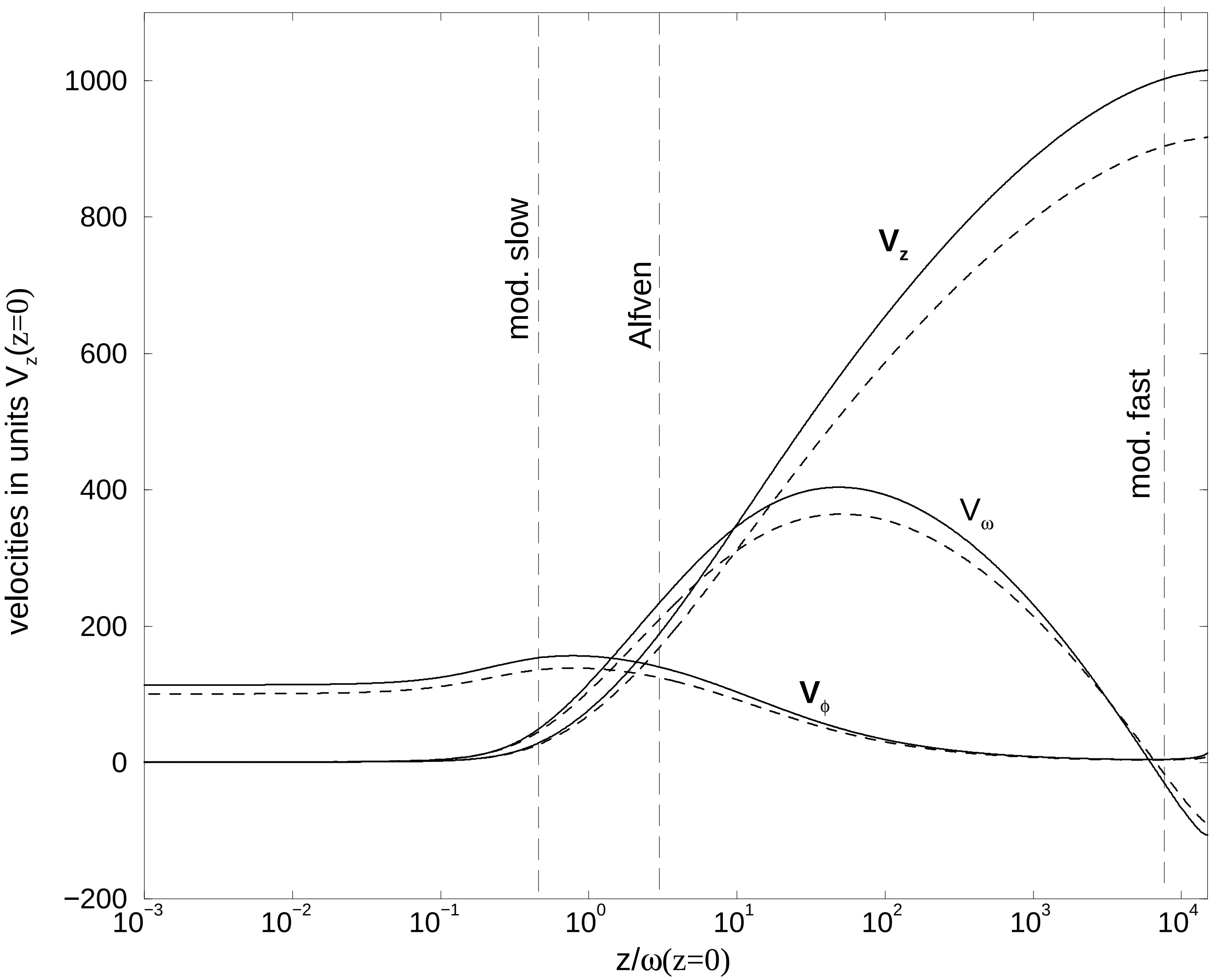

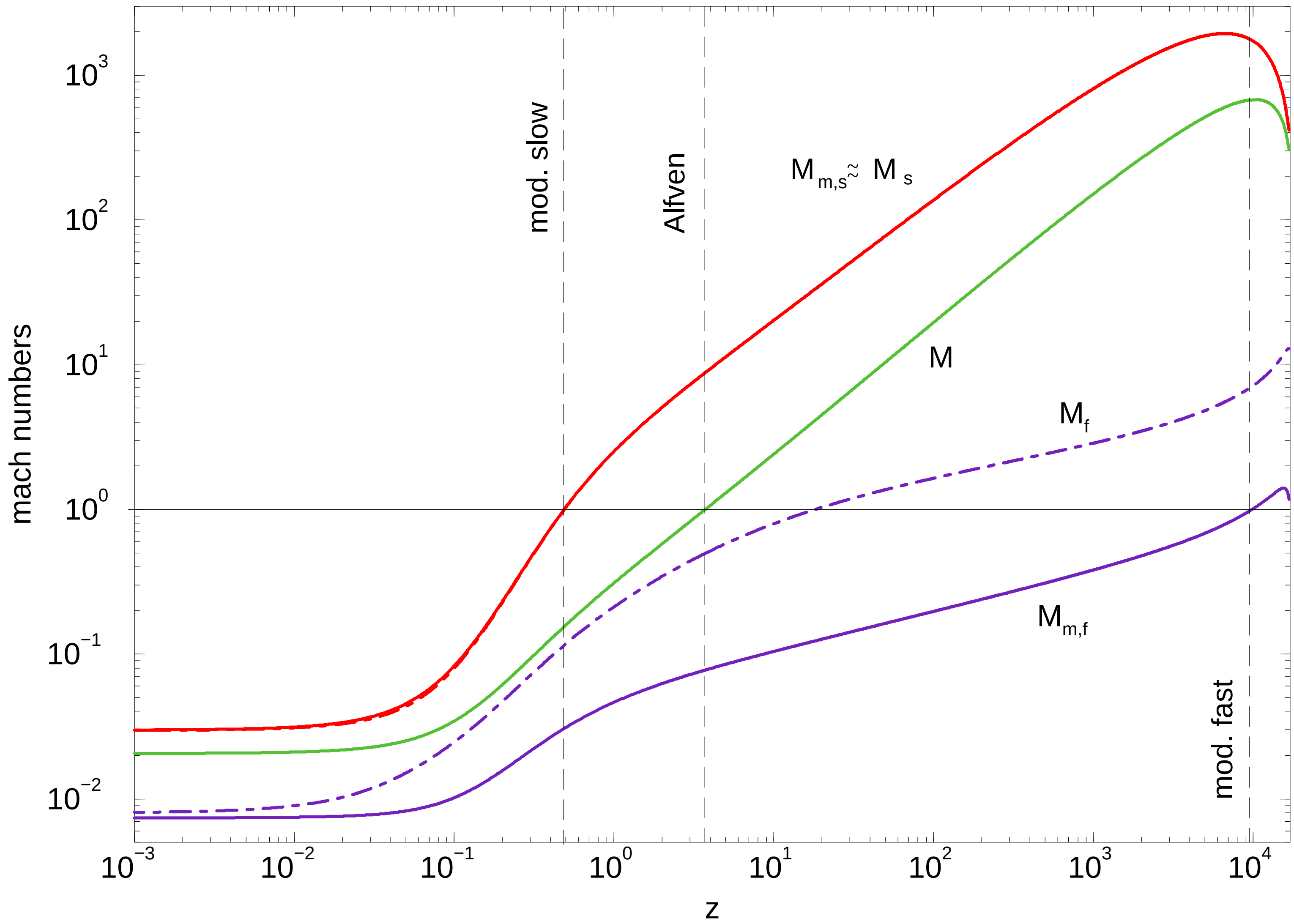
mach numbers
z
mod. slow
Alfven
mod. fast
$M_{m,s} \approx M_s$
M
M_f
$M_{m,f}$
10^3
10^2
10^1
10^0
10^{-1}
10^{-2}
10^{-3}
10^4

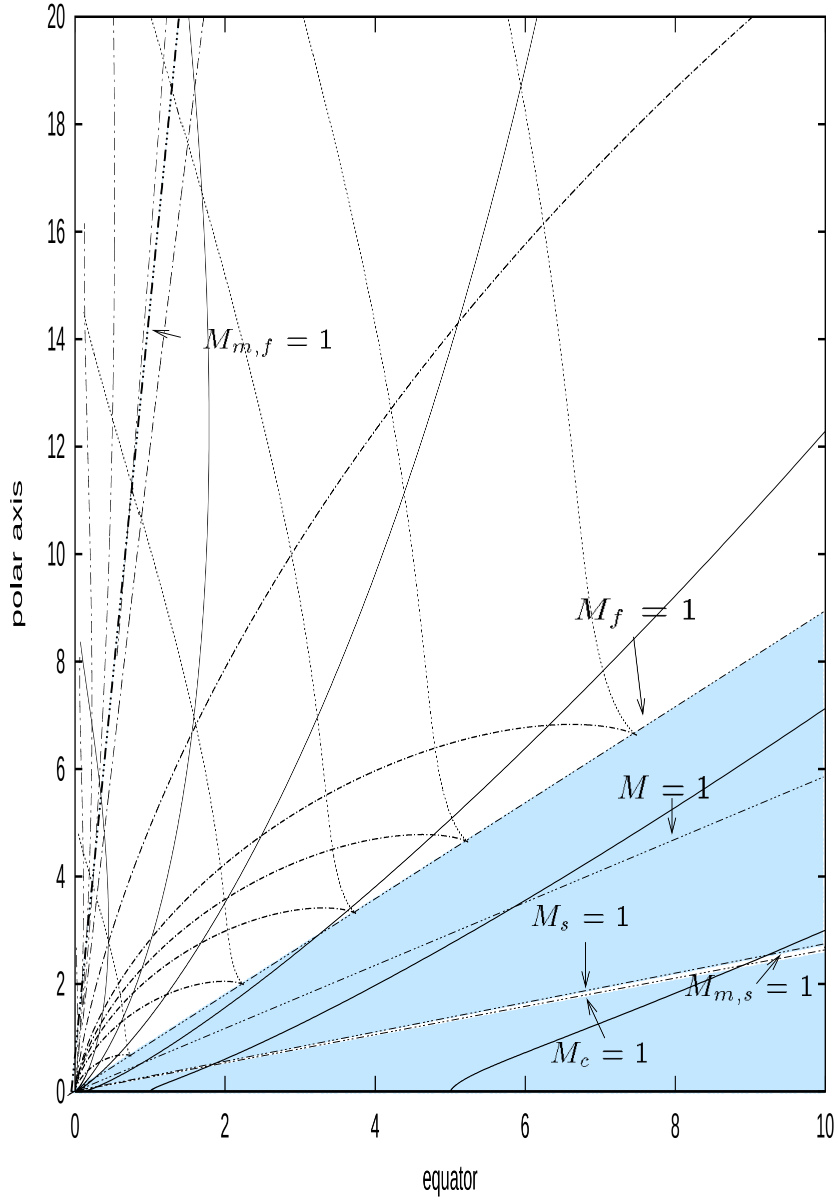

$M_{m,f} = 1$
$M_f = 1$
$M = 1$
$M_s = 1$
$M_{m,s} = 1$
$M_c = 1$
polar axis
equator

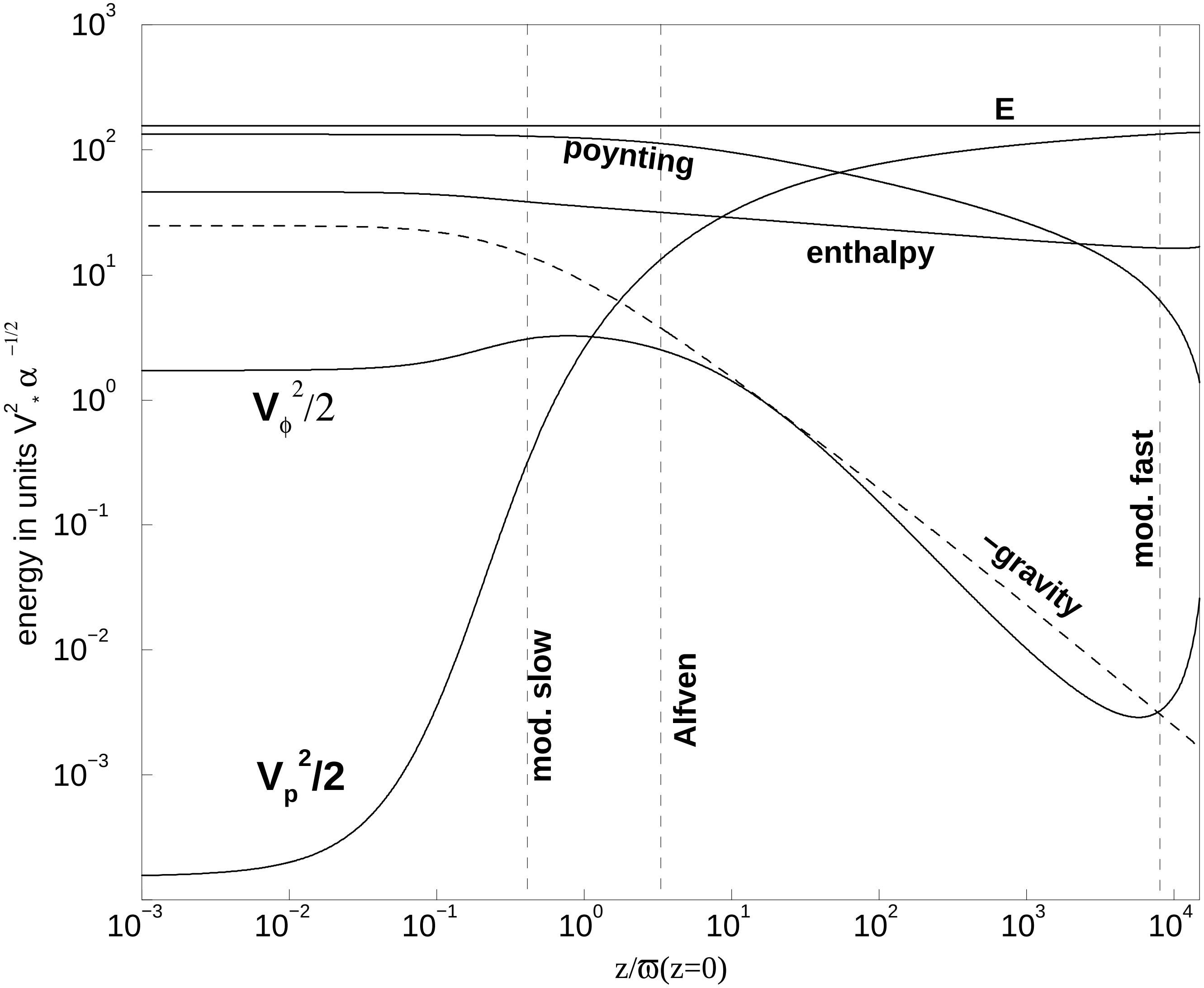
E
poynting
enthalpy
$V_\phi{}^2/2$
$V_p{}^2/2$
mod. slow
Alfven
−gravity
mod. fast
energy in units $V_*^2\,\alpha^{-1/2}$
$z/\varpi(z=0)$
10^{-3}
10^{-2}
10^{-1}
10^{0}
10^{1}
10^{2}
10^{3}
10^{4}

AGN jets (Vlahakis & Königl 2004)

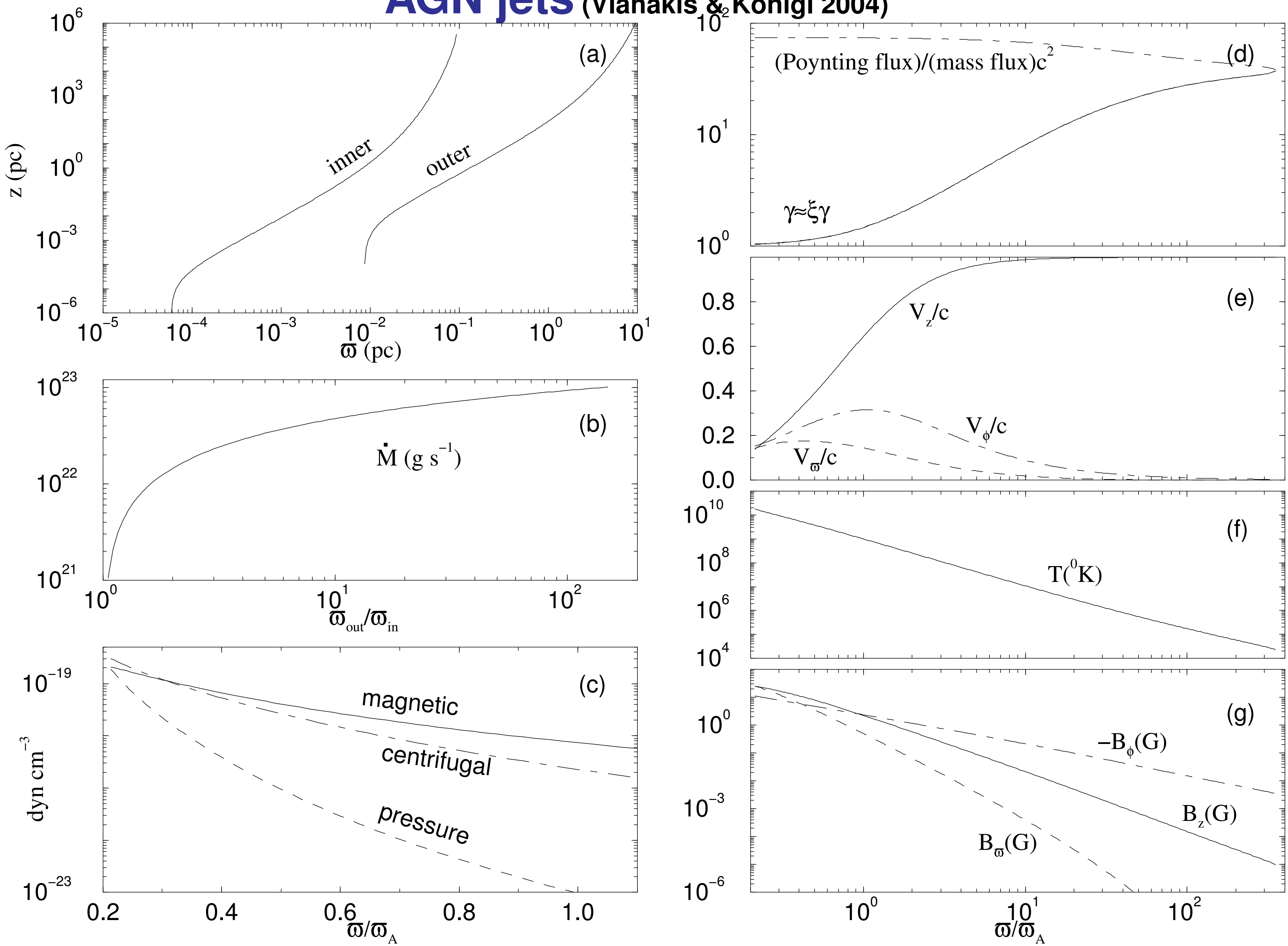

GRB Jets (NV & Königl 2001, 2003a,b)

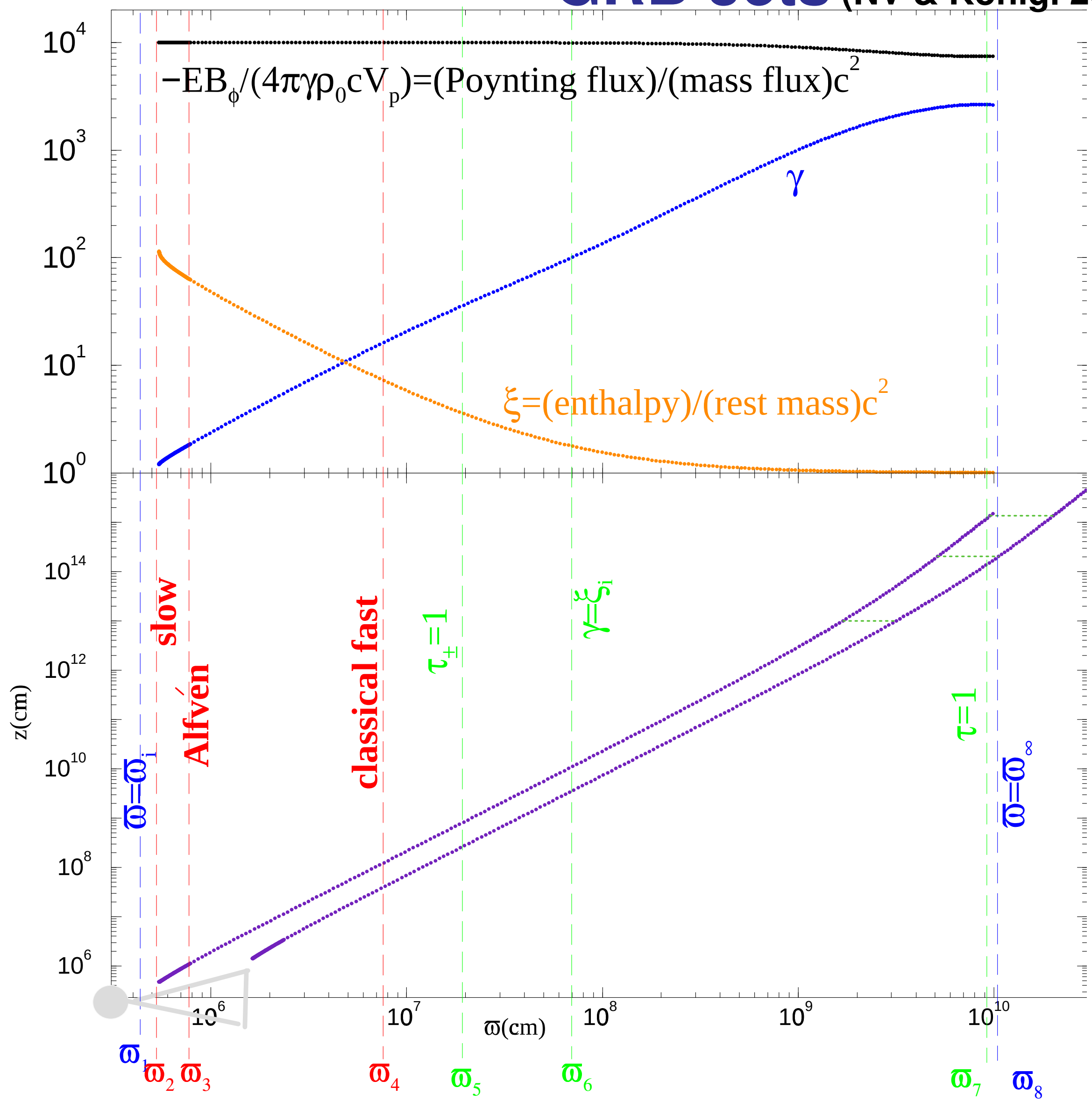

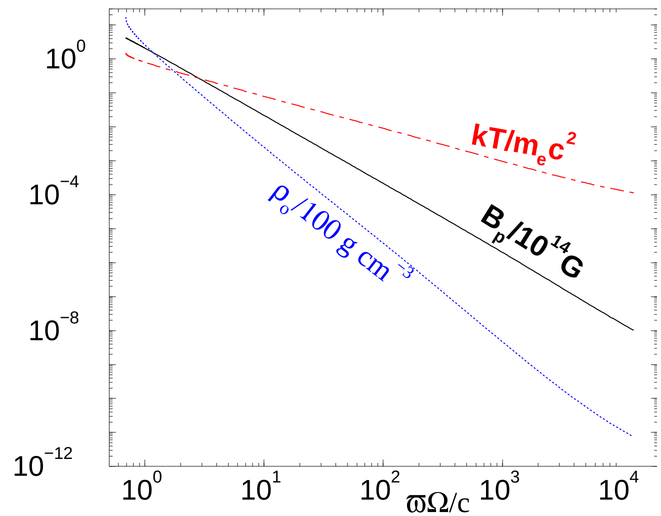

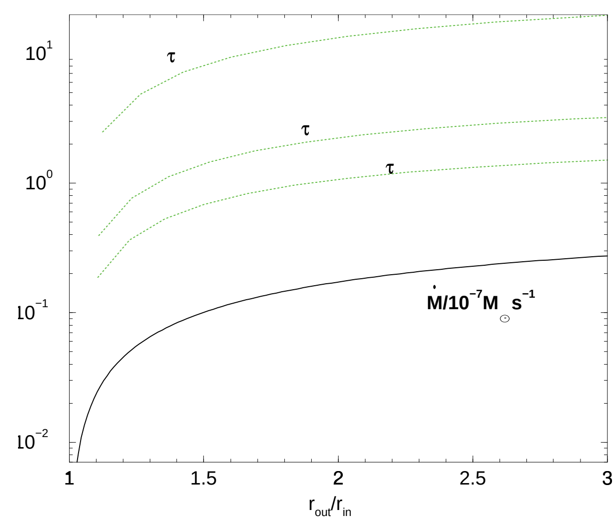

- $\varpi_1 < \varpi < \varpi_6$: Thermal acceleration - force free magnetic field
  ($\gamma \propto \varpi$, $\rho_0 \propto \varpi^{-3}$, $T \propto \varpi^{-1}$, $\varpi B_\phi = const$, parabolic shape of fieldlines: $z \propto \varpi^2$)
- $\varpi_6 < \varpi < \varpi_8$: Magnetic acceleration ($\gamma \propto \varpi$, $\rho_0 \propto \varpi^{-3}$)
- $\varpi = \varpi_8$: cylindrical regime - equipartition $\gamma_\infty \approx (-EB_\phi/4\pi\gamma\rho_0 V_p)_\infty$

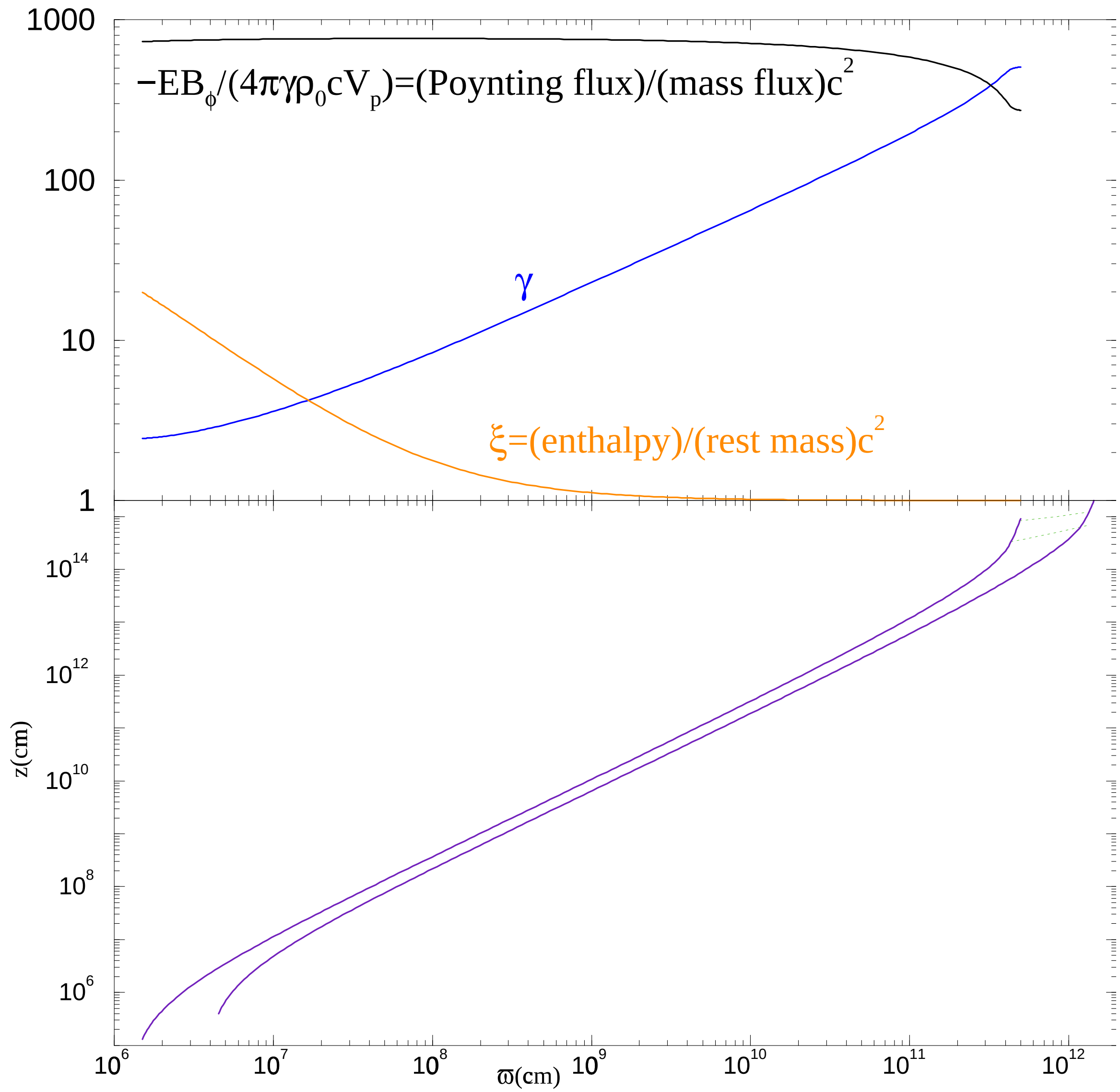

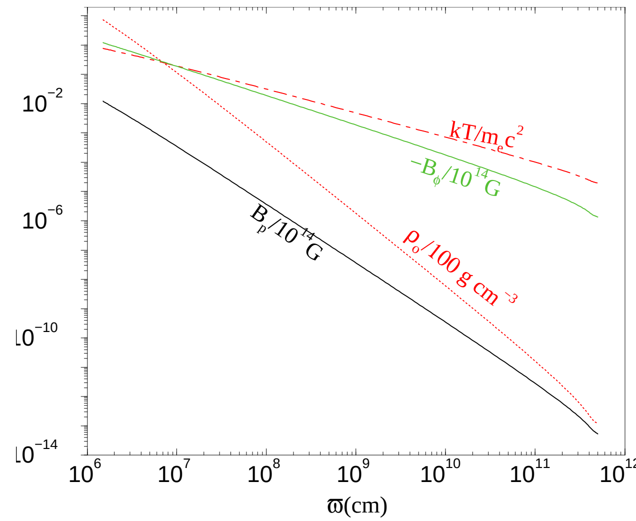

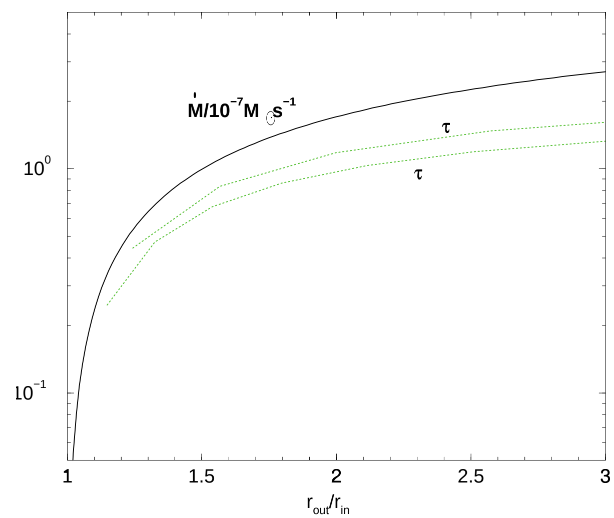

- Thermal acceleration ($\gamma \propto \varpi^{0.44}$, $\rho_0 \propto \varpi^{-2.4}$, $T \propto \varpi^{-0.8}$, $B_\phi \propto \varpi^{-1}$, $z \propto \varpi^{1.5}$)
- Magnetic acceleration ($\gamma \propto \varpi^{0.44}$, $\rho_0 \propto \varpi^{-2.4}$)
- cylindrical regime - equipartition $\gamma_\infty \approx (-EB_\phi/4\pi\gamma\rho_0 V_p)_\infty$

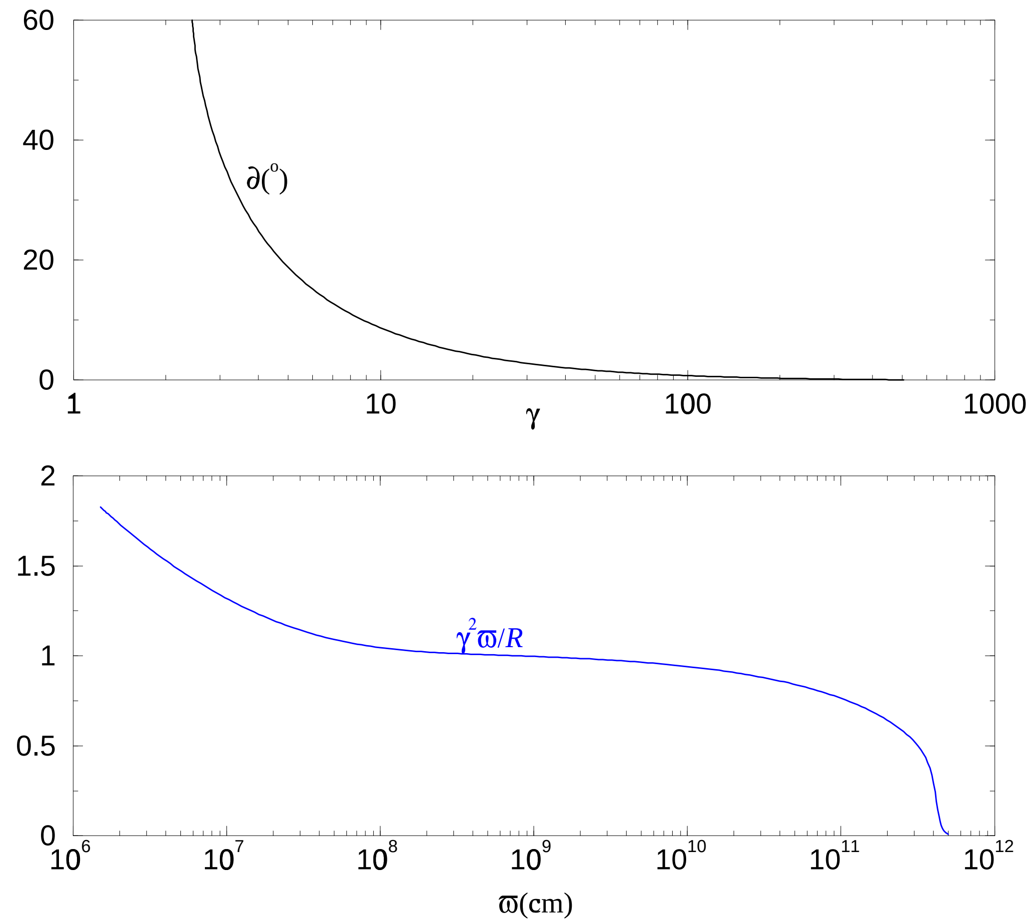

⋆ At $\varpi = 10^8$cm – where $\gamma = 10$ – the opening half-angle is already $\vartheta = 10^o$

⋆ For $\varpi > 10^8$cm, collimation continues slowly ($\mathcal{R} \sim \gamma^2 \varpi$)

Fendt & Ouyed (2004)

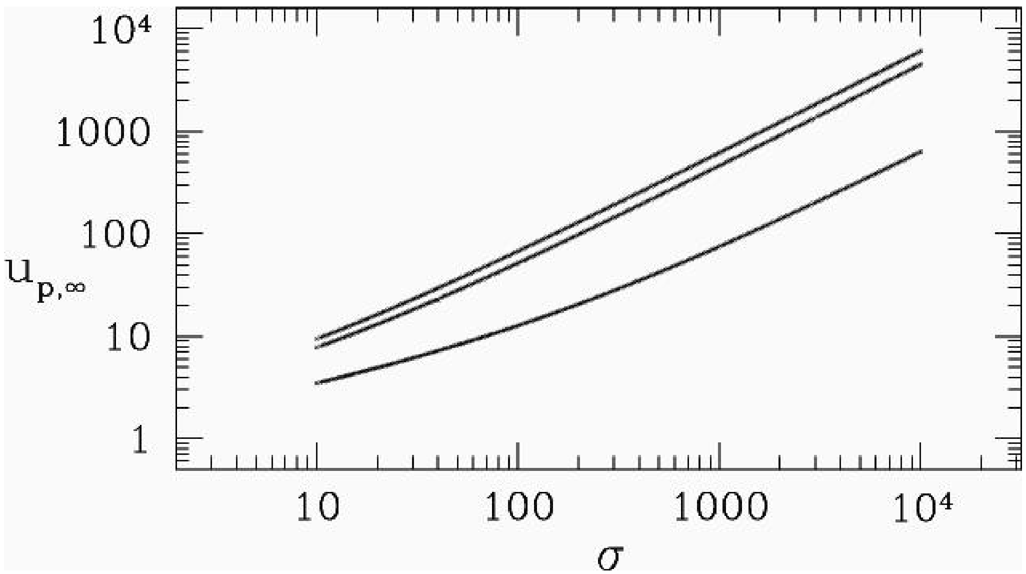

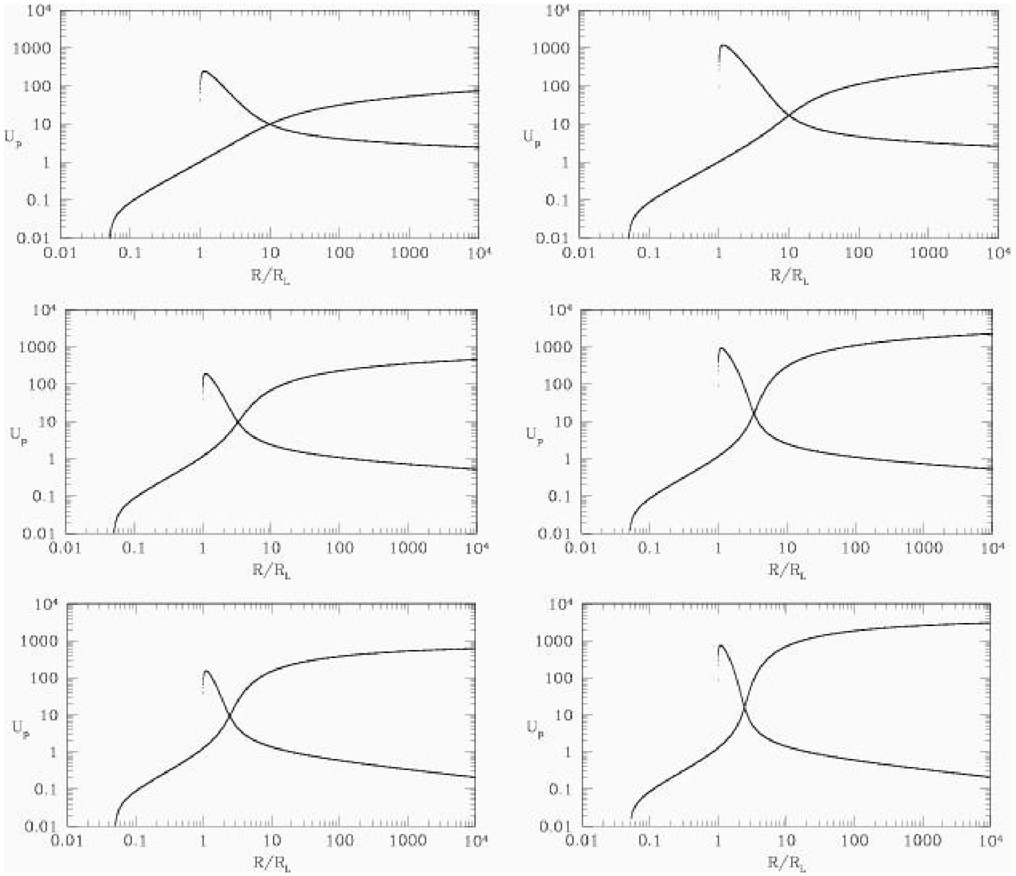

They used prescribed fieldlines (with $\varpi^2 B_p/A \propto \varpi^{-q}$) and found efficient acceleration with γ_∞ (their $u_{p,\infty}$) $\sim \mu$ (their σ).

Although the analysis is not complete (the transfield is not solved), the results show the relation between line-shape and efficiency.

Beskin & Nokhrina (2006)

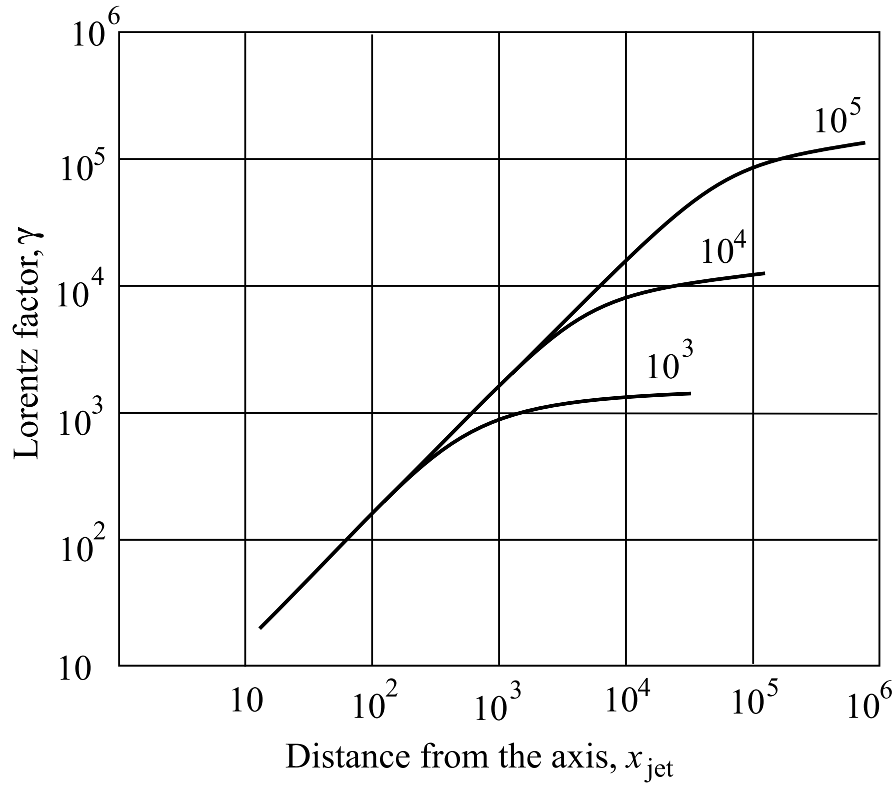

By expanding the equations wrt $2/\mu$ (their $1/\sigma$) they found a parabolic solution. The acceleration in the superfast regime is efficient, reaching $\gamma_\infty \sim \mu$.
The scaling $\gamma \propto \varpi$ is the same as in Vlahakis & Königl (2003a).

Simulations of relativistic jets
Komissarov, Barkov, Vlahakis, & Königl (2007)

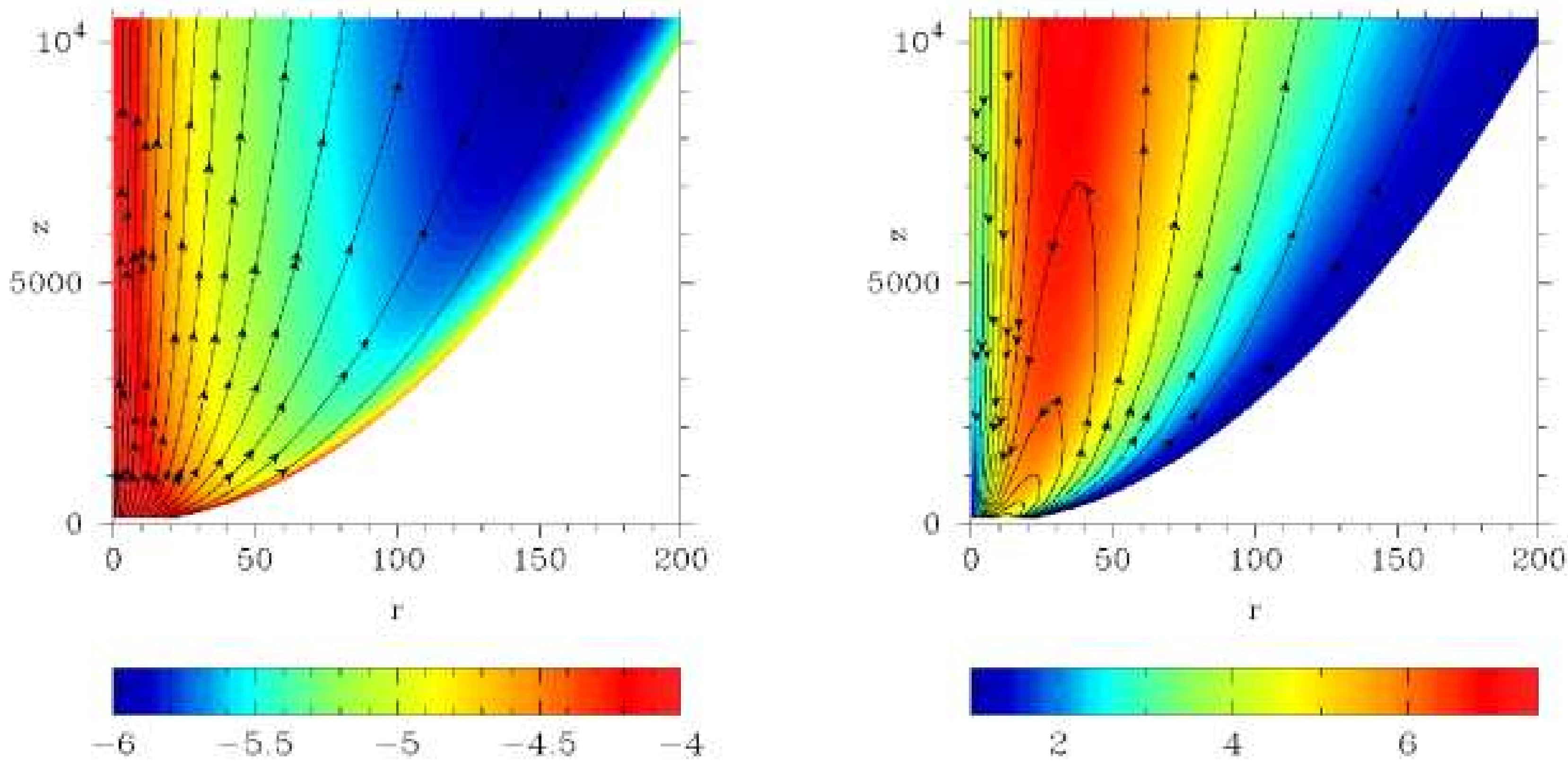

Left panel shows density (colour) and magnetic field lines. Right panel shows the Lorentz factor (colour) and the current lines.

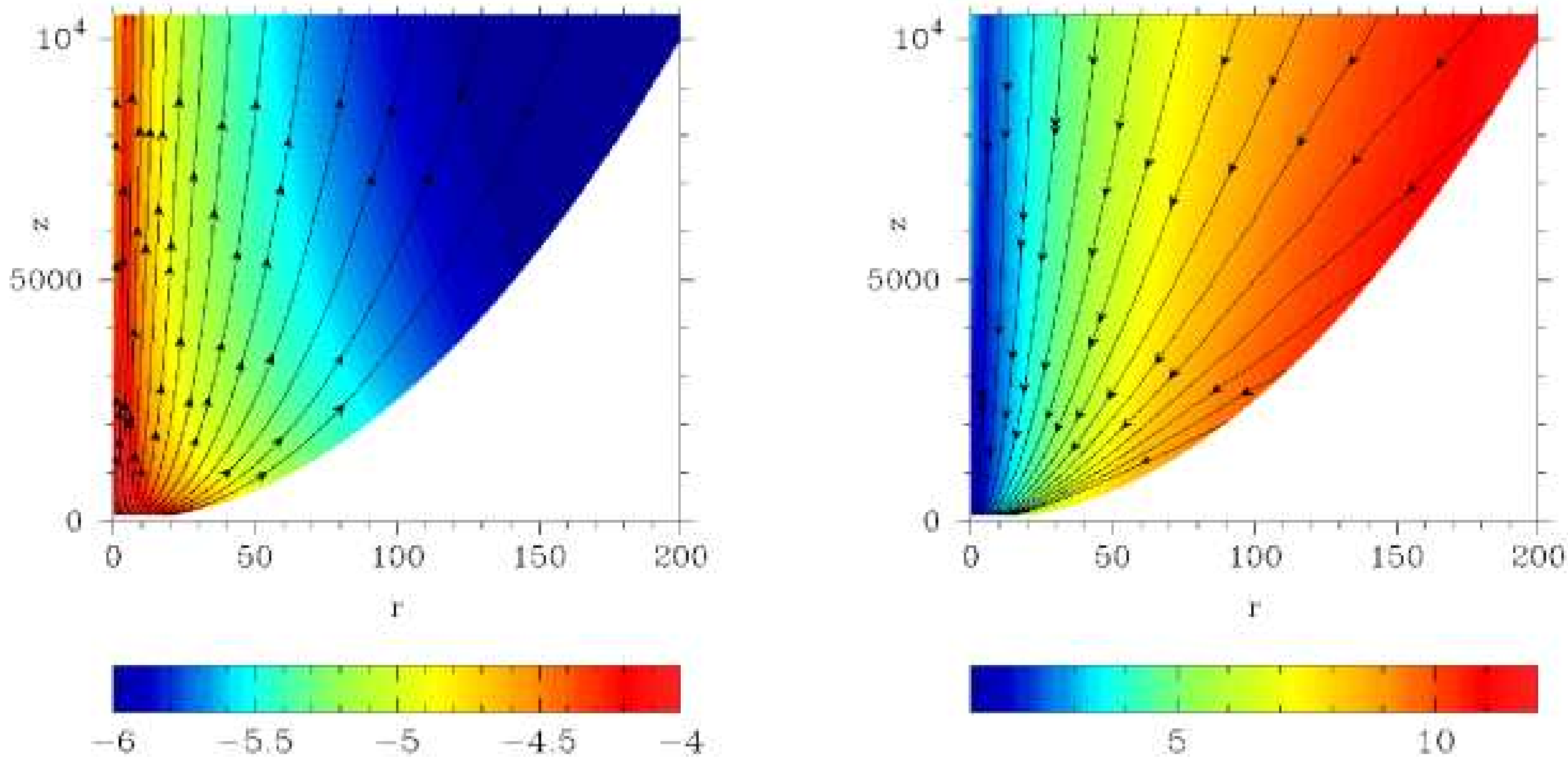

Note the difference in $\gamma(r)$ for constant z.

It depends on the current I, which is related to Ω:
$I \approx r^2 B_p \Omega/2$

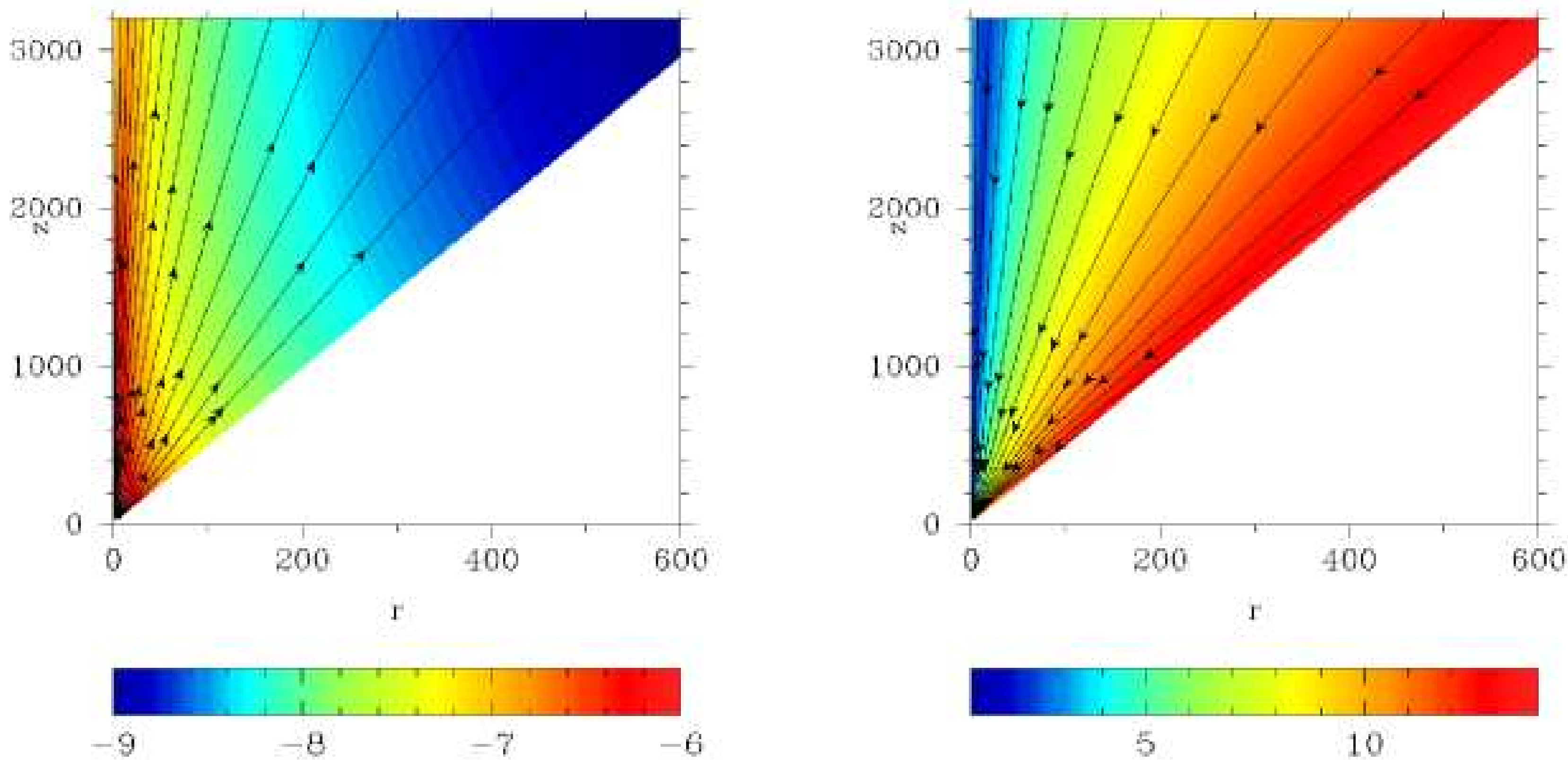
3000
2000
1000
0
z
0
200
400
600
r
−9
−8
−7
−6
5
10

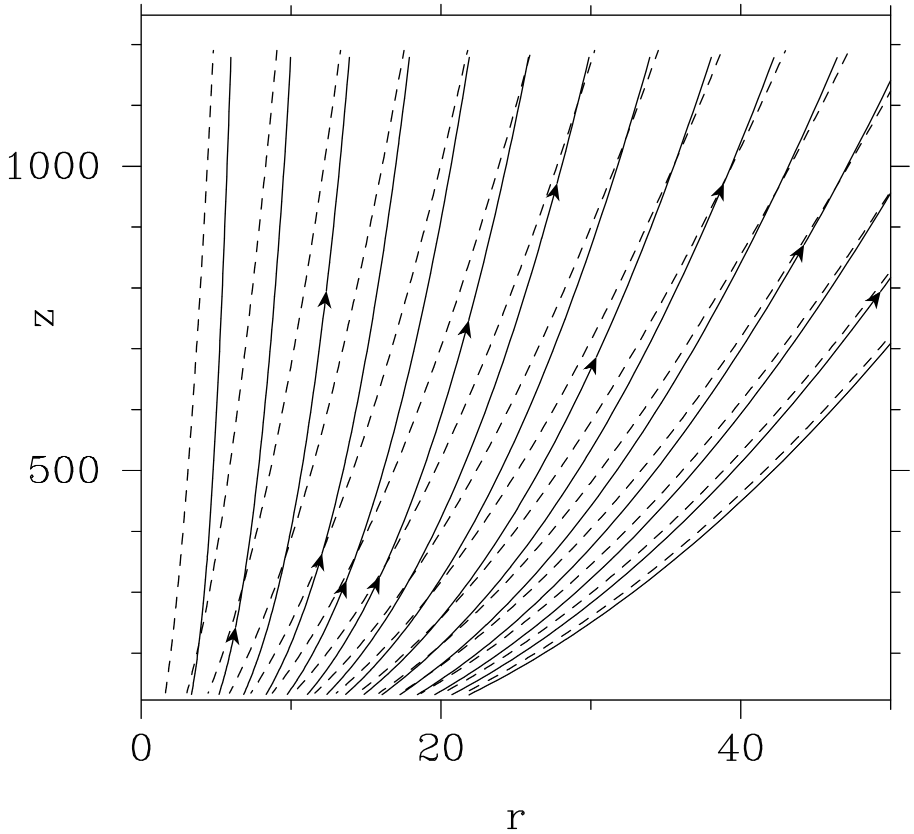

1000
500
z
0
20
40
r

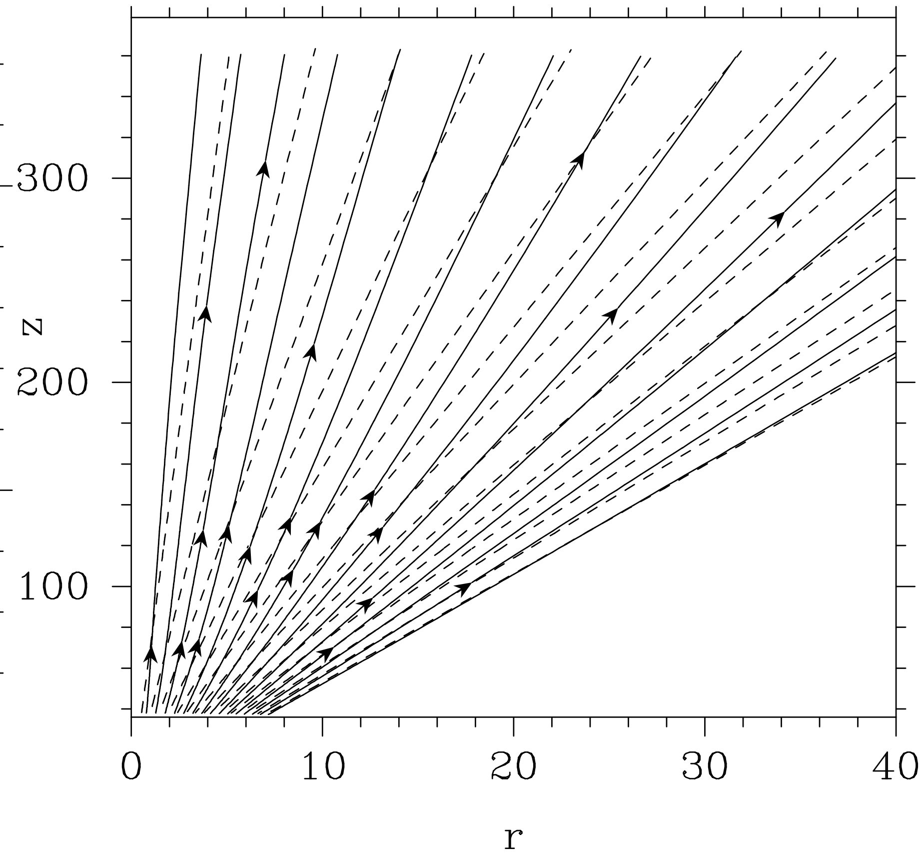

300
200
100
z
0
10
20
30
40
r

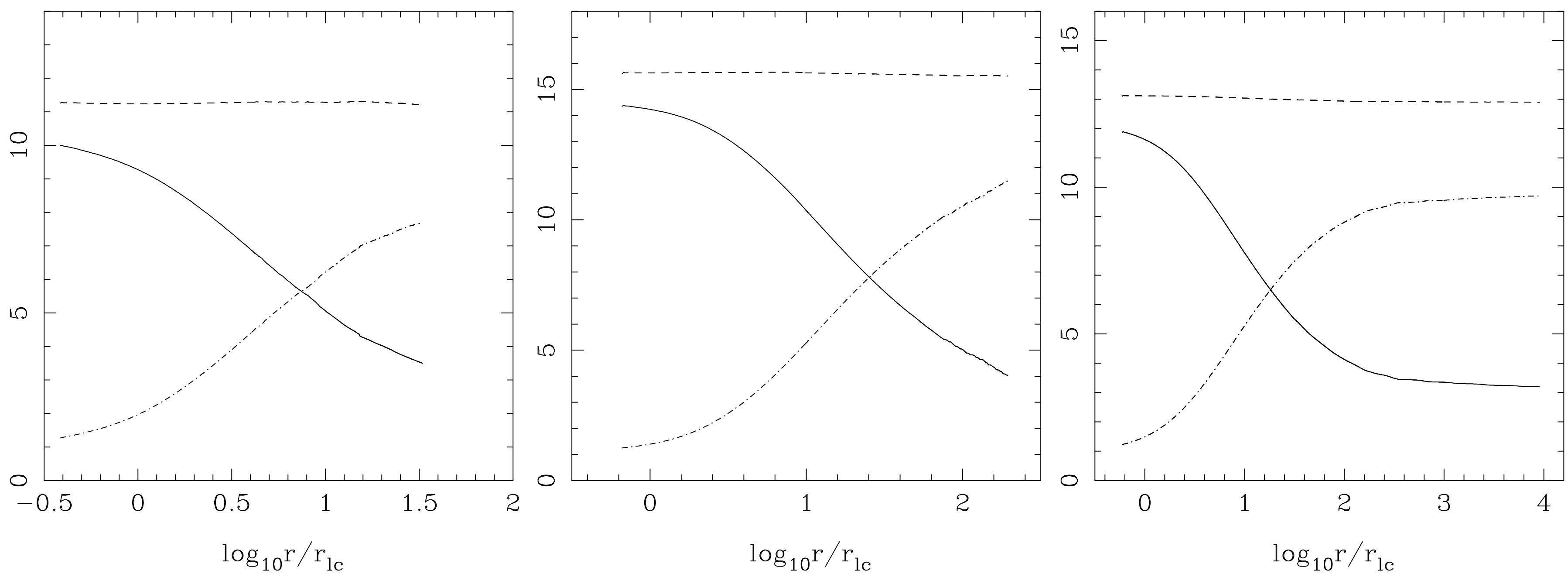

$\gamma\sigma$ (solid line), μ (dashed line) and γ (dash-dotted line) along a magnetic field line as a function of cylindrical radius for models C1 (left panel), C2 (middle panel) and A2 (right panel).

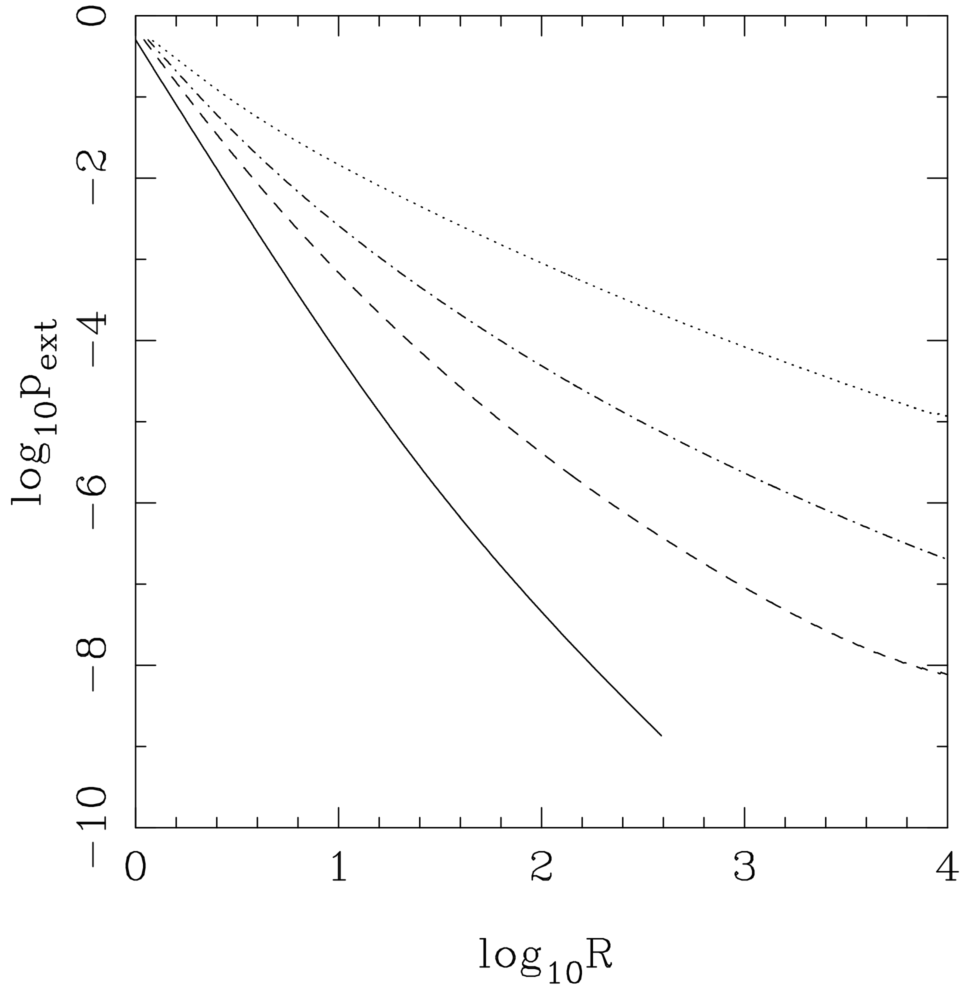

external pressure $P_{ext} = (B^2 - E^2)/8\pi$

solid line: $p_{\rm ext} \propto R^{-3.5}$ for $z \propto r$, dashed line: $p_{\rm ext} \propto R^{-2}$ for $z \propto r^{3/2}$, dash-dotted line: $p_{\rm ext} \propto R^{-1.6}$ for $z \propto r^2$, dotted line: $p_{\rm ext} \propto R^{-1.1}$ for $z \propto r^3$

Komissarov, Vlahakis, Königl, & Barkov 2009

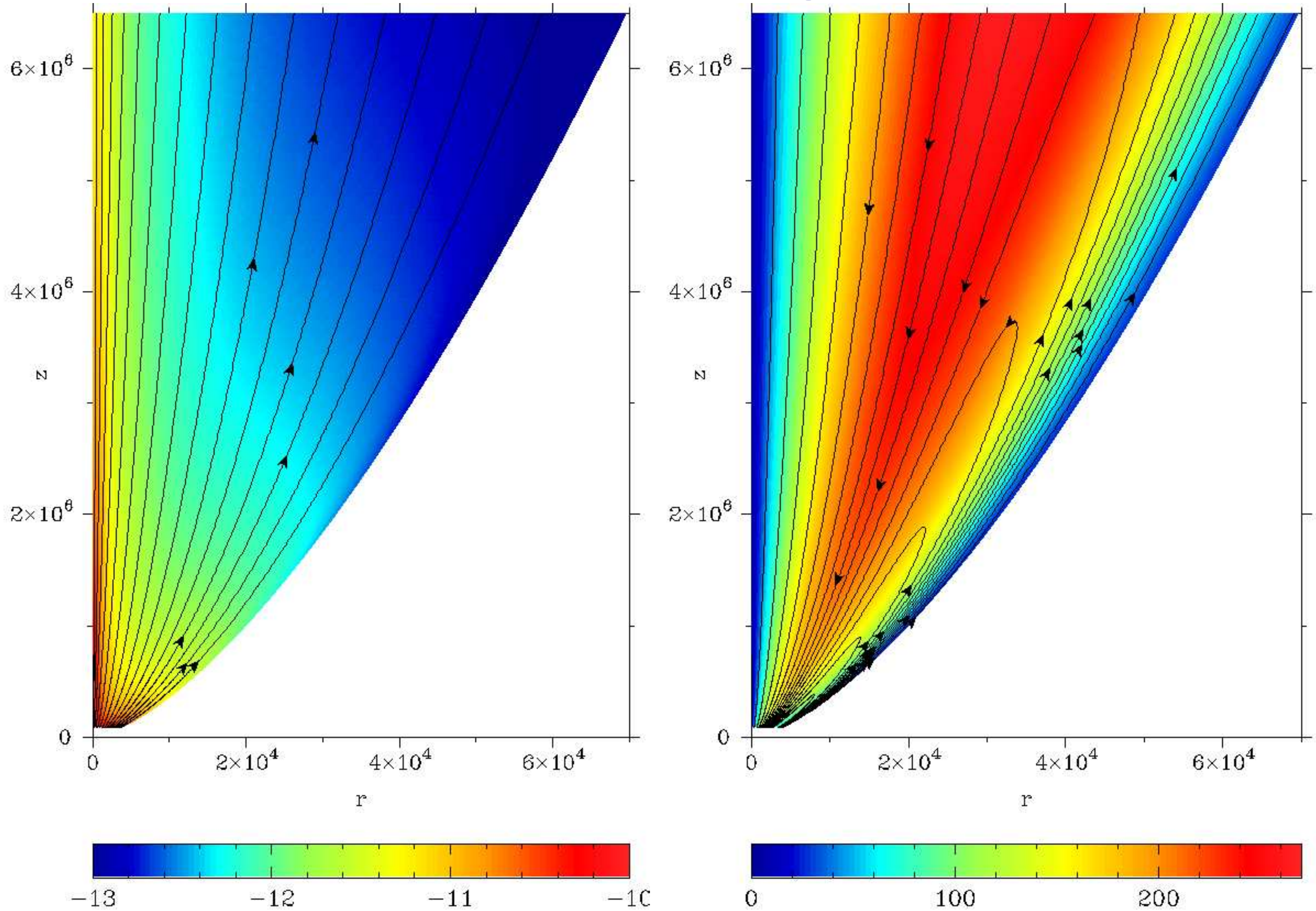

left: density/field lines, right: Lorentz factor/current lines (wall shape $z \propto r^{1.5}$)

Differential rotation $\rightarrow$ slow envelope

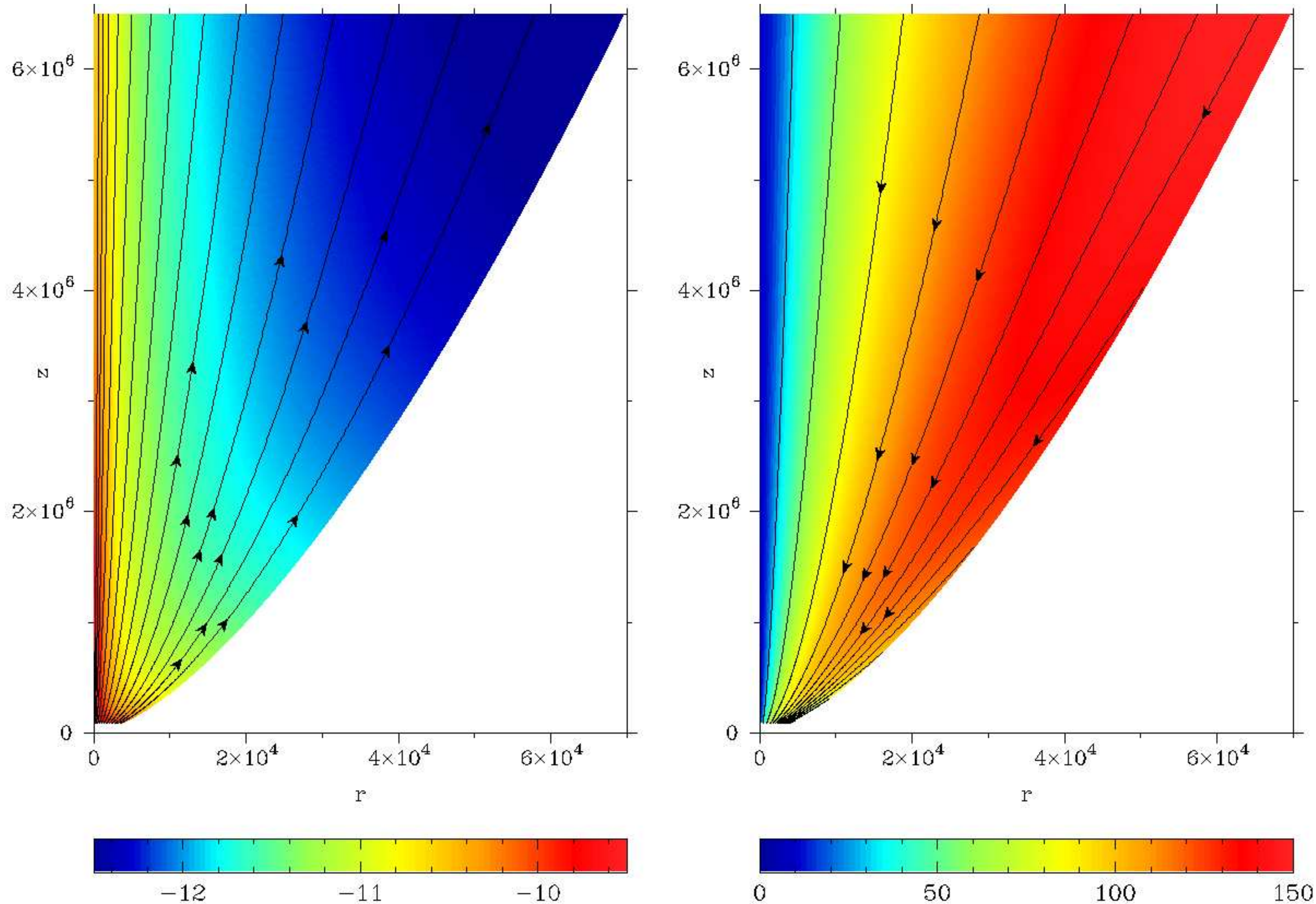

Uniform rotation $\rightarrow \gamma$ increases with r

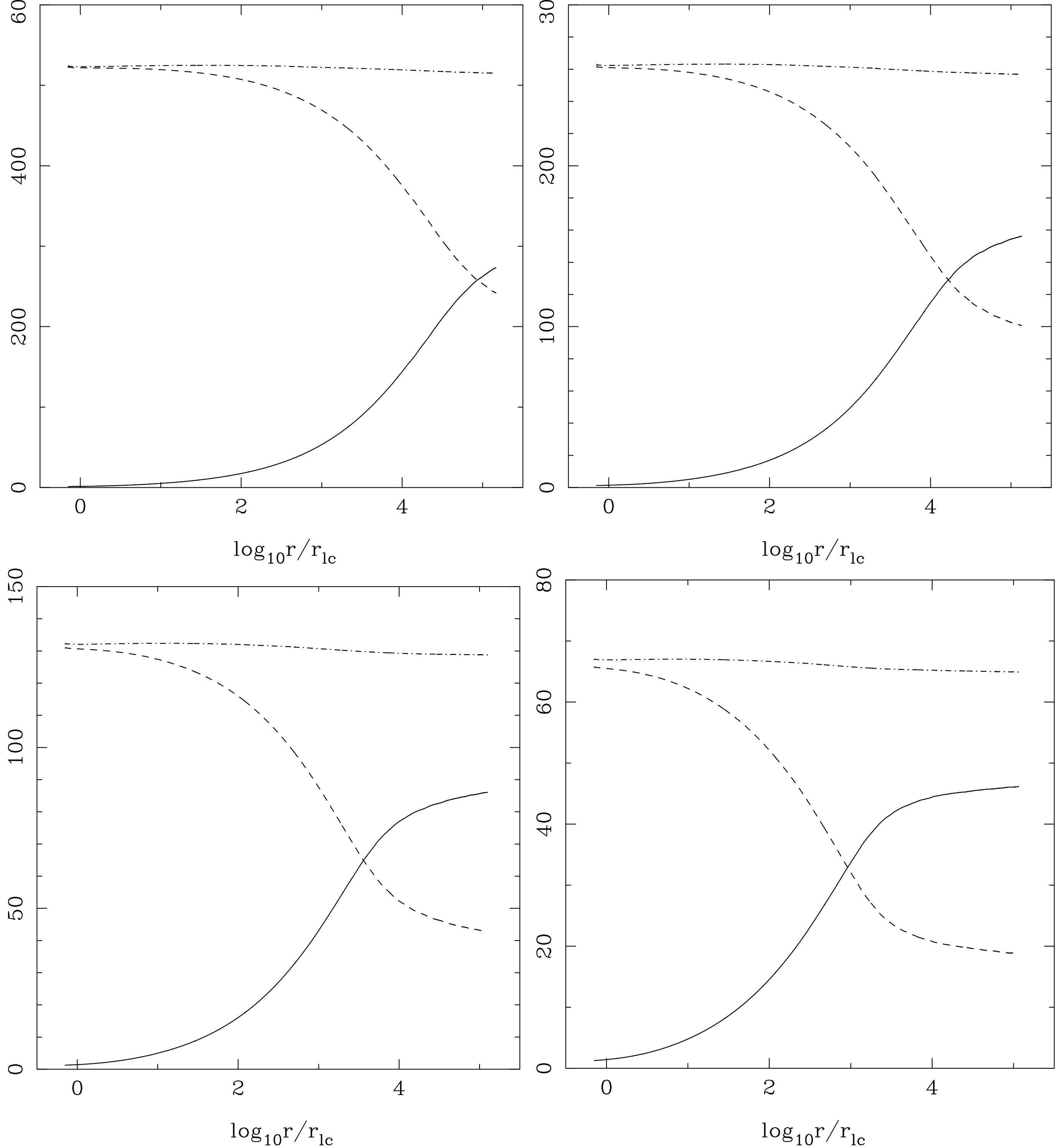
600
400
200
0
0
2
4
$\log_{10} r/r_{lc}$
300
200
100
0
0
2
4
$\log_{10} r/r_{lc}$
150
100
50
0
0
2
4
$\log_{10} r/r_{lc}$
80
60
40
20
0
0
2
4
$\log_{10} r/r_{lc}$

Caveat: $\gamma\vartheta \sim 1$ (for high γ)

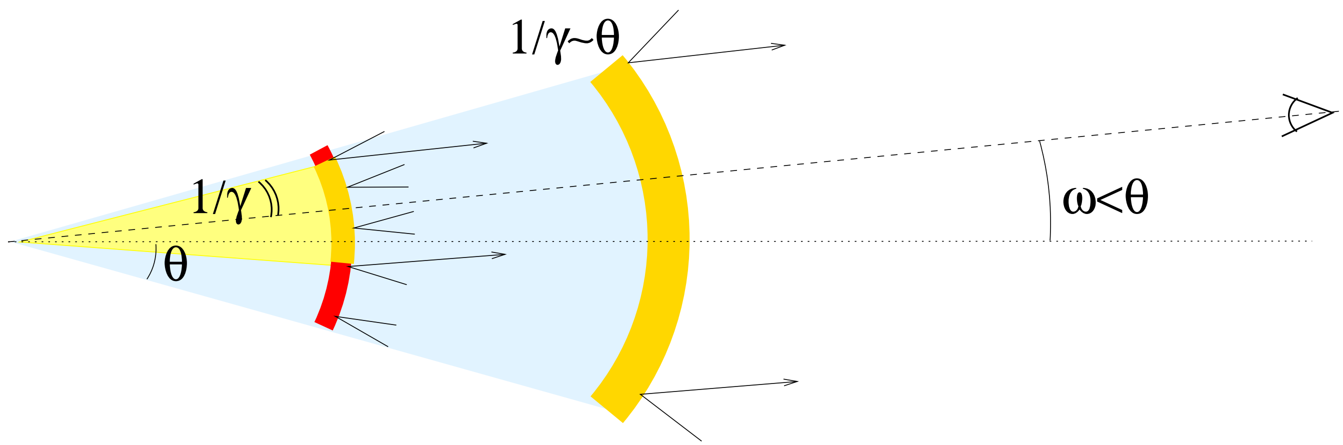

During the afterglow γ decreases
When $1/\gamma > \vartheta$ the $F(t)$ decreases faster

- with $\gamma\vartheta \sim 1$ very narrow jets ($\vartheta < 1^\circ$ for $\gamma > 100$) $\longrightarrow$ early breaks or no breaks at all
- this is a result of causality (across jet): outer lines need to know that there is space to expand
- Mach cone half-opening θ_m should be $> \vartheta$
  With $\sin\theta_m = \dfrac{\gamma_f c_f}{\gamma V_p} \approx \dfrac{\sigma^{1/2}}{\gamma}$ the requirement for causality yields $\gamma\vartheta < \sigma^{1/2}$.
  For efficient acceleration ($\sigma \sim 1$ or smaller) we always get $\gamma\vartheta \sim 1$

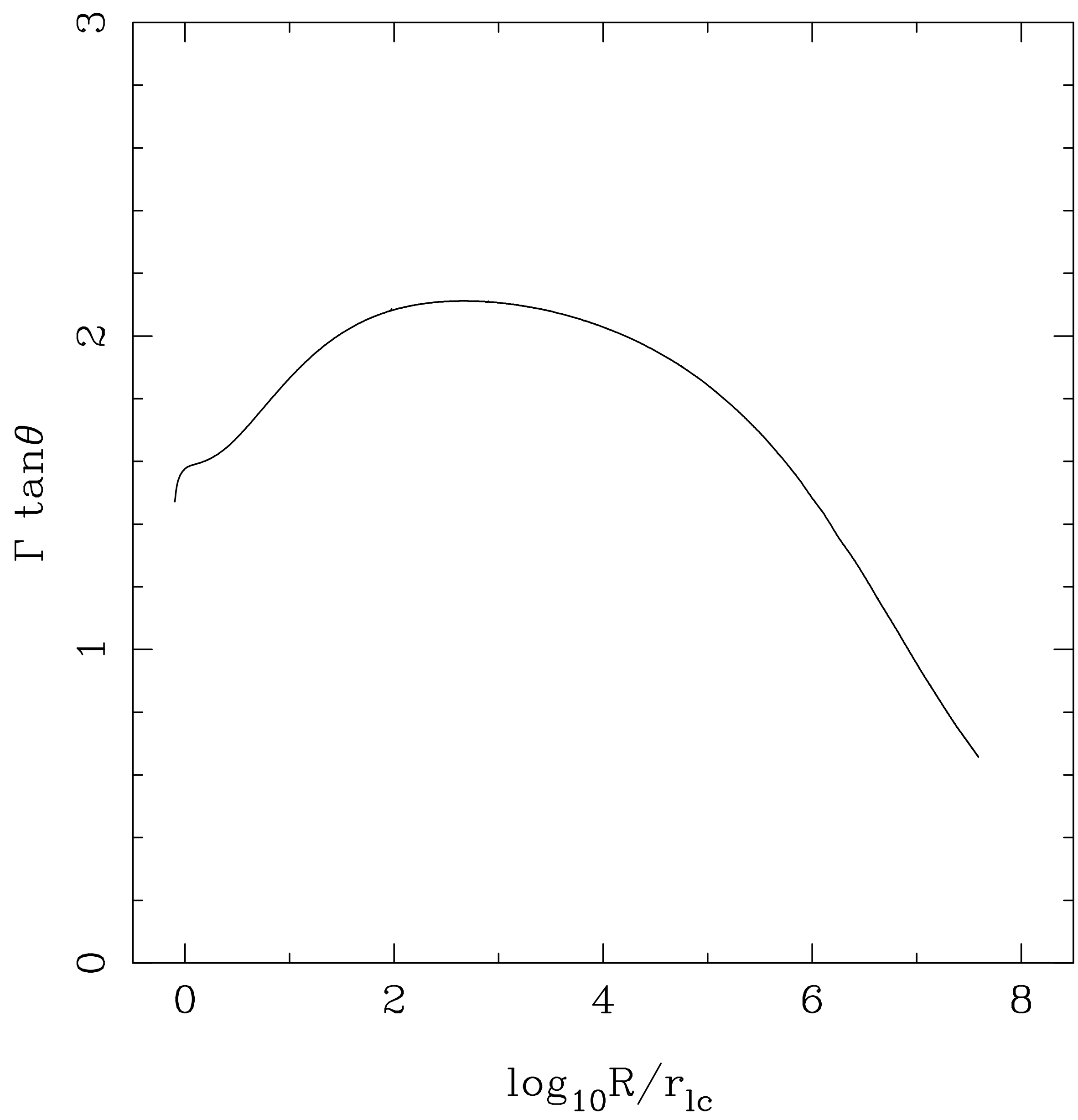
3
2
1
0
$\Gamma \tan\theta$
0
2
4
6
8
$\log_{10} R/r_{lc}$

Rarefaction acceleration

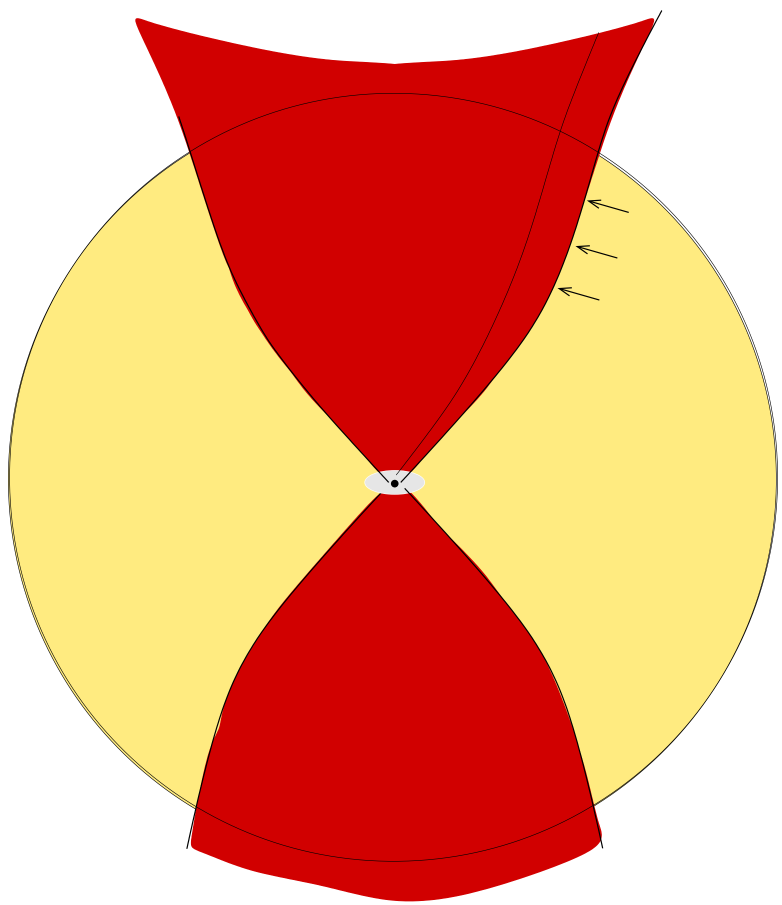

Rarefaction acceleration

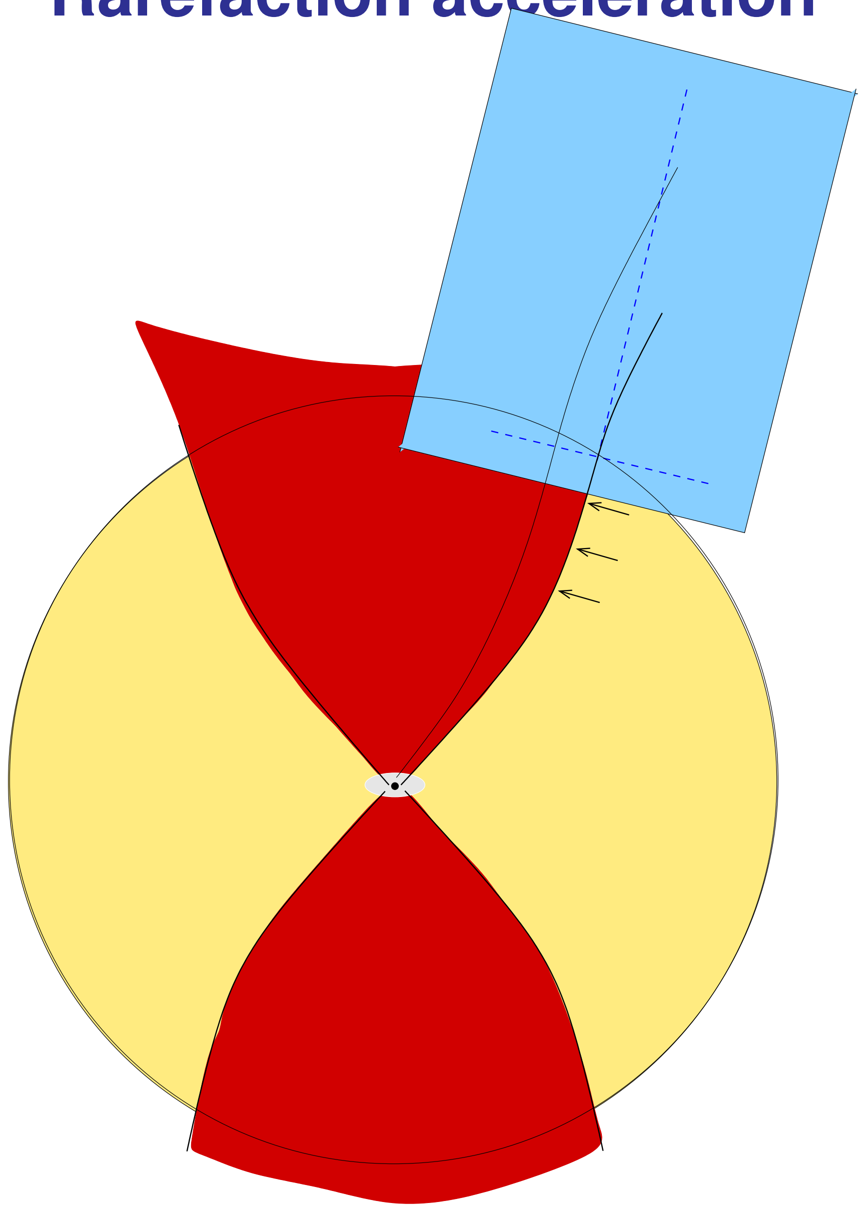

Rarefaction acceleration

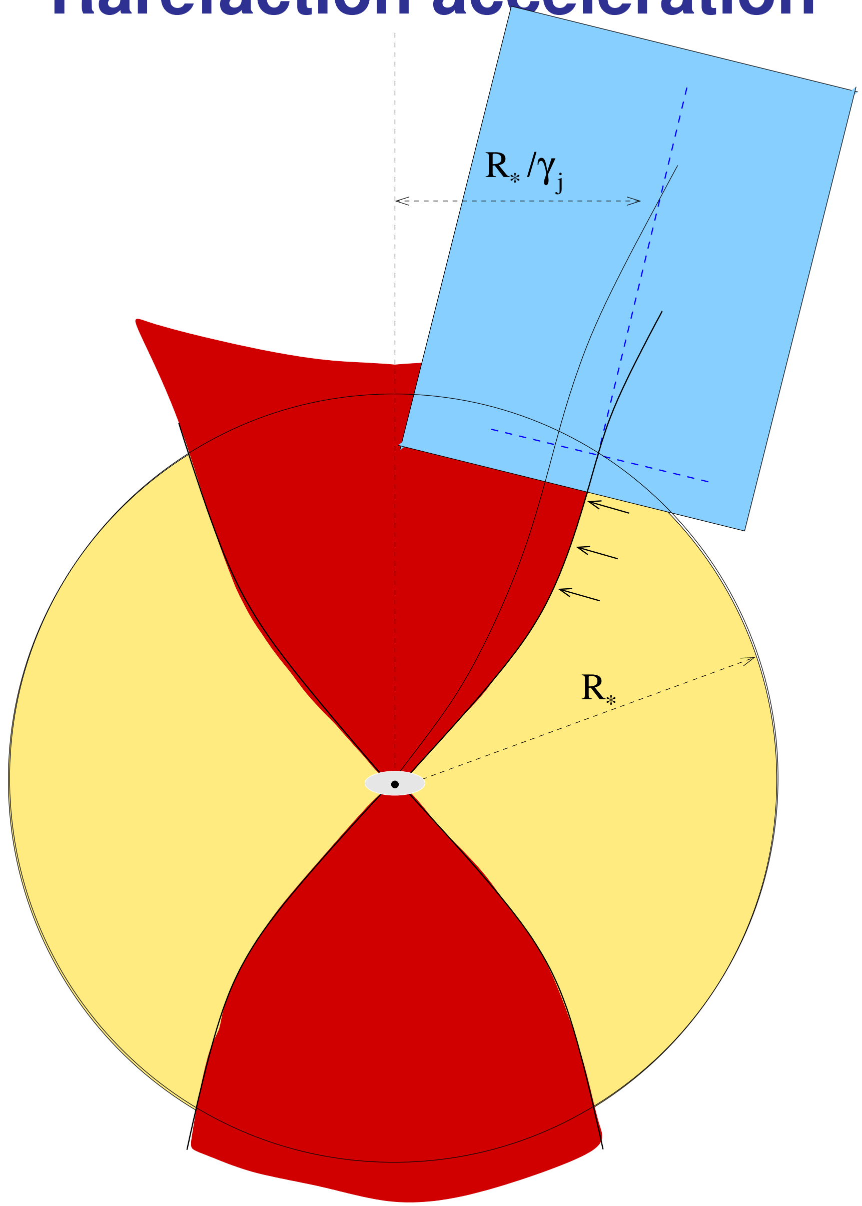

Rarefaction simple waves

At $t = 0$ two uniform states are in contact:

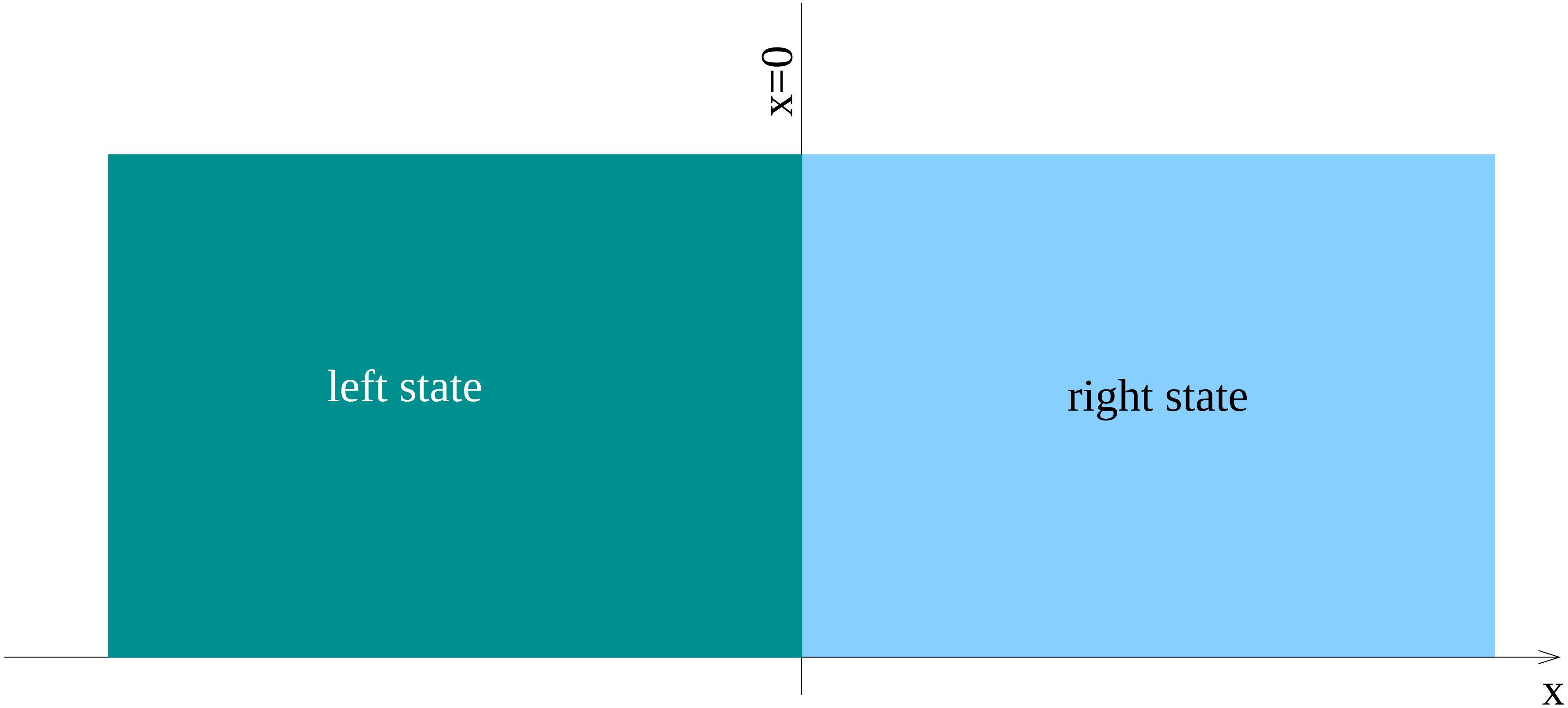

This Riemann problem allows self-similar solutions that depend only on $\xi = x/t$.

- when right=vacuum, simple rarefaction wave

At $t > 0$:

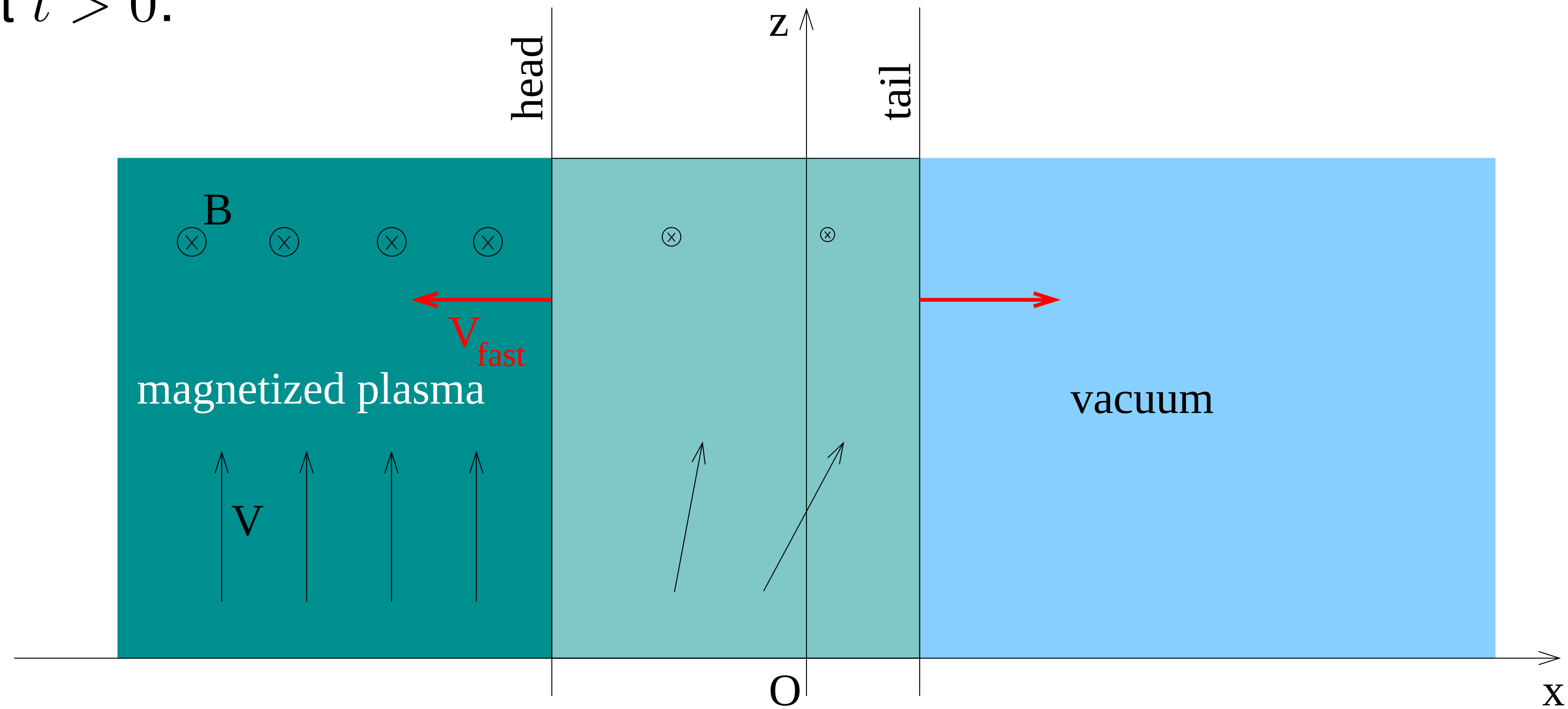

for the cold case the Riemann invariants imply

$$v_x = \frac{1}{\gamma_j}\frac{2\sigma_j^{1/2}}{1+\sigma_j}\left[1-\left(\frac{\rho}{\rho_j}\right)^{1/2}\right], \; \gamma = \frac{\gamma_j\,(1+\sigma_j)}{1+\sigma_j\rho/\rho_j}\,, \; \rho = \frac{4\rho_j}{\sigma_j}\sinh^2\left[\frac{1}{3}\mathrm{arcsinh}\left(\sigma_j^{1/2}-\frac{\mu_j}{2}\frac{x}{t}\right)\right]$$

$$V_{head} = -\frac{\sigma_j^{1/2}}{\gamma_j}\,, \qquad V_{tail} = \frac{1}{\gamma_j}\frac{2\sigma_j^{1/2}}{1+\sigma_j}\,, \qquad \Delta\vartheta = V_{tail} < 1/\gamma_i$$

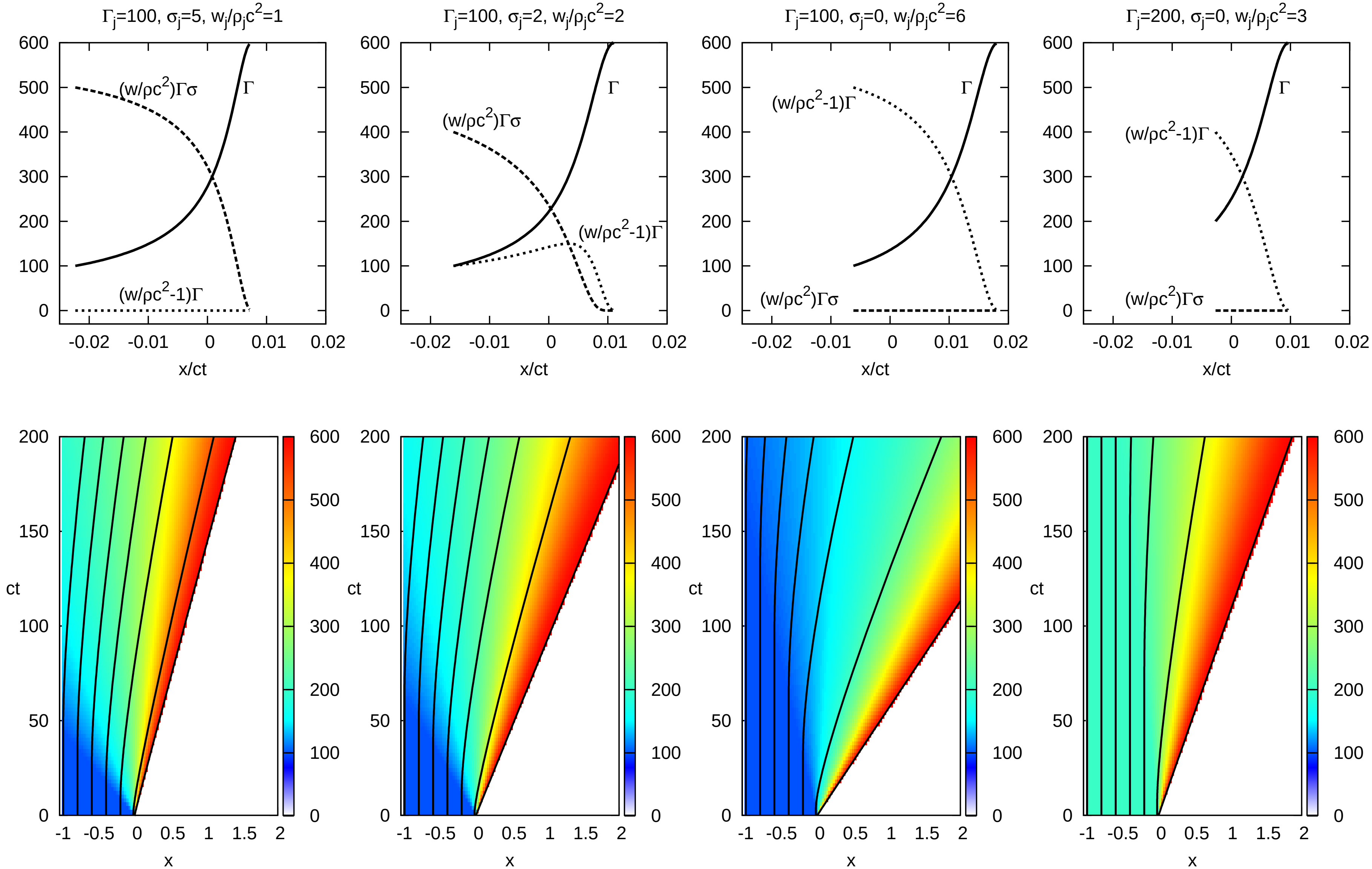

The colour image in the Minkowski diagrams represents the distribution of the Lorentz factor and the contours show the worldlines of fluid parcels initially located at $x_i = -1, -0.8, -0.6, -0.4, -0.2, -0.02, 0$.

Simulation results

Komissarov, Vlahakis & Königl 2010

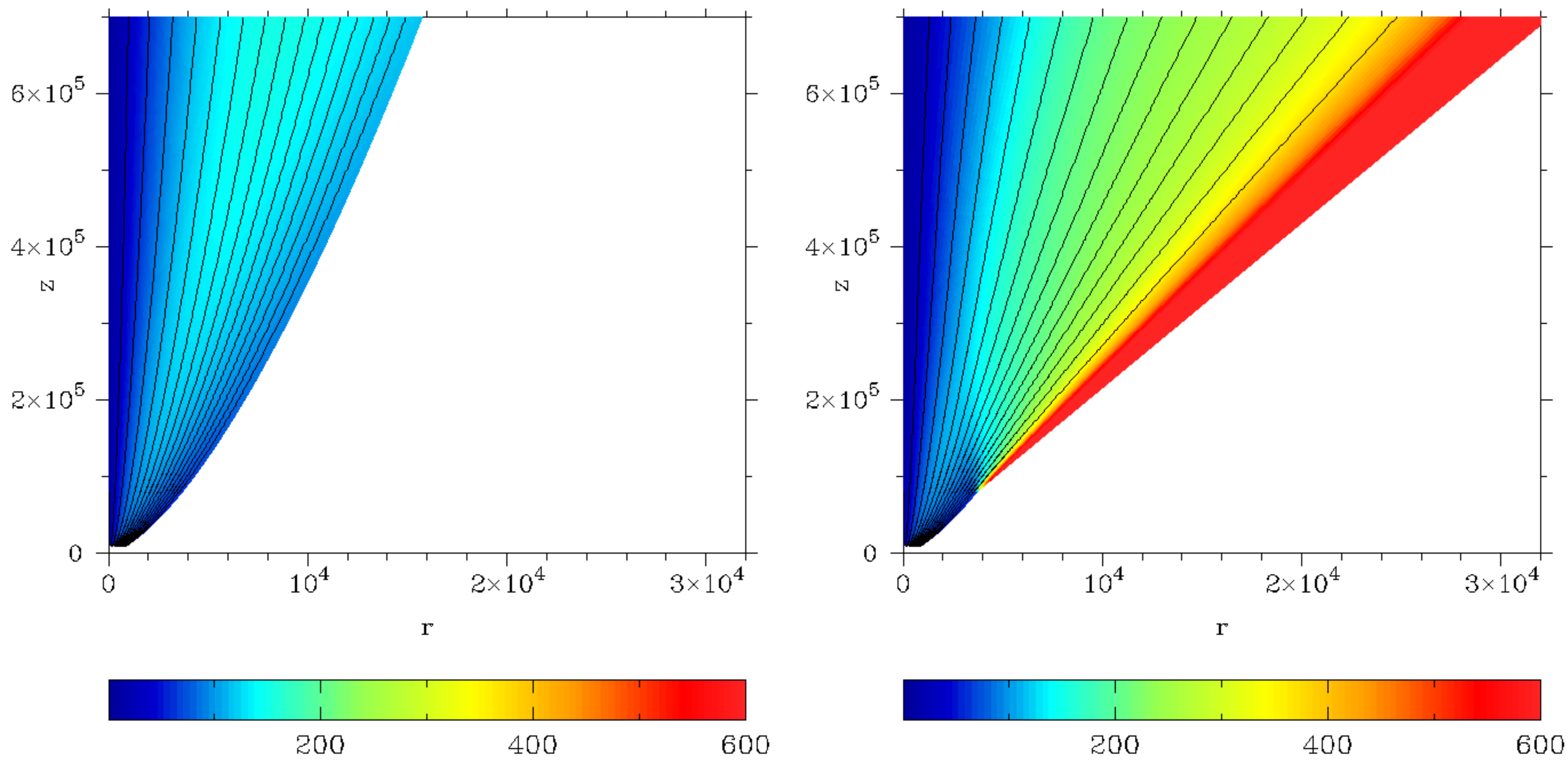

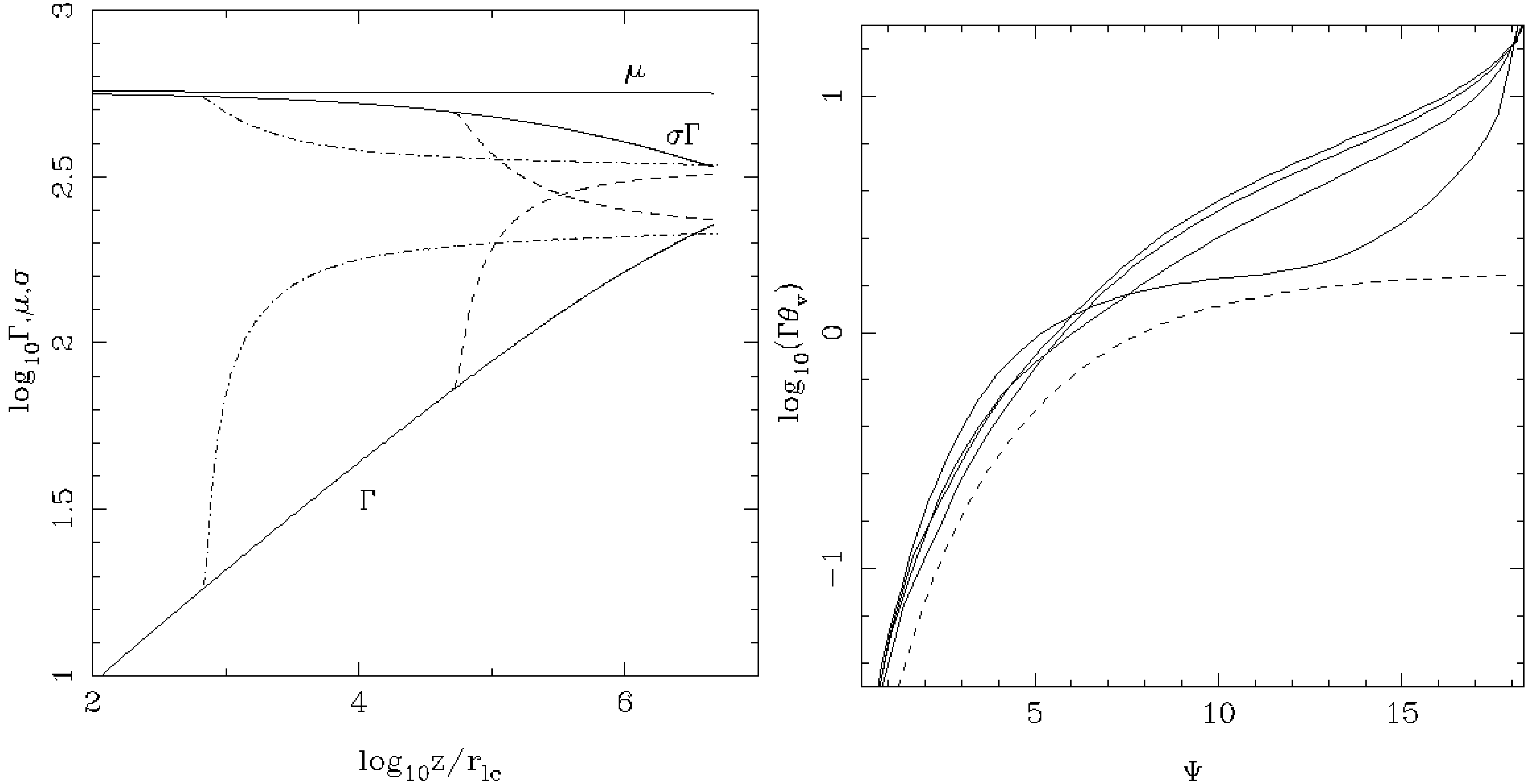

μ
$\sigma\Gamma$
Γ
$\log_{10}\Gamma,\mu,\sigma$
$\log_{10} z/r_{lc}$
$\log_{10}(\Gamma\theta_v)$
Ψ

Steady-state rarefaction wave

Sapountzis & Vlahakis (2013)

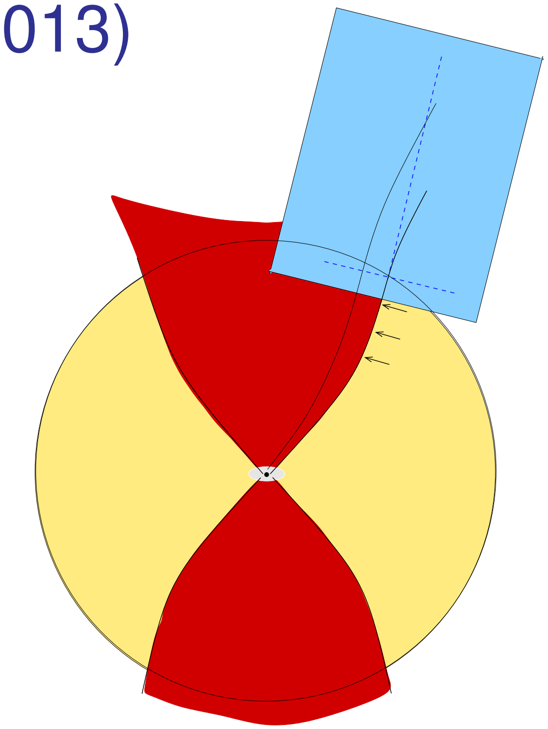

- "flow around a corner"
- planar geometry
- ignoring B_p (nonzero B_y)
- similarity variable x/z (angle θ)
- generalization of the nonrelativistic, hydrodynamic rarefaction (e.g. Landau & Lifshitz)
- in addition, allow for inhomogeneity in the "left" state

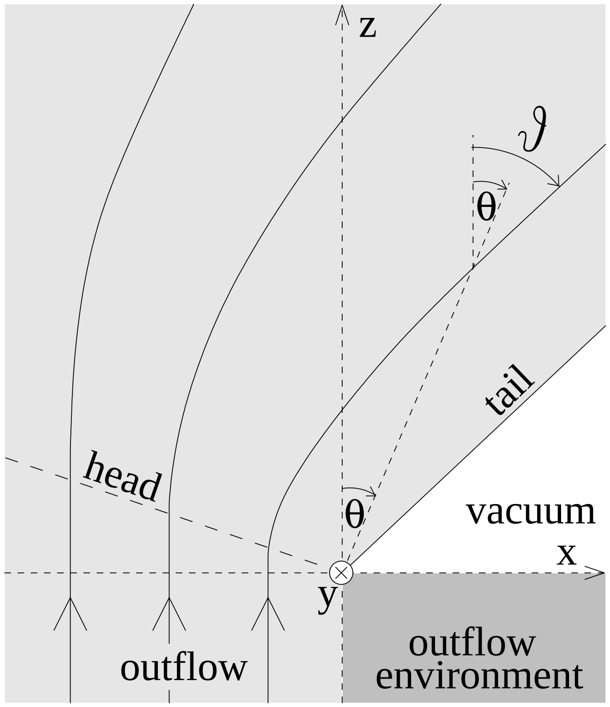

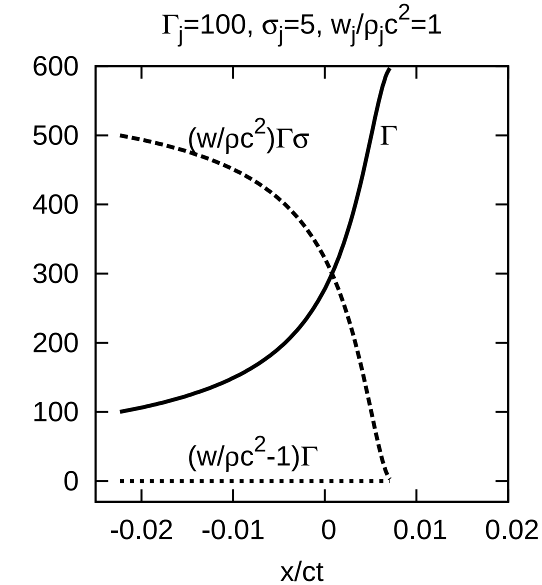

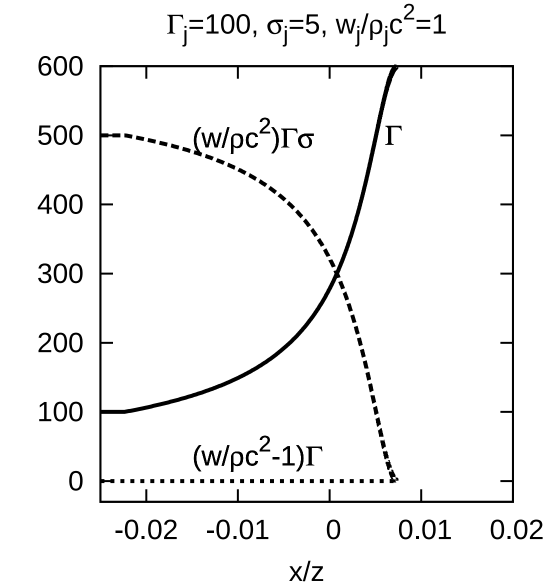

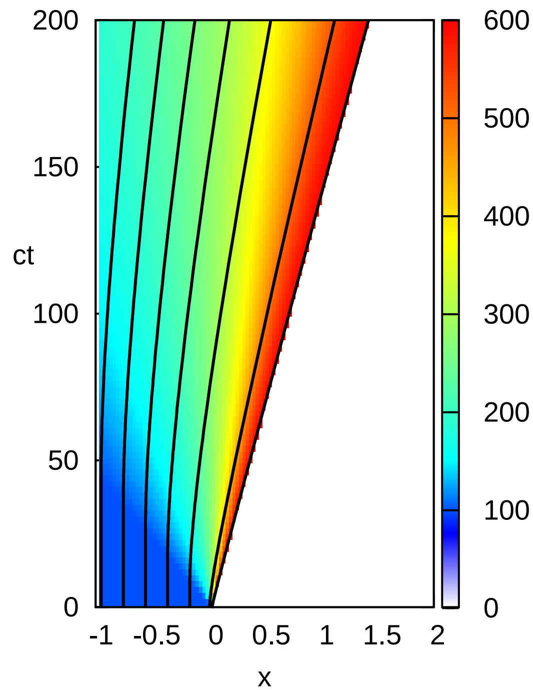

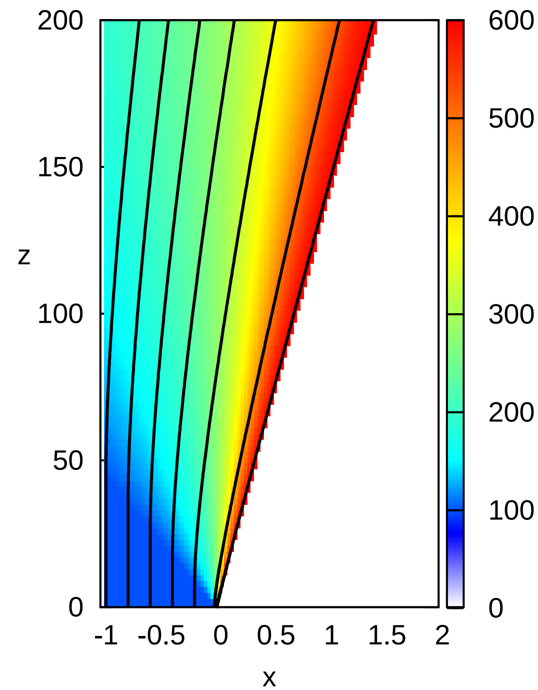

$$\theta_{\rm head} = -\frac{\sigma_j^{1/2}}{\gamma_j}$$

$$\theta_{\rm tail} = \frac{2\sigma_j^{1/2}}{\gamma_j(1+\sigma_j)}$$

$$\sigma = (\sigma_j\gamma_j x_i/z)^{2/3}$$

$\sigma = 1$ at $r = \sigma_j\gamma_j|x_i| = 7\times10^{11}\sigma_j\left(\frac{|x_i|}{R_\star/\gamma_j}\right)\left(\frac{R_\star}{10R_\odot}\right)$ cm

time-dependent (left) and steady-state (right) rarefaction (similar; $ct \to z$)
(distance unit $= R_\star/\gamma_j \sim 10^{10}$ cm)

Axisymmetric model

Solve steady-state axisymmetric MHD eqs using the method of characteristics (Sapountzis & Vlahakis in preparation)

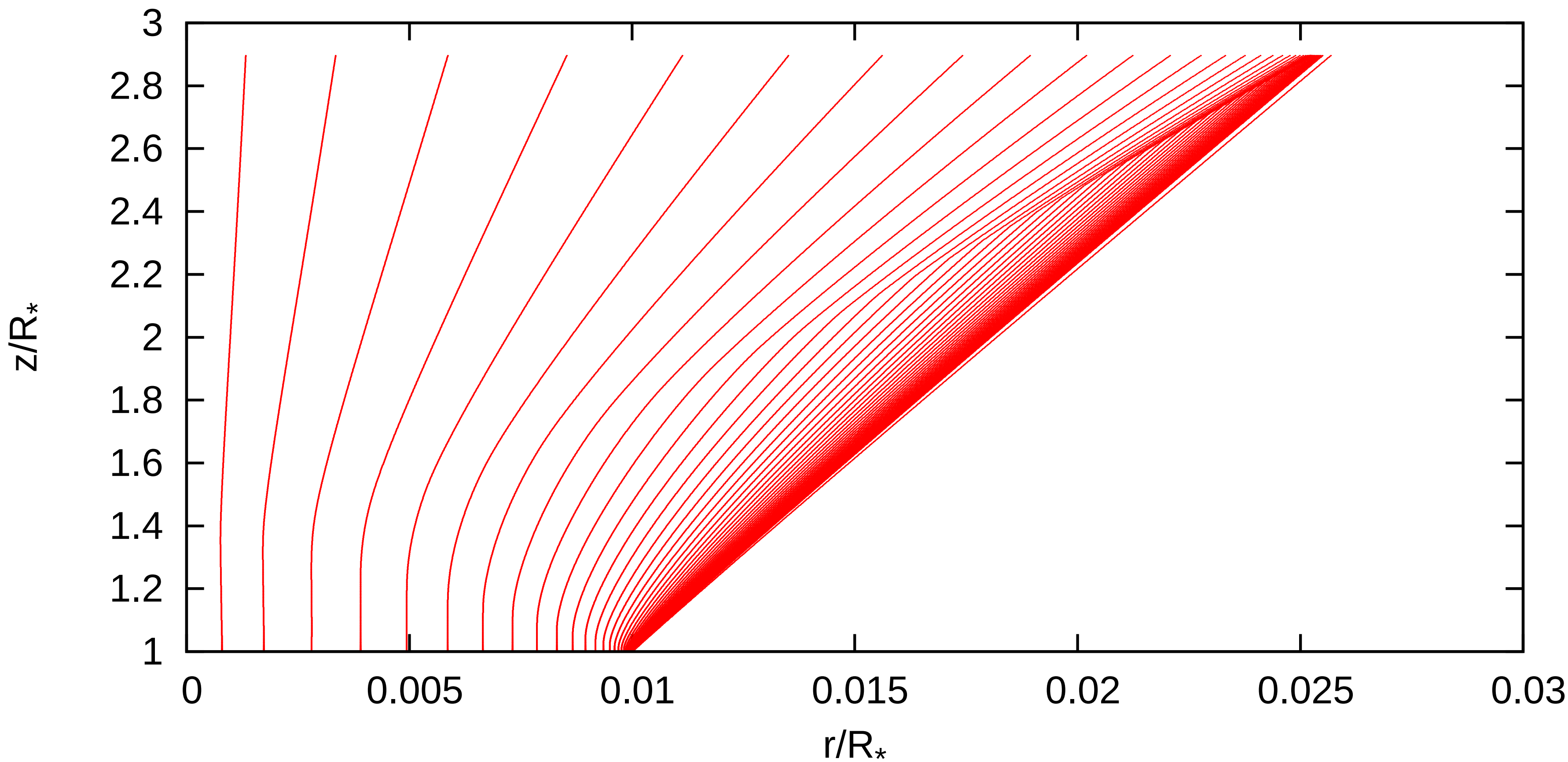

(not in scale!)

typical value of $R_\star = 10^{12}$ cm

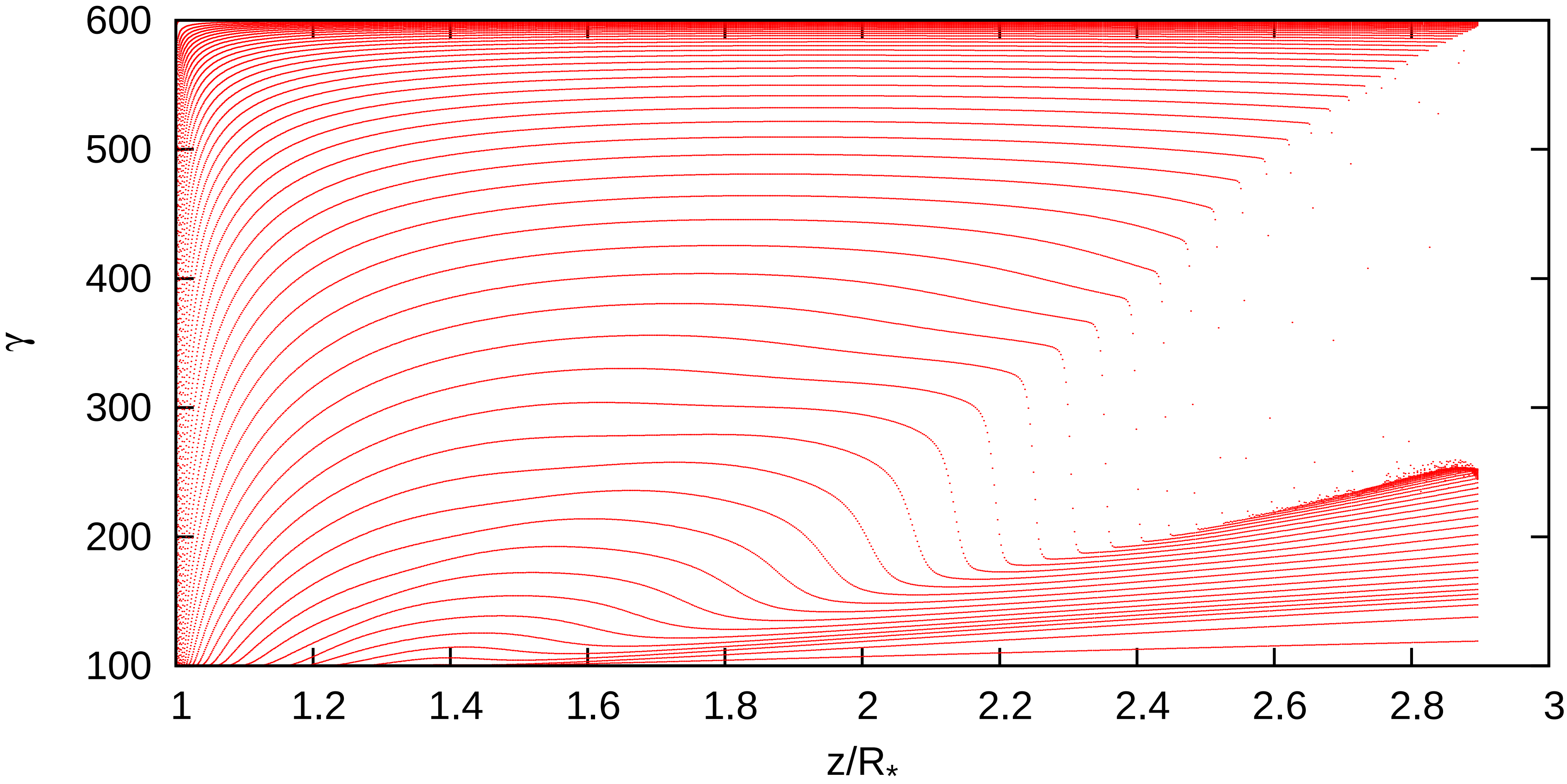

600
500
400
300
200
100
γ
1
1.2
1.4
1.6
1.8
2
2.2
2.4
2.6
2.8
3
z/R*

(Asada & Nakamura 2011)

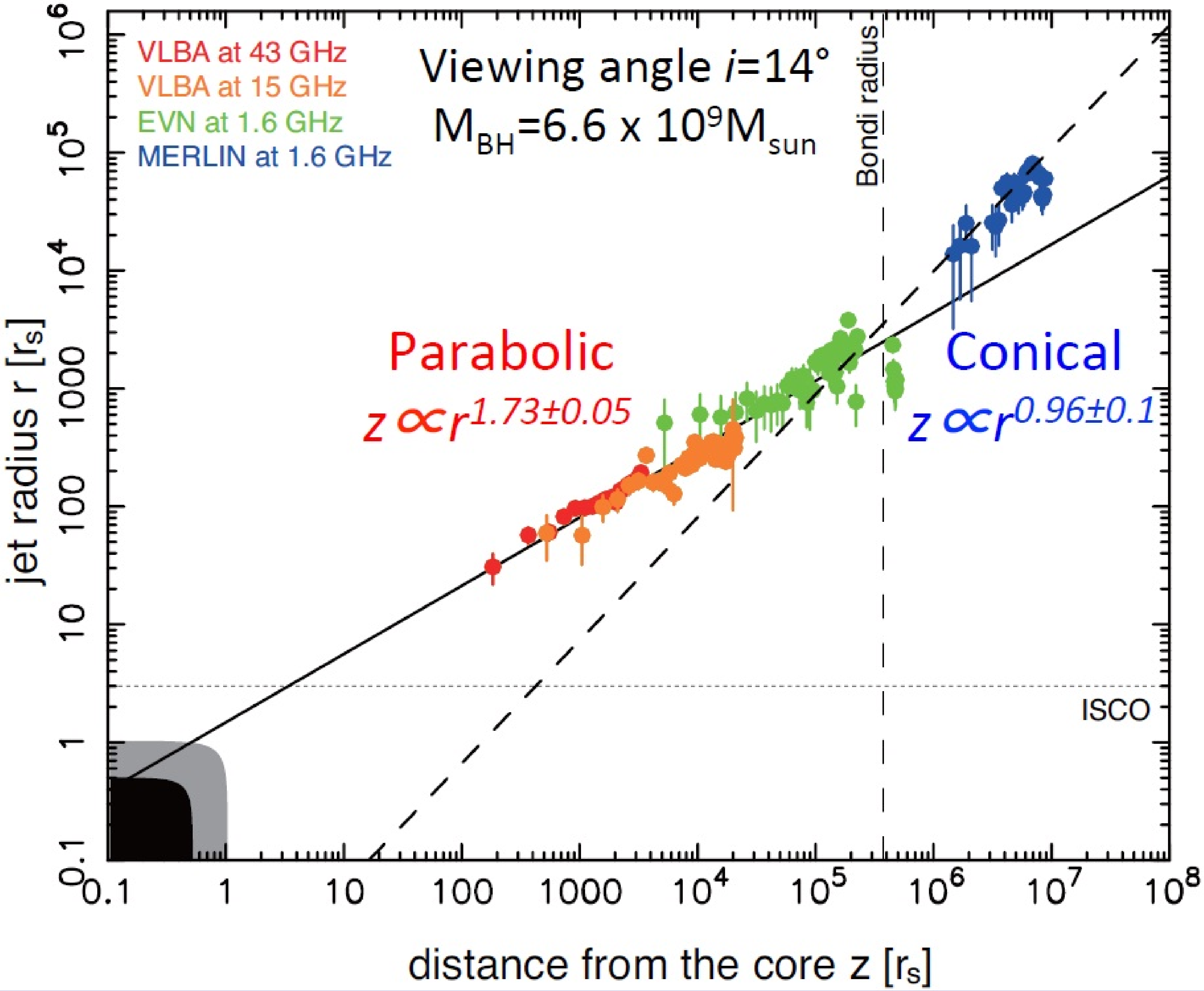

Jet kinematics

- due to precession? (e.g., Caproni & Abraham)

- instabilities? (e.g., Hardee, Meier)

bulk jet flow may play at least a partial role

to explore this possibility, we used the relativistic self-similar model (Vlahakis & Königl 2004)

since the model gives the velocity (3D) field, we can follow the motion of a part of the flow

For given $\theta_{\rm obs}$ (angle between jet axis and line of sight) and ejection area on the disk (r_o, ϕ_o), we project the trajectory on the plane of sky and compare with observations. Find the best-fit parameters r_o, $\theta_{\rm obs}$, ϕ_o.

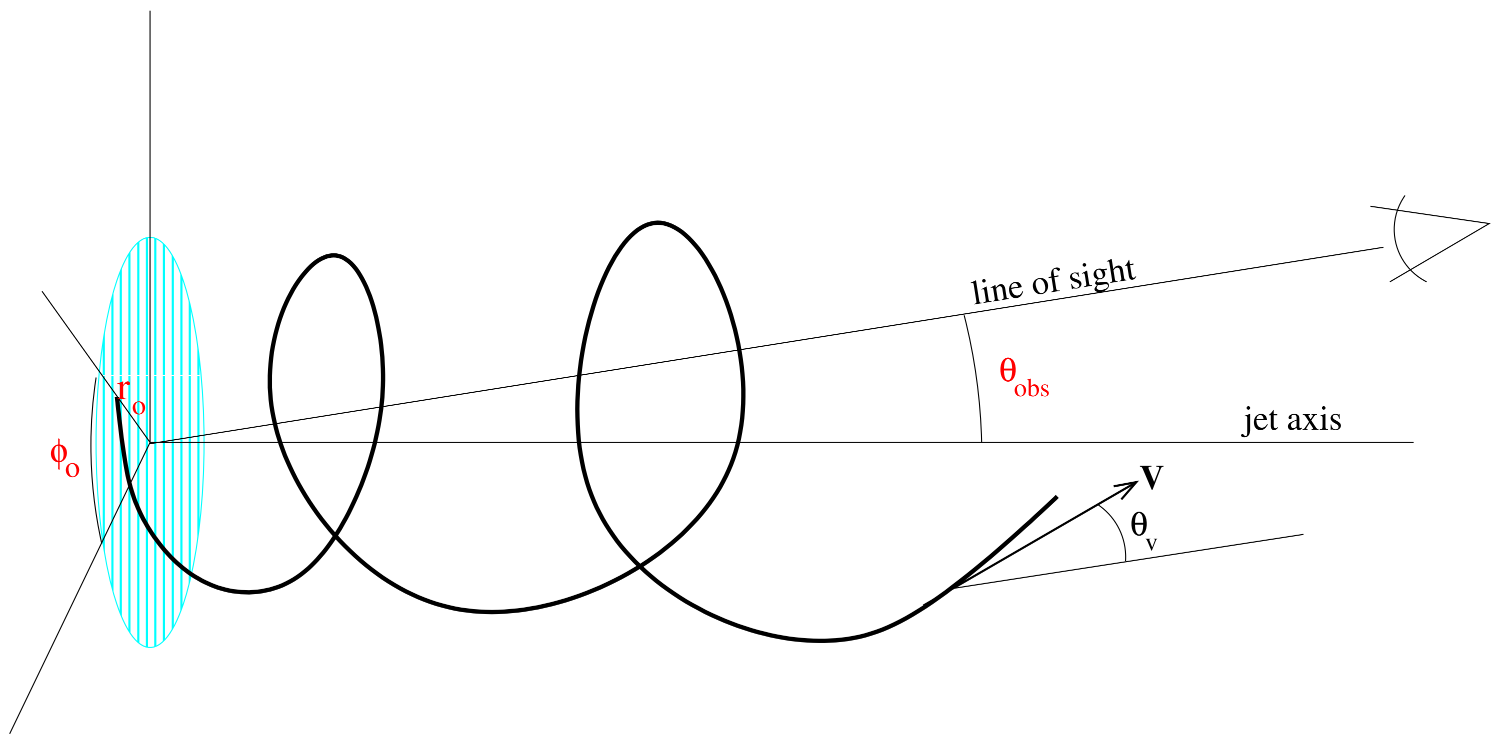

For $\theta_{\rm obs} = 1^{\rm o}$ and $\phi_o = 0^{\rm o}$, $60^{\rm o}$, $120^{\rm o}$, $180^{\rm o}$, $240^{\rm o}$, $300^{\rm o}$ (from top to bottom):

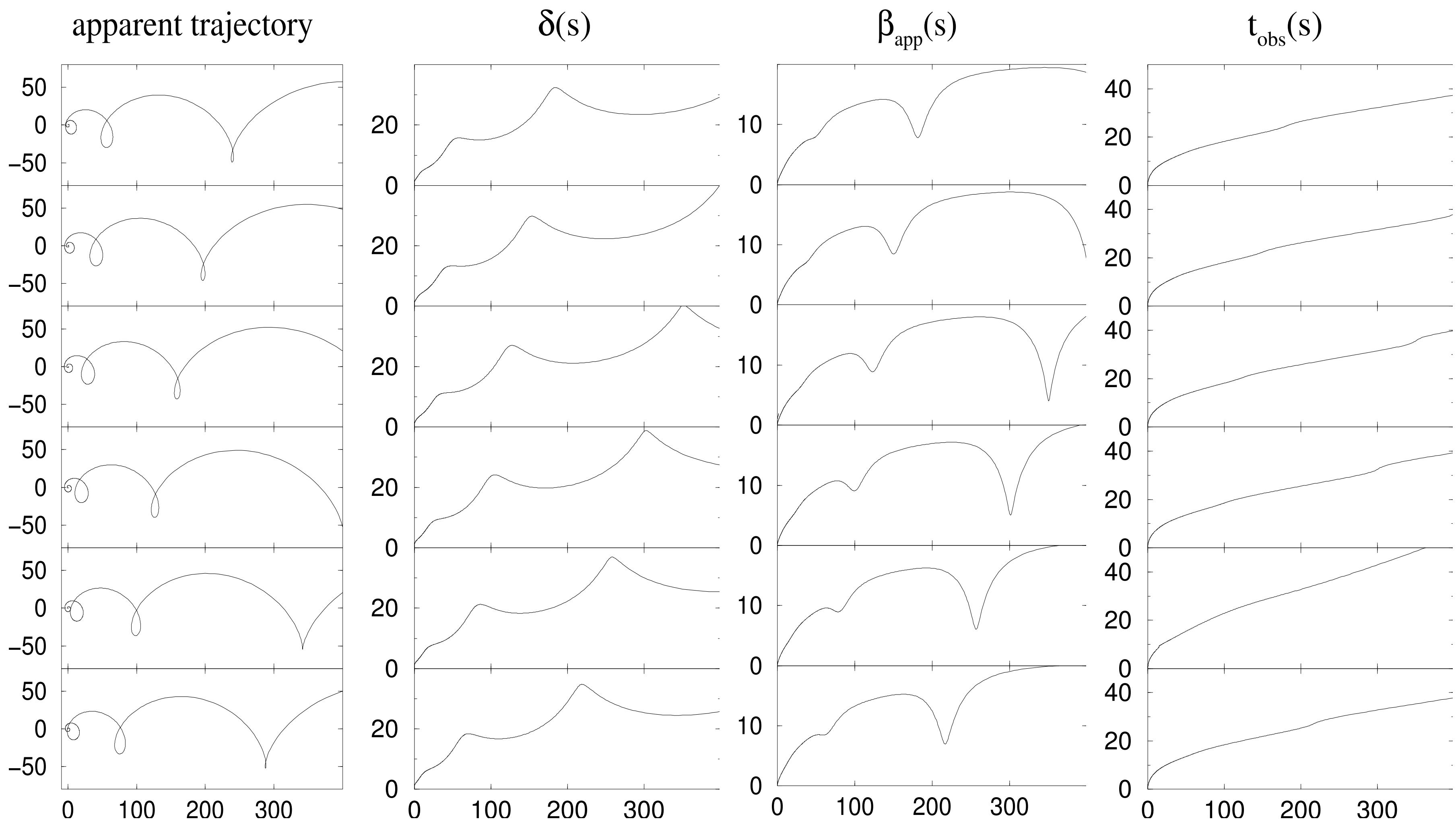

best-fit to Unwin+ results for C7 component in 3C 345:

$r_o \approx 2 \times 10^{16}$cm, ϕ_o=180^o and $\theta_{\rm obs}$=9^o

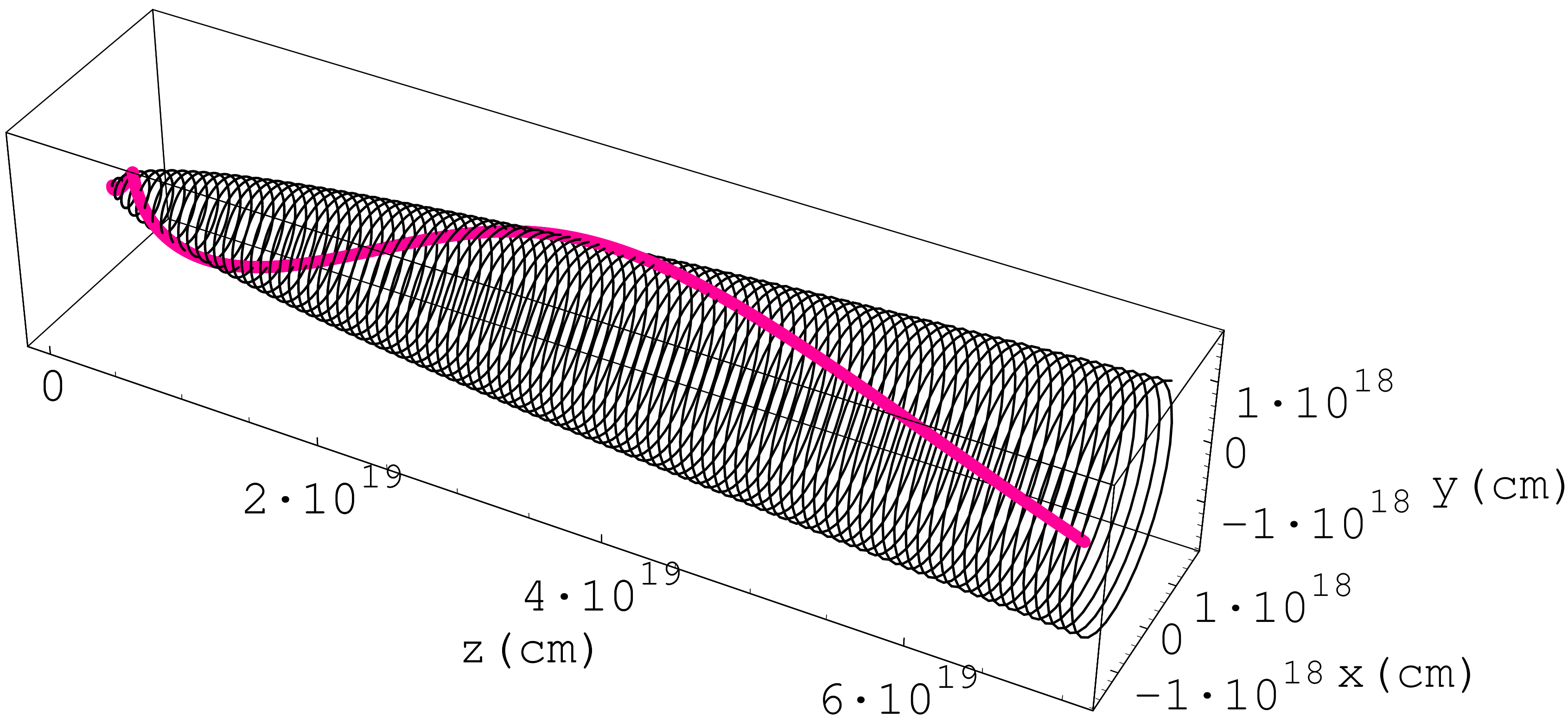

apparent trajectory

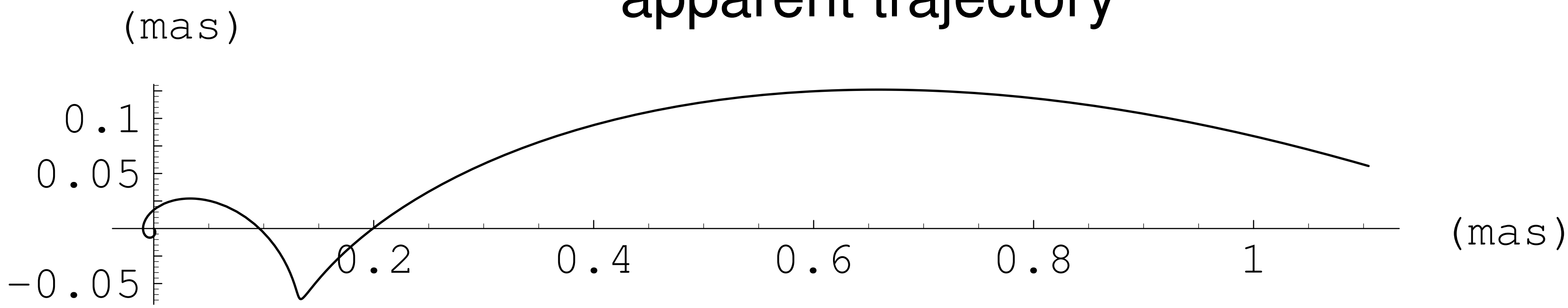

Trajectory of C7

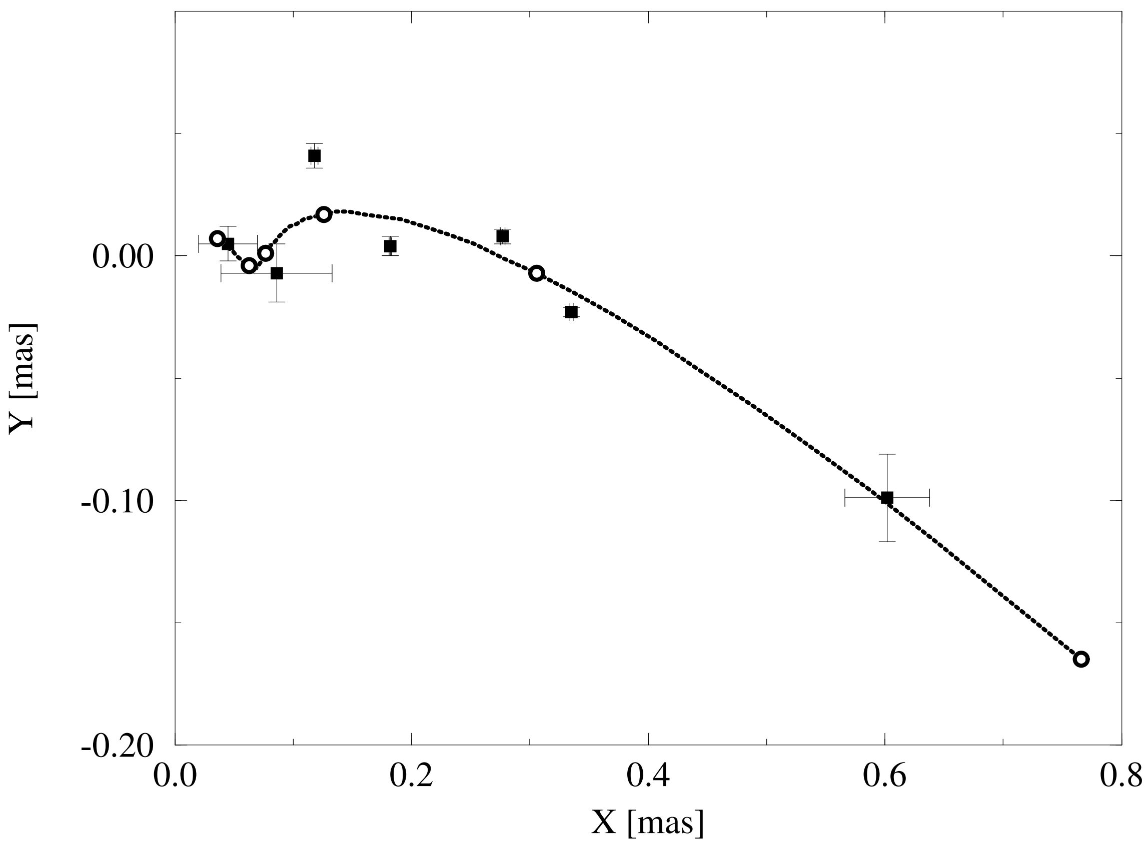

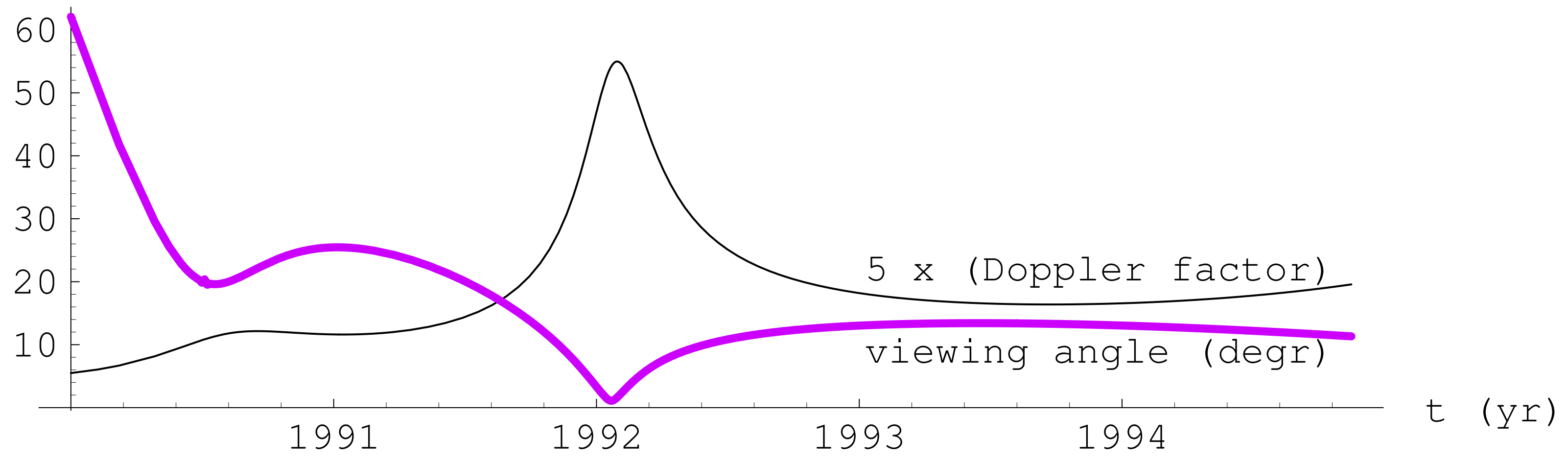
60
50
40
30
20
10
5 x (Doppler factor)
viewing angle (degr)
t (yr)
1991
1992
1993
1994

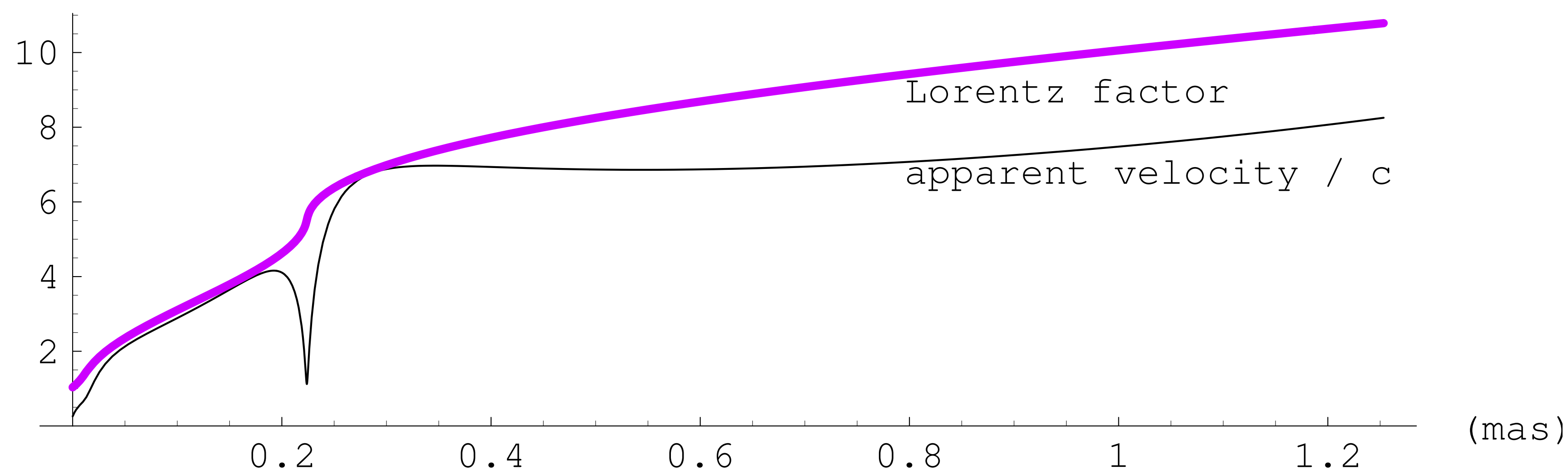
10
8
6
4
2
Lorentz factor
apparent velocity / c
(mas)
0.2
0.4
0.6
0.8
1
1.2

Polarization maps

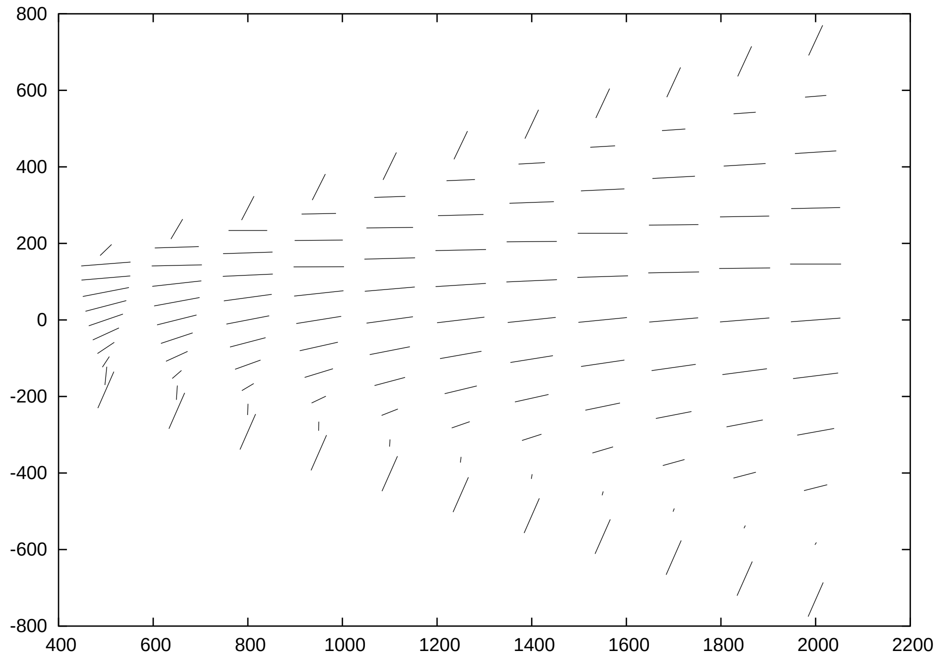

$\gamma = 10$, $\theta_{obs} = 1/2\gamma$, jet half-opening=1 degree, pitch angle at a reference diastance = 0.1 degrees
electron's energy spectrum $\propto \gamma_e^{-2.4}$

Polarization maps

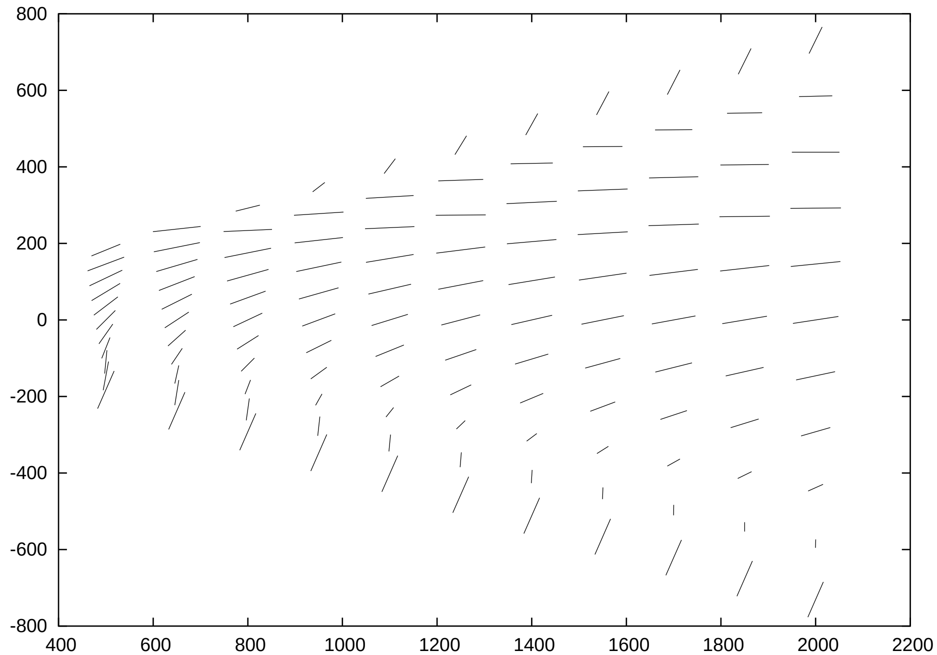

$\gamma = 10$, $\theta_{obs} = 1/2\gamma$, jet half-opening=1 degree, pitch angle at a reference diastance = 0.05 degrees
electron's energy spectrum $\propto \gamma_e^{-2.4}$

Summary

⋆ $\boldsymbol{B}$ + rotation = energy extraction
With $P_{ext} \quad \rightarrow$ jet

⋆ The collimation-acceleration paradigm provides a viable explanation of the dynamics of relativistic jets

⋆ bulk acceleration up to Lorentz factors $\gamma_\infty \gtrsim 0.5\frac{\mathcal{E}}{Mc^2}$
caveat: in ultrarelativistic GRB jets $\vartheta \sim 1/\gamma$

⋆ Rarefaction acceleration

- further increases γ
- makes GRB jets with $\gamma\vartheta \gg 1$
- interesting for AGN jets as well

the intrinsic rotation of jets could be related to the observed kinematics and to the rotation of EVPA (Marscher+2008)